NOT FOR PUBLICATION

NEANDC(J)-130/U
INDC(JPN)-116/U

PROGRESS REPORT

(JULY 1987 TO JUNE 1988 INCLUSIVE)

AUGUST 1988

EDITOR

S. KIKUCHI

JAPANESE NUCLEAR DATA COMMITTEE

JAPAN ATOMIC ENERGY RESEARCH INSTITUTE

TOKAI RESEARCH ESTABLISHMENT

TOKAI-MURA, IBARAKI-KEN, JAPAN

Editor's Note

This is a collection of reports which have been submitted to the Japanese Nuclear Data Committee at the committee's request. The request was addressed to the following individuals who might represent or be in touch with groups doing researches related to the nuclear data of interest to the development of the nuclear energy program.

Although the editor tried not to miss any appropriate addressees, there may have been some oversight. Meanwhile, contribution of a report rested with discretion of its author. The coverage of this document, therefore, may not be uniform over the related field or research.

In this progress report, each individual report is generally reproduced as it was received by the JNDC secretariat, and editor also let pass some simple obvious errors in the manuscripts if any.

This edition covers a period of July 1, 1987 to June 30, 1988. The information herein contained is of a nature of "Private Communication". <u>Data contained in this report should not be quoted without the author's permission.</u>

CONTENTS OF JAPANESE PROGRESS REPORT NEANDC(J)130/U

ELEMENT S	A	QUANTITY	ENERGY MIN	ENERGY MAX	LAB	TYPE	DOCUMENTATION REF VOL PAGE	DATE	COMMENTS
H	CXX	TOTAL	MAXW		JPN	EXPT-PROG	NEANDC(J)130	AUG 88	KADOTANI+.P101.PRESENTED AT 88MITO
LI	6	N EMISSION	1.8+7		JAE	EXPT-PROG	NEANDC(J)130	AUG 88	CHIBA+.P9.PRESENTED AT 88MITO
LI	7	DIFF INELAST	1.1+7	1.3+7	JAE	EXPT-PROG	NEANDC(J)130	AUG 88	CHIBA+.P10.PUBLISHED IN NST,25,210
LI	7	N EMISSION	1.8+7		JAE	EXPT-PROG	NEANDC(J)130	AUG 88	CHIBA+.P9.PRESENTED AT 88MITO
LI	7	(N,T)	1.4+7		YOK	EXPT-PROG	NEANDC(J)130	AUG 88	SHIRATO+.P117.PRESENTED AT 88MITO
LI	7	(N,ALPHA)	1.4+7		YOK	EXPT-PROG	NEANDC(J)130	AUG 88	SHIRATO+.P117.PRESENTED AT 88MITO
BE	9	N EMISSION	1.4+7	1.8+7	TOH	EXPT-PROG	NEANDC(J)130	AUG 88	BABA+.P123.PRESENTED AT 88MITO
B	11	DIFF ELASTIC	1.3+7		JAE	EXPT-PROG	NEANDC(J)130	AUG 88	YAMANOUTI+.P14.PRESENTED AT 88MITO
B	11	DIFF INELAST	1.3+7		JAE	EXPT-PROG	NEANDC(J)130	AUG 88	YAMANOUTI+.P14.PRESENTED AT 88MITO
C	12	N EMISSION	1.4+7	1.8+7	TOH	EXPT-PROG	NEANDC(J)130	AUG 88	BABA+.P123.PRESENTED AT 88MITO
O	16	N EMISSION	1.4+7	1.8+7	TOH	EXPT-PROG	NEANDC(J)130	AUG 88	BABA+.P123.PRESENTED AT 88MITO
O	16	RESON PARAMS	4.3+5		TIT	EXPT-PROG	NEANDC(J)130	AUG 88	KITAZAWA+.P127. PUBL IN JP/G 14 SUPPL
F	19	(N,2N)	1.4+7		KTO	EXPT-PROG	NEANDC(J)130	AUG 88	KOBAYASHI+.P37.[illegible]=41.59+-1.70 MB
NA	23	RES INT CAP	1.0+0		KTO	EXPT-PROG	NEANDC(J)130	AUG 88	KOBAYASHI+.P52.PRESENTED AT 87KII
MG		EVALUATION	NDG		JAE	EVAL-PROG	NEANDC(J)130	AUG 88	HATCHYA+.P16.FOR JENDL-3,NDG
MG		NONELA GAMMA	1.1+7		JAE	EVAL-PROG	NEANDC(J)130	AUG 88	HATCHYA+.P16.FOR JENDL-3,SPCT IN FIG
MG	24	EVALUATION	NDG		JAE	EVAL-PROG	NEANDC(J)130	AUG 88	HATCHYA+.P16.FOR JENDL-3,NDG
MG	24	(N,P)	1.4+7		KTO	EXPT-PROG	NEANDC(J)130	AUG 88	KOBAYASHI+.P37.SIG=192.2+-6.6 MB
MG	24	RESON PARAMS	4.6+4	8.4+4	TIT	EXPT-PROG	NEANDC(J)130	AUG 88	UCHIYAMA+.P132.PRESENTED AT 88MITO
MG	25	EVALUATION	NDG		JAE	EVAL-PROG	NEANDC(J)130	AUG 88	HATCHYA+.P16.FOR JENDL-3,NDG

ELEMENT S	A	QUANTITY	ENERGY MIN	MAX	LAB	TYPE	DOCUMENTATION REF VOL PAGE	DATE	COMMENTS
MG	26	EVALUATION	NDG		JAE	EVAL-PROG	NEANDC(J)130	AUG 88	HATCHYA+.P16.FOR JENDL-3,NDG
AL	27	EVALUATION	1.0-5	2.0+7	TIT	EVAL-PROG	NEANDC(J)130	AUG 88	KITAZAWA+.P128.PRESENTED AT 88MITO
AL	27	NONELA GAMMA	7.8+6		JAE	EXPT-PROG	NEANDC(J)130	AUG 88	MIZUMOTO+.P12.PRESENTED AT 88MITO
AL	27	N EMISSION	1.4+7	1.8+7	TOH	EXPT-PROG	NEANDC(J)130	AUG 88	BABA+.P124.PRESENTED AT 88MITO
AL	27	(N,P)	NDG		KYU	EVAL-PROG	NEANDC(J)130	AUG 88	KANDA+.P88.PRESENTED AT 88MITO
AL	27	(N,P)	NDG		KYU	EVAL-PROG	NEANDC(J)130	AUG 88	KANDA+.P89.PRESENTED AT 87KIEV
AL	27	(N,P)	1.4+7		KTO	EXPT-PROG	NEANDC(J)130	AUG 88	KOBAYASHI+.P37.SIG=77.07+-2.71 MB
AL	27	(N,P)	5.0+6	2.0+7	JPN	EXPT-PROG	NEANDC(J)130	AUG 88	KUDO+.P3.VDG,C-W,ACT-SIG IN FIG
AL	27	(N,ALPHA)	NDG		KYU	EVAL-PROG	NEANDC(J)130	AUG 88	KANDA+.P88.PRESENTED AT 88MITO
AL	27	(N,ALPHA)	NDG		KYU	EVAL-PROG	NEANDC(J)130	AUG 88	KANDA+.P89.PRESENTED AT 87KIEV
SI		NONELA GAMMA	7.8+6		JAE	EXPT-PROG	NEANDC(J)130	AUG 88	MIZUMOTO+.P12.PRESENTED AT 88MITO
SI	28	EVALUATION	1.0-5	2.0+7	TIT	EVAL-PROG	NEANDC(J)130	AUG 88	KITAZAWA+.P128.PRESENTED AT 88MITO
SI	28	RESON PARAMS	1.9+5	8.1+5	TIT	EXPT-PROG	NEANDC(J)130	AUG 88	KITAZAWA+.P127.PUBL IN JP/G 14 SUPPL
SI	28	RESON PARAMS	5.6+4	1.8+5	JAE	EXPT-PROG	NEANDC(J)130	AUG 88	ZENG+.P13.LINAC,RES-E AND WN GIVEN
SI	29	EVALUATION	1.0-5	2.0+7	TIT	EVAL-PROG	NEANDC(J)130	AUG 88	KITAZAWA+.P128.PRESENTED AT 88MITO
SI	30	EVALUATION	1.0-5	2.0+7	TIT	EVAL-PROG	NEANDC(J)130	AUG 88	KITAZAWA+.P128.PRESENTED AT 88MITO
S	32	RESON PARAMS	1.0+5	2.0+5	TIT	EXPT-PROG	NEANDC(J)130	AUG 88	KITAZAWA+.P127.PUBL IN JP/G 14 SUPPL
TI		N EMISSION	1.4+7		TOH	EXPT-PROG	NEANDC(J)130	AUG 88	BABA+.P124.PRESENTED AT 88MITO
TI	46	(N,P)	1.4+7		KTO	EXPT-PROG	NEANDC(J)130	AUG 88	KOBAYASHI+.P37.SIG=267.8+-9.3 MB
TI	47	(N,P)	1.4+7		KTO	EXPT-PROG	NEANDC(J)130	AUG 88	KOBAYASHI+.P37.SIG=289.6+-9.8 MB

ELEMENT S	A	QUANTITY	ENERGY MIN	ENERGY MAX	LAB	TYPE	DOCUMENTATION REF	VOL	PAGE	DATE	COMMENTS
TI	48	(N,P)	1.4+7		KTO	EXPT-PROG	NEANDC(J)		130	AUG 88	KOBAYASHI+.P37.SIG=58.60+-1.88MB
TI	50	RES INT CAP	1.0+0		KTO	EXPT-PROG	NEANDC(J)		130	AUG 88	KOBAYASHI+.P52.PRESENTED AT 87KIEV
V	51	RES INT CAP	1.0+0		KTO	EXPT-PROG	NEANDC(J)		130	AUG 88	KOBAYASHI+.P52.PRESENTED AT 87KIEV
V	51	N EMISSION	1.4+7		TOH	EXPT-PROG	NEANDC(J)		130	AUG 88	BABA+.P124.PRESENTED AT 88MITO
V	51	(N,ALPHA)	1.4+7		KTO	EXPT-PROG	NEANDC(J)		130	AUG 88	KOBAYASHI+.P37.SIG=15.03+-0.65 MB
CR		N EMISSION	1.4+7		TOH	EXPT-PROG	NEANDC(J)		130	AUG 88	BABA+.P124.PRESENTED AT 88MITO
MN	55	RES INT CAP	1.0+0		KTO	EXPT-PROG	NEANDC(J)		130	AUG 88	KOBAYASHI+.P52.PRESENTED AT 87KIEV
MN	55	(N,2N)	1.4+7		KTO	EXPT-PROG	NEANDC(J)		130	AUG 88	KOBAYASHI+.P37.SIG=775.4+-28.6 MB
MN	55	N EMISSION	1.4+7		TOH	EXPT-PROG	NEANDC(J)		130	AUG 88	BABA+.P124.PRESENTED AT 88MITO
MN	55	(N,ALPHA)	1.4+7		NAG	EXPT-PROG	NEANDC(J)		130	AUG 88	KATOH+.P105.ACT-SIG CFD OTHER IN FIG
FE		(N,GAMMA)	1.0+4	6.0+5	TIT	EXPT-PROG	NEANDC(J)		130	AUG 88	IGASHIRA+.P130.PRESENTED AT 88MITO
FE		NONELA GAMMA	7.8+6		JAE	EXPT-PROG	NEANDC(J)		130	AUG 88	MIZUMOTO+.P12.PRESENTED AT 88MITO
FE		N EMISSION	1.4+7	1.8+7	TOH	EXPT-PROG	NEANDC(J)		130	AUG 88	BABA+.P124.PRESENTED AT 88MITO
FE	54	(N,P)	NDG		KYU	EVAL-PROG	NEANDC(J)		130	AUG 88	KANDA+.P89.PRESENTED AT 87KIEV
FE	54	(N,P)	1.4+7		KTO	EXPT-PROG	NEANDC(J)		130	AUG 88	KOBAYASHI+.P37.SIG=405.1+-15.3 MB
FE	54	(N,P)	NDG		KYU	EVAL-PROG	NEANDC(J)		130	AUG 88	KANDA+.P88.PRESENTED AT 88MITO
FE	56	(N,P)	NDG		KYU	EVAL-PROG	NEANDC(J)		130	AUG 88	KANDA+.P89.PRESENTED AT 87KIEV
FE	56	(N,P)	NDG		KYU	EVAL-PROG	NEANDC(J)		130	AUG 88	KANDA+.P88.PRESENTED AT 88MITO
FE	56	(N,P)	1.4+7		KTO	EXPT-PROG	NEANDC(J)		130	AUG 88	KOBAYASHI+.P37.SIG=112.3+-3.9 MB
CO	59	RES INT CAP	1.0+0		KTO	EXPT-PROG	NEANDC(J)		130	AUG 88	KOBAYASHI+.P52.PRESENTED AT 87KIEV

ELEMENT S	A	QUANTITY	ENERGY MIN	MAX	LAB	TYPE	DOCUMENTATION REF VOL PAGE	DATE	COMMENTS
CO	59	(N,2N)	1.4+7		KTO	EXPT-PROG	NEANDC(J)130	AUG 88	KOBAYASHI+.P37.SIG=729.0+-29.0 MB
CO	59	(N,ALPHA)	NDG		KYU	EVAL-PROG	NEANDC(J)130	AUG 88	KANDA+.P88.PRESENTED AT 88MITO
CO	59	(N,ALPHA)	NDG		KYU	EVAL-PROG	NEANDC(J)130	AUG 88	KANDA+.P89.PRESENTED AT 87KIEV
CO	59	(N,ALPHA)	1.4+7		KTO	EXPT-PROG	NEANDC(J)130	AUG 88	KOBAYASHI+.P37.SIG=29.72+-1.04 MB
NI		(N,GAMMA)	1.0+4	6.0+5	TIT	EXPT-PROG	NEANDC(J)130	AUG 88	IGASHIRA+.P130.PRESENTED AT 88MITO
NI		N EMISSION	1.4+7	1.8+7	TOH	EXPT-PROG	NEANDC(J)130	AUG 88	BABA+.P124.PRESENTED AT 88MITO
NI	58	(N,2N)	1.4+7		KTO	EXPT-PROG	NEANDC(J)130	AUG 88	KOBAYASHI+.P37.SIG=25.33+-0.83 MB
NI	58	(N,P)	NDG		KYU	EVAL-PROG	NEANDC(J)130	AUG 88	KANDA+.P89.PRESENTED AT 87KIEV
NI	58	(N,P)	NDG		KYU	EVAL-PROG	NEANDC(J)130	AUG 88	KANDA+.P88.PRESENTED AT 88MITO
NI	58	(N,P)	1.4+7		KTO	EXPT-PROG	NEANDC(J)130	AUG 88	KOBAYASHI+.P37.SIG=397.9+-13.3 MB
NI	64	RES INT CAP	1.0+0		KTO	EXPT-PROG	NEANDC(J)130	AUG 88	KOBAYASHI+.P52.PRESENTED AT 87KIEV
CU		N EMISSION	1.4+7	1.8+7	TOH	EXPT-PROG	NEANDC(J)130	AUG 88	BABA+.P124.PRESENTED AT 88MITO
CU	63	(N,2N)	1.4+7		NAG	EXPT-PROG	NEANDC(J)130	AUG 88	KATOH+.P105.ACT-SIG CFD OTHER IN FIG
CU	63	(N,ALPHA)	1.4+7		NAG	EXPT-PROG	NEANDC(J)130	AUG 88	KATOH+.P105.ACT-SIG CFD OTHER IN FIG
ZN	64	(N,P)	1.4+7		KTO	EXPT-PROG	NEANDC(J)130	AUG 88	KOBAYASHI+.P37.SIG=172.8+-12.7 MB
ZN	90	(N,2N)	1.4+7		KTO	EXPT-PROG	NEANDC(J)130	AUG 88	KOBAYASHI+.P37.SIG TO M+G
GA	71	RES INT CAP	1.0+0		KTO	EXPT-PROG	NEANDC(J)130	AUG 88	KOBAYASHI+.P52.PRESENTED AT 87KIEV
AS	75	DIFF INELAST	1.4+7		KYU	THEO-PROG	NEANDC(J)130	AUG 88	KUMABE+.P72.ANG-DIST IN FIG
ZR		N EMISSION	1.4+7	1.8+7	TOH	EXPT-PROG	NEANDC(J)130	AUG 88	BABA+.P124.PRESENTED AT 88MITO
ZR	90	(N,2N)	1.4+7		NAG	EXPT-PROG	NEANDC(J)130	AUG 88	KATOH+.P105.ACT-SIG CFD OTHER IN FIG

ELEMENT S	A	QUANTITY	ENERGY MIN	MAX	LAB	TYPE	DOCUMENTATION REF VOL PAGE	DATE	COMMENTS
NB	93	DIFF INELAST	1.4+7		KYU	THEO-PROG	NEANDC(J)130	AUG 88	KUMABE+.P72.ANG-DIST IN FIG
NB	93	DIFF INELAST	NDG		JAE	EVAL-PROG	NEANDC(J)130	AUG 88	IKEDA+.P23.ACT-SIG TO ISOMER IN TBL
NB	93	RES INT CAP	1.0+0		KTO	EXPT-PROG	NEANDC(J)130	AUG 88	KOBAYASHI+.P52.PRESENTED AT 87KIEV
NB	93	(N,2N)	1.4+7		KTO	EXPT-PROG	NEANDC(J)130	AUG 88	KOBAYASHI+.P37.S(M)=464.3+-15.1 MB
NB	93	(N,P)	1.4+7		KYU	THEO-PROG	NEANDC(J)130	AUG 88	KUMABE+.P72.ANG-DIST IN FIG
MO	92	(N,2N)	1.4+7		NAG	EXPT-PROG	NEANDC(J)130	AUG 88	KATOH+.P105.ACT-SIG CFD OTHER IN FIG
MO	92	(N,P)	1.4+7		KTO	EXPT-PROG	NEANDC(J)130	AUG 88	KOBAYASHI+.P37.S(M)=73.67+-4.14 MB
MO	92	(N,ALPHA)	1.4+7		NAG	EXPT-PROG	NEANDC(J)130	AUG 88	KATOH+.P105.ACT-SIG CFD OTHER IN FIG
AG		DIFF INELAST	1.4+7		KYU	THEO-PROG	NEANDC(J)130	AUG 88	KUMABE+.P72.ANG-DIST IN FIG
AG		N EMISSION	1.4+7		KYU	EXPT-PROG	NEANDC(J)130	AUG 88	WATANABE+.P68.PUBL IN PR/C37,963(88)
AG	107	RES INT CAP	1.0+0		KTO	EXPT-PROG	NEANDC(J)130	AUG 88	KOBAYASHI+.P52.PRESENTED AT 87KIEV
AG	109	RES INT CAP	1.0+0		KTO	EXPT-PROG	NEANDC(J)130	AUG 88	KOBAYASHI+.P52.PRESENTED AT 87KIEV
CD		N EMISSION	1.4+7		KYU	EXPT-PROG	NEANDC(J)130	AUG 88	WATANABE+.P68.PUBL IN PR/C37,963(88)
IN		N EMISSION	1.4+7		KYU	THEO-PROG	NEANDC(J)130	AUG 88	WATANABE+.P76.PREDIU ANG-DIST IN FIG
IN		N EMISSION	1.4+7		KYU	EXPT-PROG	NEANDC(J)130	AUG 88	WATANABE+.P68.PUBL IN PR/C37,963(88)
IN	115	DIFF INELAST	1.4+7		KTO	EXPT-PROG	NEANDC(J)130	AUG 88	KOBAYASHI+.P37.S(M)=65.03+-2.47 MB
IN	115	RES INT CAP	1.0+0		KTO	EXPT-PROG	NEANDC(J)130	AUG 88	KOBAYASHI+.P52.PRESENTED AT 87KIEV
SN		N EMISSION	1.4+7		KYU	EXPT-PROG	NEANDC(J)130	AUG 88	WATANABE+.P68.PUBL IN PR/C37,963(88)
SN	118	DIFF ELASTIC	1.5+7	1.8+7	JAE	EXPT-PROG	NEANDC(J)130	AUG 88	CHIBA+.P11.PUBLISHED IN NST,25,511
SN	118	DIFF INELAST	1.5+7	1.8+7	JAE	EXPT-PROG	NEANDC(J)130	AUG 88	CHIBA+.P11.PUBLISHED IN NST,25,511

ELEMENT S	A	QUANTITY	ENERGY MIN	MAX	LAB	TYPE	DOCUMENTATION REF VOL PAGE	DATE	COMMENTS
SB		N EMISSION	1.4+7		KYU	EXPT-PROG	NEANDC(J)130	AUG 88	WATANABE+.P68.PUBL IN PR/C37,963(88)
TE		N EMISSION	1.4+7		KYU	EXPT-PROG	NEANDC(J)130	AUG 88	WATANABE+.P68.PUBL IN PR/C37,963(88)
SM		TOTAL	MAXW		JPN	EXPT-PROG	NEANDC(J)130	AUG 88	HIGURASHI+.P99.PRESENTED AT 88MITO
GD		TOTAL	MAXW		JPN	EXPT-PROG	NEANDC(J)130	AUG 88	HIGURASHI+.P99.PRESENTED AT 88MITO
DY		TOTAL	MAXW		JPN	EXPT-PROG	NEANDC(J)130	AUG 88	HIGURASHI+.P99.PRESENTED AT 88MITO
TA	181	RES INT CAP	1.0+0		KTO	EXPT-PROG	NEANDC(J)130	AUG 88	KOBAYASHI+.P52.PRESENTED AT 87KIEV
TA	181	RESON PARAMS	1.0+2	4.3+3	KYU	EXPT-PROG	NEANDC(J)130	AUG 88	TSUBONE+.P94.PUBL NST 24,975(87)
W		EVALUATION	NDG		JAE	EVAL-PROG	NEANDC(J)130	AUG 88	ASAMI+.P18.FOR JENDL3,NDG
W		(N,2N)	TR	2.0+7	JAE	EVAL-PROG	NEANDC(J)130	AUG 88	ASAMI+.P18.FOR JENDL3,CFD EXP IN FIG
W	182	EVALUATION	NDG		JAE	EVAL-PROG	NEANDC(J)130	AUG 88	ASAMI+.P18.FOR JENDL3,NDG
W	183	EVALUATION	NDG		JAE	EVAL-PROG	NEANDC(J)130	AUG 88	ASAMI+.P18.FOR JENDL3,NDG
W	184	EVALUATION	NDG		JAE	EVAL-PROG	NEANDC(J)130	AUG 88	ASAMI+.P18.FOR JENDL3,NDG
W	186	EVALUATION	NDG		JAE	EVAL-PROG	NEANDC(J)130	AUG 88	ASAMI+.P18.FOR JENDL3,NDG
W	186	RES INT CAP	1.0+0		KTO	EXPT-PROG	NEANDC(J)130	AUG 88	KOBAYASHI+.P52.PRESENTED AT 87KIEV
AU	197	RES INT CAP	1.0+0		KTO	EXPT-PROG	NEANDC(J)130	AUG 88	KOBAYASHI+.P52.PRESENTED AT 87KIEV
AU	197	(N,2N)	1.4+7		KTO	EXPT-PROG	NEANDC(J)130	AUG 88	KOBAYASHI+.P37.SIG=2125+-79 MB
HG	199	DIFF INELAST	NDG		JAE	EVAL-PROG	NEANDC(J)130	AUG 88	IKEDA+.P23.ACT-SIG TO ISOMER IN TBL
PB		TOTAL	4.3+0	3.9+1	KTO	EXPT-PROG	NEANDC(J)130	AUG 88	KOBAYASHI+.P47.FILTERED BEAM,FIG+TBL
PB		NONELA GAMMA	7.8+6		JAE	EXPT-PROG	NEANDC(J)130	AUG 88	MIZUMOTO+.P12.PRESENTED AT 88MITO
PB	204	DIFF INELAST	1.4+7		KTO	EXPT-PROG	NEANDC(J)130	AUG 88	KOBAYASHI+.P37.S(M)=63.81+-3.30 MB

ELEMENT S A	QUANTITY	ENERGY MIN	MAX	LAB	TYPE	DOCUMENTATION REF VOL PAGE	DATE	COMMENTS
PB 204	(N,2N)	1.4+7		KTO	EXPT-PROG	NEANDC(J)130	AUG 88	KOBAYASHI+.P37.[illegible] 1910+-63 MB
BI 209	NONELA GAMMA	7.8+6		JAE	EXPT-PROG	NEANDC(J)130	AUG 88	MIZUMOTO+.P12.PRESENTED AT 88MITO
TH 232	RES INT CAP	1.0+0		KTO	EXPT-PROG	NEANDC(J)130	AUG 88	KOBAYASHI+.P52.PRESENTED AT 87KIEV
TH 232	FISSION	1.0+6	1.0+7	KYU	EVAL-PROG	NEANDC(J)130	AUG 88	KANDA+.P92.PRESENTED AT 88MITO
TH 232	RESON PARAMS	NDG		KTO	EXPT-PROG	NEANDC(J)130	AUG 88	KOBAYASHI+.P43.SUBMITTED TO ANE
PA 231	(N,GAMMA)	MAXW		KTO	EXPT-PROG	NEANDC(J)130	AUG 88	HASHIMOTO+.P42.PUBL IN JRN,120,185
PA 231	(N,2N)	FISS		KTO	EXPT-PROG	NEANDC(J)130	AUG 88	HASHIMOTO+.P42.PUBL IN JRN,120,185
U 233	FISSION	1.0+6	1.0+7	KYU	EVAL-PROG	NEANDC(J)130	AUG 88	KANDA+.P92.PRESENTED AT 88MITO
U 233	NU	2.5-2		KTO	EXPT-PROG	NEANDC(J)130	AUG 88	NAKAGOME+.P55.CFD OTHERS IN FIG
U 234	FISSION	1.0+6	1.0+7	KYU	EVAL-PROG	NEANDC(J)130	AUG 88	KANDA+.P92.PRESENTED AT 88MITO
U 235	FISSION	1.0+6	1.0+7	KYU	EVAL-PROG	NEANDC(J)130	AUG 88	KANDA+.P92.PRESENTED AT 88MITO
U 235	FISSION	1.4+7		TOH	EXPT-PROG	NEANDC(J)130	AUG 88	IWASAKI+.P121.PRESENTED AT 88MITO
U 235	NU	2.5-2		KTO	EXPT-PROG	NEANDC(J)130	AUG 88	NAKAGOME+.P55.CFD OTHERS IN FIG
U 236	FISSION	1.0+6	1.0+7	KYU	EVAL-PROG	NEANDC(J)130	AUG 88	KANDA+.P92.PRESENTED AT 88MITO
U 238	RES INT CAP	1.0+0		KTO	EXPT-PROG	NEANDC(J)130	AUG 88	KOBAYASHI+.P52.PRESENTED AT 87KIEV
U 238	FISSION	1.0+6	1.0+7	KYU	EVAL-PROG	NEANDC(J)130	AUG 88	KANDA+.P92.PRESENTED AT 88MITO
NP 237	FISSION	1.0+6	1.0+7	KYU	EVAL-PROG	NEANDC(J)130	AUG 88	KANDA+.P92.PRESENTED AT 88MITO
PU 239	FISSION	1.0+6	1.0+7	KYU	EVAL-PROG	NEANDC(J)130	AUG 88	KANDA+.P92.PRESENTED AT 88MITO
PU 239	FISSION	6.0+5	7.0+6	TOH	EXPT-PROG	NEANDC(J)130	AUG 88	HIRAKAWA+.P122.PRESENTED AT 88MITO
PU 242	FISSION	6.0+5	7.0+6	TOH	EXPT-PROG	NEANDC(J)130	AUG 88	HIRAKAWA+.P122.PRESENTED AT 88MITO

ELEMENT S	A	QUANTITY	ENERGY MIN	MAX	LAB	TYPE	DOCUMENTATION REF VOL PAGE	DATE	COMMENTS
AM	241	EVALUATION	1.0-5	2.0+7	JAE	EVAL-PROG	NEANDC(J)130	AUG 88	NAKAGAWA+.P20.PRESENTED AT 88MITO
AM	242	EVALUATION	1.0-5	2.0+7	JAE	EVAL-PROG	NEANDC(J)130	AUG 88	NAKAGAWA+.P20.PRESENTED AT 88MITO
AM	243	EVALUATION	1.0-5	2.0+7	JAE	EVAL-PROG	NEANDC(J)130	AUG 88	NAKAGAWA+.P20.PRESENTED AT 88MITO
AM	244	EVALUATION	1.0-5	2.0+7	JAE	EVAL-PROG	NEANDC(J)130	AUG 88	NAKAGAWA+.P20.PRESENTED AT 88MITO
CM	242	EVALUATION	1.0-5	2.0+7	JAE	EVAL-PROG	NEANDC(J)130	AUG 88	NAKAGAWA+.P20.PRESENTED AT 88MITO
CM	243	EVALUATION	1.0-5	2.0+7	JAE	EVAL-PROG	NEANDC(J)130	AUG 88	NAKAGAWA+.P20.PRESENTED AT 88MITO
CM	244	EVALUATION	1.0-5	2.0+7	JAE	EVAL-PROG	NEANDC(J)130	AUG 88	NAKAGAWA+.P20.PRESENTED AT 88MITO
CM	245	EVALUATION	1.0-5	2.0+7	JAE	EVAL-PROG	NEANDC(J)130	AUG 88	NAKAGAWA+.P20.PRESENTED AT 88MITO
CM	246	EVALUATION	1.0-5	2.0+7	JAE	EVAL-PROG	NEANDC(J)130	AUG 88	NAKAGAWA+.P20.PRESENTED AT 88MITO
CM	247	EVALUATION	1.0-5	2.0+7	JAE	EVAL-PROG	NEANDC(J)130	AUG 88	NAKAGAWA+.P20.PRESENTED AT 88MITO
CM	248	EVALUATION	1.0-5	2.0+7	JAE	EVAL-PROG	NEANDC(J)130	AUG 88	NAKAGAWA+.P20.PRESENTED AT 88MITO
CM	249	EVALUATION	1.0-5	2.0+7	JAE	EVAL-PROG	NEANDC(J)130	AUG 88	NAKAGAWA+.P20.PRESENTED AT 88MITO
BK	249	EVALUATION	1.0-5	2.0+7	JAE	EVAL-PROG	NEANDC(J)130	AUG 88	NAKAGAWA+.P20.PRESENTED AT 88MITO
BK	250	EVALUATION	1.0-5	2.0+7	JAE	EVAL-PROG	NEANDC(J)130	AUG 88	NAKAGAWA+.P21.PUBL IN JAERI-M 88-004
BK	250	EVALUATION	1.0-5	2.0+7	JAE	EVAL-PROG	NEANDC(J)130	AUG 88	NAKAGAWA+.P20.PRESENTED AT 88MITO
CF	249	EVALUATION	1.0-5	2.0+7	JAE	EVAL-PROG	NEANDC(J)130	AUG 88	NAKAGAWA+.P20.PRESENTED AT 88MITO
CF	250	EVALUATION	1.0-5	2.0+7	JAE	EVAL-PROG	NEANDC(J)130	AUG 88	NAKAGAWA+.P20.PRESENTED AT 88MITO
CF	251	EVALUATION	1.0-5	2.0+7	JAE	EVAL-PROG	NEANDC(J)130	AUG 88	NAKAGAWA+.P20.PRESENTED AT 88MITO
CF	252	EVALUATION	1.0-5	2.0+7	JAE	EVAL-PROG	NEANDC(J)130	AUG 88	NAKAGAWA+.P20.PRESENTED AT 88MITO
CF	252	EVALUATION	1.0-5	2.0+7	JAE	EVAL-PROG	NEANDC(J)130	AUG 88	NAKAGAWA+.P21.PUBL IN JAERI-M 88-004

ELEMENT S A	QUANTITY	ENERGY MIN	ENERGY MAX	LAB	TYPE	DOCUMENTATION REF VOL PAGE	DATE	COMMENTS
MANY	EVALUATION	NDG		JAE	REVW-PROG	NEANDC(J)130	AUG 88	ASAMI+.P15.JENDL-3.PRSNTED AT 88MITO
MANY	(N,P)	1.4+7		KYU	THEO-PROG	NEANDC(J)130	AUG 88	KUMABE+.P65.PUBLISHED IN NST,24,839
MANY	(N,ALPHA)	1.4+7		KYU	THEO-PROG	NEANDC(J)130	AUG 88	KUMABE+.P65.PUBLISHED IN NST,24,839
MANY	(N,ALPHA)	NDG		JAE	THEO-PROG	NEANDC(J)130	AUG 88	SHIBATA+.P22.PRESENTED AT 88MITO
MANY	A EMISSION	1.5+7		KYU	EXPT-PROG	NEANDC(J)130	AUG 88	KANDA+.P90.SIG OF VARIOUS ELEMENTS,NDG
MANY	LVL DENSITY	NDG		KYU	EVAL-PROG	NEANDC(J)130	AUG 88	UENOHARA+.P87.PRESENTED AT 88MITO

The content table in the CINDA format was compiled by the JNDC CINDA group;

S. Chiba (JAERI), M. Kawai (NAIG),
H. Kitazawa (Tokyo Inst. of Tech.), T. Nakagawa (JAERI),
R. Nakasima (Hosei Univ.), M. Sakamoto (JAERI).

I. Electrotechnical Laboratory

A. Quantum Technology Division

I-A-1 Cross Sections of $^{27}Al(n,p)^{27}Mg$ Reaction at 5 MeV and between 14.6 and 19.9 MeV

K.Kudo, T.Kinoshita, Y.Hino, Y.Kawada
and K.Takeuchi*

The threshold reaction of the $^{27}Al(n,p)^{27}Mg$ gives advantageous features as one of activation reactions for reactor dosimetry as well as such $^{27}Al(n,\alpha)^{24}Na$ and $^{56}Fe(n,p)^{56}Mn$ reactions which have been included among the standard reference data by IAEA(1). ETL provided the $^{27}Al(n,\alpha)^{24}Na$ and the $^{56}Fe(n,p)^{56}Mn$ cross sections for the energies between 14.0 and 19.9 MeV(2), and has been extending the measurements to other important reactions. The present study covers precise measurements of the cross sections presented for the $^{27}Al(n,p)^{27}Mg$ reaction at the energy point of 5.0 MeV and in the energy range between 14.6 and 19.9 MeV.

Neutron Irradiations and Fluence Monitoring

Runs using the Cockcroft type accelerator were performed with the Ti-T target set at 45° inclination to the incident deuteron beam of 220 keV. The

---

* Ship Research Institute

foil was irradiated at an angle of 45° to the deuteron beam. The mean neutron energy corresponding to the angle was determined as 14.6 MeV by using an associated α-particle counting technique. The distance from the target was varied in the range from 50 to 100 mm.

Runs using the van de Graaff accelerator, were made with an activation foil placed along the deuteron beam axis behind the Ti-T or Ti-D target at distances from 50 to 100 mm. The neutron flux at 5.0 MeV was determined absolutely by using a Si surface barrier detector with a 1 mm thick polyethylene radiator.

The aluminum foils used in all irradiation runs were of purity exceeding 99.99 %, and the thickness ranged from 0.05 mm to 0.5 mm with the diameter of 25.4 mm. The foil was irradiated with a deuteron beam current ranging 3 - 10 μA, which ensured a fairly stable neutron yield. Variation in time of the neutron flux was monitored by α-particle counters or else by long counters. The irradiation time was about 30 min.

Radioactivity Measurement

The ^{27}Mg activity from the $^{27}Al(n,p)^{27}Mg$ reaction was measured by the γ counting method with a calibrated pure Ge detector or by the 4πβ-γ counting technique. For the half-life of ^{27}Mg and the γ-ray intensity for 844 keV, 9.462 min.(3) and 71.8 % (4) were adopted respectively. The recent evaluation(5) adopted 71.8 % instead of 73.0 %(3) as the γ-ray intensity. Our measurements also suggested the value of 71.8 % to be more preferable rather than 73.0 % by comparing the results between the γ counting and the β counting method.

Effect of d+D Neutrons in d+T Neutron Field

The d+D neutrons deriving from deuteron implantation in a Ti-T target will increase rapidly with augmentation of incident deuteron energy, to produce additional ^{27}Mg radioactivity. In the present study, the neutron yield from the D(d,n)^{3}He reaction was measured by means of a calibrated ^{3}He proportional detector of cylindrical type filled with ^{3}He 400 kPa and Kr 200 kPa. The correction required to the final ^{27}Mg activity measurement amounted to about 20 % at 19.9 MeV and about 5 % at 18.04 MeV.

Effect of Secondary Neutrons from Surroundings

The spectra of secondary neutrons produced from the target assembly and the construction of the experimental room were calculated by the PALLAS code(6). The dominant contribution of the secondary neutrons comes from the target assembly compared to that from the room construction. The additional activity of ^{27}Mg presented by these secondary neutrons was calculated using the calculated neutron spectrum and the ^{27}Al(n,p)^{27}Mg cross section given in ENDF/B-V.

Results

The results for the ^{27}Al(n,p)^{27}Mg reaction cross section are presented graphically in Fig.1 covering the energies of 5 MeV and between 14.6 and 19.9 MeV with Ryves' measurements(7), together with evaluations given in ENDF/B-V, as well as those by Evain(8) and Ryves(5). The plots indicating the present results are seen to be in agreement with Ryves' measuremets above 14.6 MeV energy region and with the recent evaluations at 14.6 MeV, but deviate largely from the ENDF/B-V evaluation in whole energy region except 19.9 MeV(9).

References

1. IAEA/NEANDC Nuclear Standards File: Nuclear Standards for Nuclear Measurements, IAEA Tech. Ser., No.227 (1985)
2. K.Kudo et al.: J. Nucl. Sci. Tech. 24,684 (1987)
3. C.M.Lederer: Table of Isotopes(7th Ed.) (1978)
4. U.Reus et al.: Atomic Data and Nucl. Data Tables 29, (1983)
5. T.B.Ryves: private communication (1987)
6. K.Takeuchi: JAERI-M 84-244 (1985)
7. T.B.Ryves: J. Phys. G 4,1783 (1978)
8. B.P.Evain et al.: ANL/NDM-89, (1985)
9. K.Kudo et al.: Proceedings of Int. Conf. on Nucl. Data in Mito, (1988)

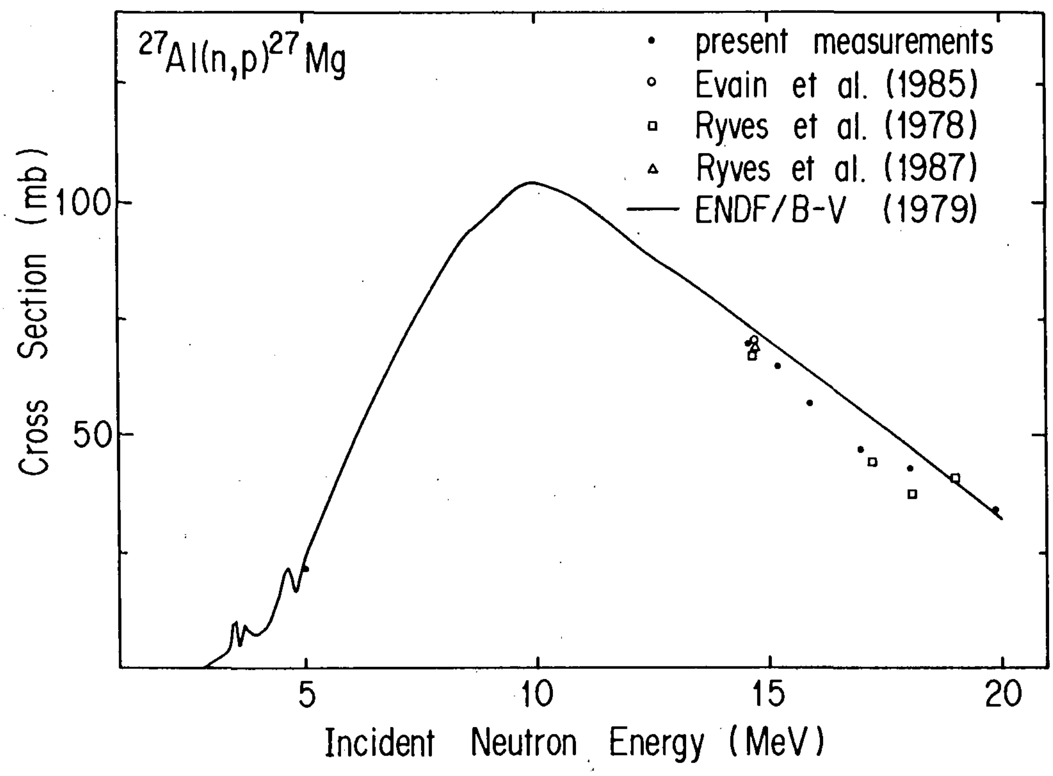

Fig.1 Cross sections of ^{27}Al(n,p)^{27}Mg reaction for incident neutron energies

II. Japan Atomic Energy Research Institute

A. Linac laboratory

Department of Physics

II-A-1

Measurement of Neutron-Induced Neutron-Producing Cross Sections of ^{6}Li and ^{7}Li at 18.0 MeV

Satoshi Chiba, Mamoru Baba*, Naohiro Yabuta*, Tsukasa Kikuchi*, Masumi Ishikawa*, Naohiro Hirakawa* and Kazusuke Sugiyama*

A paper on this subject was presented at the International Conference on Nuclear Data for Science and Technology, which was held in Mito during May 30 to June 3, 1988, with the following abstract:

The energy and angular double-differential neutron emission cross sections (DDX), $d^2\sigma/dE'd\Omega$, of ^{6}Li and ^{7}Li have been measured at 12 angles from 30 to 150^{o} with incident neutrons of 18.0 MeV. The measurement was based on the time-of-flight (TOF) method. Measured DDXs have been compared with predictions from evaluated nuclear data and some problems with the evaluations were found. It was also found that the angular distributions of the continuum energy neutrons have a clear systematic trend that is dependent on their Q-values. Neutrons corresponding to low excitation energy in residual nucleus showed strong forward angular distributions. A spherical optical model calculation was performed for the elastically scattered neutrons of ^{6}Li. The continuum neutron spectra of ^{6}Li were analyzed in terms of the Final-State Interaction theory. The analysis could reproduce the experimental spectra very well with a large contribution from the $^{3}S_{1}$ partial wave in the d-α system.

---

* : Tohoku University

II-A-2

Measurement of Fast Neutron Scattering Cross Sections of Li-7 at 11.0 and 13.0 MeV

Satoshi Chiba, Yoshimaro Yamanouti, Motoharu Mizumoto, Mikio Hyakutake*1 and Shin Iwasaki*2

A paper on this subject was published in Jour. Nucl. Sci. Technol. 25, 210(1988) with the following abstract:

Fast neutron cross sections below 14 MeV are very important for the development of D-T fusion reactors. Among them, those of ^{7}Li are of special importance, because ^{7}Li is the major tritium breeding material as well as ^{6}Li. The inelastic scattering to the 4.63-MeV state of ^{7}Li accounts for about half of the total ^{7}Li(n,n't)α reaction. In spite of its importance, the cross section is not confirmed well between 7 and 13 MeV. The present experiments have been made to resolve the discrepancy in the 4.63-MeV level cross sections of ^{7}Li reported by several authors. The incident neutron energies were selected to be 11.0 and 13.0 MeV, because there are no experimental data except those measured at TUNL in this energy range. The experiments were based on the time-of-flight (TOF) method.

---

*1 : Kyushu University

*2 : Tohoku University

II-A-3

Fast Neutron Scattering Cross Sections of Sn-118 at 14.9 and 18.0 MeV

Satoshi Chiba, Yoshimaro Yamanouti, Masayoshi Sugimoto, Motoharu Mizumoto, Yutaka Furuta, Mikio Hyakutake*1 and Shin Iwasaki*2

A paper on this subject will be published in Jour. Nucl. Sci. Technol. 25, 511(1988) with the following abstract:

The neutron scattering cross sections of ^{118}Sn have been measured at incident neutron energies of 14.9 and 18.0 MeV using the JAERI tandem fast neutron time-of-flight spectrometer. Measured are the angular distributions of the elastically scattered neutrons, and of inelastically scattered neutrons to the first 2^+ state (Q=-1.23 MeV) and to the 3^- state (Q=-2.32 MeV). The angular distributions of the inelastic scattering were strongly forward peaked. Thus the direct reaction process is dominant in this energy range. The measured angular distributions were analyzed in terms of the spherical optical model, the distorted-wave Born approximation and the coupled-channel theory. The optical potential and deformation parameters were deduced. The obtained deformation parameters were compared with other experimental results and the relation of $\beta_{p,p'}/\beta_{n,n'}>1$ was confirmed for the quadrupole deformation. This ratio was found to be consistent with the prediction of the schematic model for treatment of core-polarization. For the octupole deformation, however, this ratio was essentially unity. Isoscaler deformation parameters were also deduced.

---

*1 : Kyushu University

*2 : Tohoku University

II-A-4

Gamma-ray Production Cross Sections of Some Structural and Shielding Materials

M. Mizumoto, K. Hasegawa, S. Chiba, Y. Yamanouti, Y. Kawarasaki, M. Igashira*1, T. Uchiyama*1, H. Kitazawa*1, M. Drosg*2

A paper on this subject was presented at the International Conference on Nuclera Data for Sicence and Technology, May 30-June3, 1988, Mito with an abstract as follows:

Gamma-ray production cross sections have been measured for structural and shielding materials such as Al, Si, Fe, Pb and Bi at a neutron incident energy of 7.8 MeV. Neutrons were produced by the $^{2}H(d,n)^{3}He$ reaction at the JAERI Tandem Accelerator. Emitted gamma-rays were measured with a 7.6 cm diameter x 15 cm long NaI(Tl) detector surrounded by an 25.4 cm diameter x 25.4 cm long annular NaI(Tl) detector. The time-of-flight technique was used to eliminate the background caused by the scattered neutrons. In addition to corrections for neutron multiple scattering and gamma-ray self-shielding, special attention was paid to make an accurate correction for gamma-rays emitted due to Compton scattering in the samples. This effect appears to increase the observed low energy parts of the gamma-ray spectra by as much as 40 % in our samples. The measured results were compared with existing data and with the new evaluated data JENDL-3T based on the multi-step Hauser Feshbach calculation.

---

*1 Tokyo Institute of Technology, O-okayama, Tokyo, Japan
*2 University of Wien, Wien, Austria

II-A-5 Neutron Resonance Parameters of Si-28

Zeng Xiantang*1, M. Mizumoto, M. Sugimoto, S. Chiba
K. Hasegawa

Neutron transmission through a natural silicon sample has been measured in the neutron energy range between 30 keV and 500 keV. The JAERI Electron Linear Accelerator was used to provide neutrons. A 56-m flight path with a Li-6 glass scintillation detector was used for this measurement. Resonance parameters of Si-28 in this energy range were obtained to be: E_0 = 55.76 ± 0.01 keV, Γ_n = 0.63 ± 0.02 keV and E_0 = 179.78 ± 0.23 keV, Γ_n = 28.1 ± 0.5 keV, and compared with the three main evaluation values JENDL-3T, BNL-325 and Hermsdorf. Among them, the evaluation values adopted in JENDL-3T are close to our experimental results.

---

*1 Through the STA Scientist Exchange Program, on leave from Nuclear Physics Division, Institute of Atomic Energy China

II-A-6

Collective Model Analysis of Neutron Scattering from ^{11}B

Y.Yamanouti, M.Sugimoto, Y.Furuta, M.Mizumoto, M.Hyakutake*
and T.Methasiri**

Differential cross sections for elastic and inelastic scattering of 13 MeV neutrons from ^{11}B have been measured by using the JAERI tandem accelerator. The experimental cross sections were analyzed by the DWBA formalism in order to study to what extent the collective model can describe the light mass nucleus ^{11}B. In the theoretical calculations the best fit optical potential parameters obtained in the optical model analysis were used, and compound inelastic cross sections were taken into account. The collective model calculation based on the rotational model well reproduces the experimental cross section for the first $5/2^-$ excited state of ^{11}B. A paper on this subject was presented at the International Conference on Nuclear Data for Science and Technology, May 30- June 3, 1988, Mito, Japan.

* Department of Nuclear Engineering, Kyushu University
** Department of Physics, Chulalongkorn University

B. Nuclear Data Center, Department of Physics and Working Groups of Japanese Nuclear Data Committee

II-B-1

Status of Japanese Evaluated Nuclear Data Library Version 3

T. Asami, T. Nakagawa, M. Mizumoto*, T. Narita, K. Shibata, S. Chiba*, T. Fukahori, A. Hasegawa** and S. Igarasi

A paper on this subject was submitted to International Conference on Nuclear Data for Science and Technology, May 30 to June 3, 1988, Mito, Japan, with the abstract as follows:

The compilation of the Japanese Evaluated Nuclear Data Library, Version 3 (JENDL-3) has been made in the Japanese Nuclear Data Committee and is now in a final stage. JENDL-3 has been planned so as to meet requirements from fields of fusion researches and radiation shieldings as well as designs of thermal- and fast reactors. In JENDL-3, much emphasis was placed on improvement of high-energy neutron data, inclusion of photon production data and consideration of measured double differential neutron emission cross sections. Much efforts were also made in full revisions of JENDL-2 data for fissile nuclides and structural materials. This paper gives an outline of JENDL-3 project and the present status of its compilation.

* Linac Laboratory, Department of Physics
** Shielding Laboratory, Department of Reactor Engineering

II-B-2 Evaluation of Neutron Nuclear Data for Magnesium

Masanori HATCHYA* and Tetsuo ASAMI

The evaluation of neutron nuclear data was made for the magnesium element and its three stable isotopes (^{24}Mg, ^{25}Mg and ^{26}Mg). This work was made to be newly adopted their evaluated data to JENDL-3. The evaluation for the Mg element were made so as to give the data consistent with the ones for the Mg isotopes. The neutron cross sections for low energies were reproduced from a set of the resonance parameters evaluated in this work, using a multi-level Breit-Wigner formula. The parameters for a few resolved resonances lying in the low energies were adjusted in detail so that the total cross sections reproduced were fitted to their experimental data. The data for fast neutrons were estimated mainly with theoretical calculations. The GNASH code was used to calculate the threshold reaction cross sections and the photon-production data including precompound effect. The inelastic scattering data for the discrete levels were calculated by using the CASTHY code. The contribution from the direct process in inelastic scattering was estimated by using the DWUCK code. The photon production data contain photon production cross sections, secondary gamma-ray spectra and gamma-ray multiplicities. The data evaluation has almost finished and the work on the file making for JENDL-3 is now in progress. As an example of the evaluated data, Fig. 1 shows the evaluated spectrum of the secondary gamma-ray induced by the 11-MeV neutrons for the Mg element in comparing with the experimental ones.

---

* Data Engineering Co., Ltd.

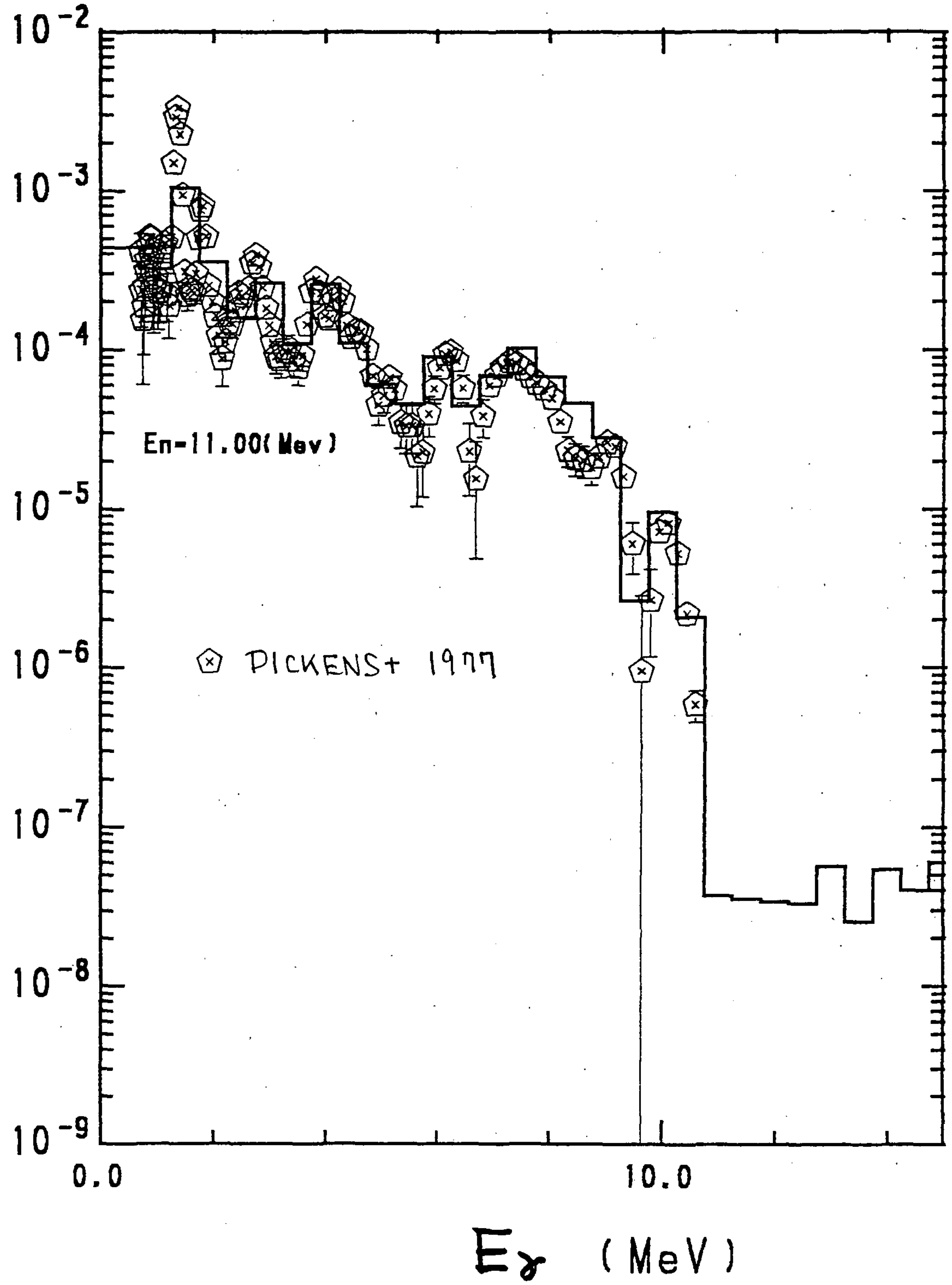

Fig. 1 Evaluated Secondary Gamma-Ray Spectrum for the Mg element at the Neutron Energy of 11 MeV.

II-B-3 Evaluation of Neutron Nuclear Data for Tungsten

Tetsuo ASAMI and Takashi WATANABE*

The evaluation of neutron nuclear data was made for the tungsten element and its four stable isotopes (^{182}W, ^{183}W, ^{184}W and ^{186}W). In the evaluation ^{180}W was ignored because of its very low abundance (0.13 %). The data evaluation includes the photon production data i.e. photon production cross sections, secondary gamma-ray spectra and gamma-ray multiplicities as well as the reaction data significant below 20 MeV. The evaluation for the W element were made so as to give the data consistent with the ones for the W stable isotopes. The neutron cross sections for low energy below 15 keV were reproduced from a set of the resonance parameters evaluated in the present work, using a multi-level Breit-Wigner formula. The data for fast neutrons were estimated mainly with theoretical calculations. The GNASH code was used to calculate the threshold reaction cross sections and photon-production data including precompound effect. A joined code of CASTHY and ECIS was used to estimate the inelastic scattering data including the contribution from direct process. The data evaluation has almost finished and the file making for JENDL-3 is now in progress. As an example of the evaluated data, Fig. 1 shows the (n,2n) cross sections of the W element which were composed from the evaluated ones for each W stable isotopes, in comparing with the experimental ones.

---

* Kawasaki Heavy Industries Inc.

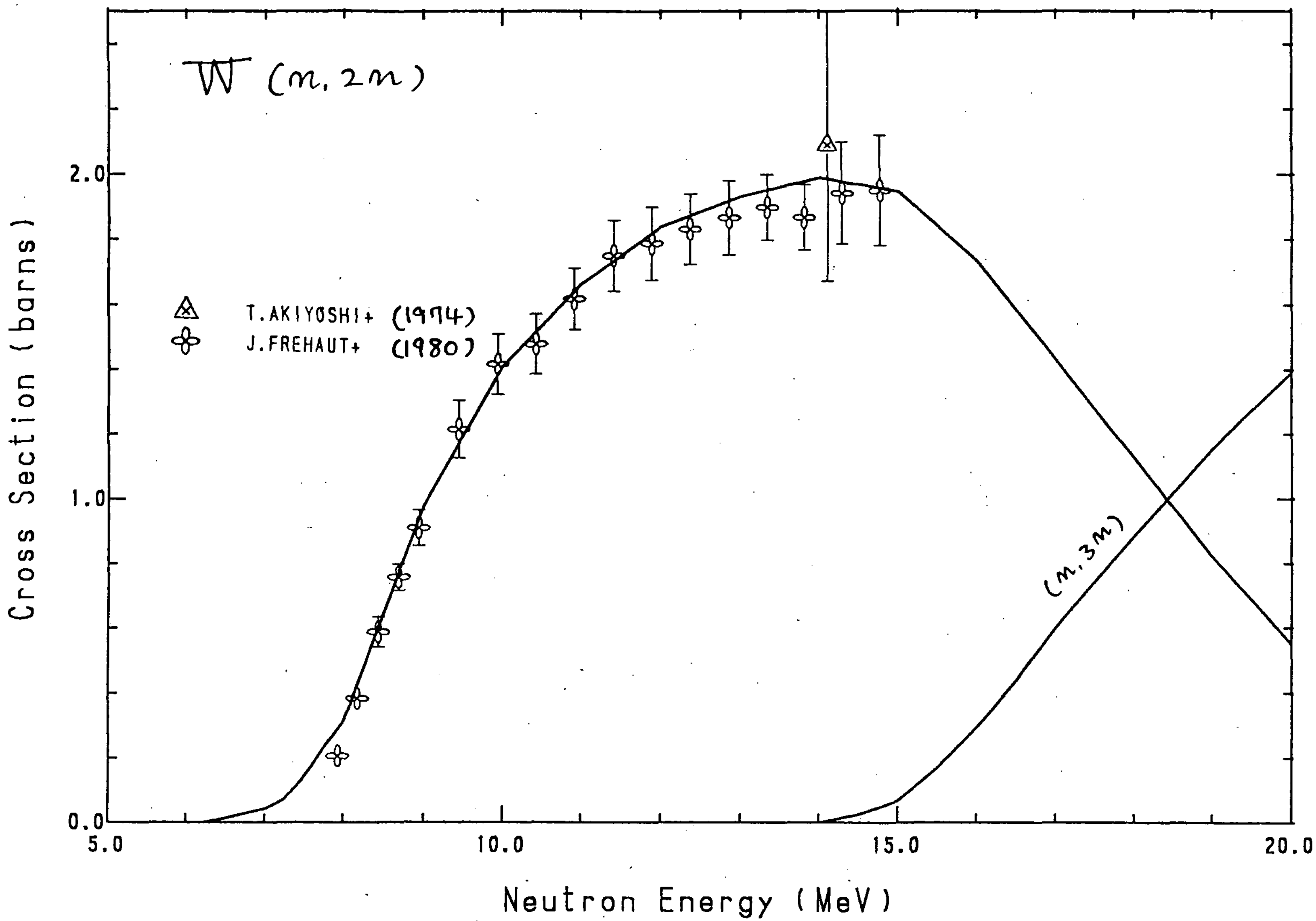

Fig. 1 Evaluated Cross Sections of the (n,2n) and (n,3n) Reactions for the W element.

II-B-4 Evaluation of Transplutonium Nuclear Data

Tsuneo Nakagawa, Yasuyuki Kikuchi and Sin-iti Igarasi

A paper on this subject was presented at the International Conference on Nuclear Data for Science and Technology, May 30 - June 3, 1988, Mito with the following abstract:

Evaluation of nuclear data for transplutonium nuclides has been performed in the energy range from 0.01 meV to 20 MeV. The quantities evaluated are cross sections of total, elastic and inelastic scattering, fission, (n,2n), (n,3n) and (n,4n) reactions. The angular distributions and energy distributions of emitted neutrons and the number of neutrons per fission were also given for each nuclide. In a low energy range, resolved and unresolved resonance parameters were given to reproduce the cross sections. In a high energy region, theoretical calculations with optical, statistical and evaporation models were used except for the fission cross section which was determined from the experimental data or systematic trend. So far, evaluated data have been given for 20 nuclides; Am-241, 242, 242m, 243, 244, 244m, Cm-242, 243, 244, 245, 246, 247, 248, 249, Bk-249, 250 and Cf-249, 250, 251, 252. The evaluated results were compiled in the ENDF-5 format and will be stored in JENDL-3.

II-B-5

Evaluation of Neutron Nuclear Data for ^{252}Cf and ^{250}Bk

Tsuneo Nakagawa

A paper on this subject was published as JAERI-M 88-004 (1988) with an abstract as follows:

Neutron nuclear data of ^{252}Cf and ^{250}Bk have been evaluated in the neutron energy range from 10^{-5} eV to 20 MeV. The cross sections evaluated are the total, elastic and inelastic scattering, (n,2n), (n,3n), (n,4n) reaction, fission and capture cross sections. For the both nuclides, cross sections below 30 keV were represented with resolved and unresolved resonance parameters. For ^{252}Cf, the resolved resonance parameters were evaluated in the energy range from 10^{-5} eV to 1 keV and the unresolved resonance parameters above 1 keV. For ^{250}Bk, no resonance parameters have been reported. Therefore, hypothetical resolved resonance parameters were given below 100 eV. In addition, angular and energy distributions of emitted neutrons and average number of emitted neutrons per fission were also evaluated. Existing experimental data are only those for the fission cross section of ^{252}Cf, thermal cross sections and resonance integrals of ^{252}Cf and the fission cross section of ^{250}Bk at the thermal neutron energy. The present evaluation, therefore, was mainly based on the systematics of the data from neighboring nuclides and optical- and statistical-model calculations.

II-B-6 **Analysis of (n,α) Reaction by Use of Modified TNG Code**

Keiichi SHIBATA and Kichinosuke HARADA*

A paper on this subject was submitted to Int. Conf. Nuclear Data for Science and Technology, May 30 - June 3, 1988, Mito, Japan with the following abstract:

The nuclear-model code TNG is modified to treat alpha-particle emission more physically. Information of the intrinsic wave function of alpha-particle is contained in the formation factor proposed by Iwamoto and Harada. The spectra of alpha-particle emitted from structural materials are calculated and compared with experimental data in order to verify the present modification. Furthermore, activation cross sections for the (n,α) reactions are calculated by using the modified code.

* Nuclear Energy Data Center, Tokai-mura, Ibaraki-ken, Japan

II-B-7 Evaluation and Verifications of Dosimetry Cross-section in JENDL-3T

Y. Ikeda, K. Sakurai, T. Nakagawa, S.Iijima,[*]
K. Kobayashi,[**] S. Iwasaki[***] and M. Nakazawa[****]

We have a plan to develop the special purpose file for dosimetry applications from JENDL-3, and both works on evaluations and verifications of dosimetry cross-sections are in progress in the dosimetry sub-working group.

For the evaluation works, recentry Sakurai has completed the two reactions of $^{93}Nb(n,n')^{93m}Nb$ and $^{199}Hg(n,n')^{199m}Hg$. Integral check of his evaluated reactions has been summarized in Table 1.

For the verification works, 35 dosimetry reactions from JENDL-3T have been systematically tested using the integral benchmark data of Cf-252 and U-235 fission spectra, CFRMF, YAYOI, JAERI-FNS-14MeV neutron fields. According to the result of this integral test, re-check of some cross-sections has been requested for cross-section evaluation group. And covariance data are now expected for more quantitative comparison with experimental data, and also for the neutron spectrum unfolding / adjustment applications.

(*)NAIG, (**)Kyoto Univ. Research Reactor Inst.,
(***)Tohoku Univ., (****)Univ. of Tokyo

Table 1. C/E ratio of $^{93}Nb(n,n')$ and $^{199}Hg(n,n')$ reaction rates in U-235 fission spectrum

$^{93}Nb(n,n')^{93m}Nb$		$^{199}Hg(n,n')^{199m}Hg$	
IRDF-82	1.07	Grigorev	0.81
Lippincott	0.90	present	0.84
present	0.96		

C. Fast Reactor Physics Laboratory

Department of Reactor Engineering

II-C-1 EVALUATION AND ADJUSTMENT OF ACTINIDE CROSS SECTIONS USING INTEGRAL DATA MEASURED AT FCA

S.Okajima, T.Mukaiyama, J.D.Kim*, M.Obu and T.Nemoto

Actinide intergral measurements were carried out in FCA IX series assemblies to evaluate and adjust the fission and capture cross sections of higher actinides[1,2]. The assemblies built for this purpose cover the systematic change of neutron spectrum shape[3]. The experimental program and result were given in references (1) and (2) respectively.

Here, 20 group fission and capture cross sections of actinide nuclides processed from JENDL-2 library were evaluated and adjusted using integral data. It was shown that the adjusted data could be generally used in fast spectrum.

Neutron field calculation of IX series assemblies was carried out with JENDL-2 library. The collision probability code, SP-2000, was used to calculate a fine group (1970 groups) fundamental-mode spectrum. The 20 group cell averaged, self shielded cross sections were generated using the fine group spectrum. Real and adjoint fluxes were obtained from the two dimensional transport calculation using the R-Z model of each assembly.

---

*On leave from Korea Advanced Energy Research Institute

The higher actinides fission and capture cross sections of JENDL-2 library were collapsed into 20 groups. In this collapsion, a fine group fundamental-mode spectrum of the assembly IX-4 was used as a weighting function. Higher actinide cross sections were evaluated by comparing calculated and measured values. In the calculation of these integral values, the real and adjoint fluxes and the 20 group cross sections mentioned above were used.

The sensitivity coefficients for the integral data were calculated with the generalized perturbation theory. The group cross sections were adjusted by the least squares fitting method[4].

Evaluation for actinide cross sections

Figure 1 shows the comparison of values between JENDL-2 calculations (C) and experiments (E) as C/E values.

The calculated and experimental fission rate ratios of Np-237 and Pu-238 agree within experimental errors ($\pm$2%). For those of other nuclides, the calculation gives 6 to 15% larger values than the experiments.

For sample reactivity worth ratios, the harder a neutron spectrum becomes, the larger the descrepancy of C/E from 1.

Adjustment for actinide cross sections

The comparison between measured (E) and calculated values (C) using the adjusted cross sections is shown in Fig.2. The adjustment effect is clearly shown by comparing Fig.1 and Fig.2.

For the fission rate ratios, the calculation with the adjusted actinide cross sections agrees with the experimental values within experimental errors except for in the assembly IX-6. The C/E values of the sample reactivity worth ratios are 0.9 to 1.1.

We can conclude, therefore, that the adjustment of higher actinides was successfully done.

Application of the adjusted actinide cross sections

The reliability of the adjusted cross sections was tested for the actinide integral data measured in FCA assemblies X-1 and XI-1. Neutron spectrum of the assembly XI-1 was softer than those of FCA IX assemblies.

The adjusted cross sections give a better agreement between calculated and experimental values than the original ones.

In the above mentioned cross section adjustment, these integral data measured in the assemblies X-1 and XI-1 were not used. Even though, the calculation using the adjusted cross sections gives a better agreement with the experimental values. Therefore, it is concluded that the adjusted data can be used generally in fast spectrum.

The adjusted data used are preliminary ones because, in the adjustment procedure, we didn't consider the effects caused by the experimental errors of U-235 fission rate and of Pu-239 reactivity worth and the heterogeneity effects associated with the measurement of the sample reactivity worth.

References

1. T.Mukaiyama, et al., in Proc. Int. Conf. Nuclear Cross Sections for Technology (Knoxville, 1979), NBS SP 594 (1980), p.552
2. T.Mukaiyama, et al., in Proc. Int. Conf. Nuclear Data for Basic and Applied Science (Santa Fe, 1985), Gordon and Breach Science Publishers (1985), p.483
3. M.Nakano, et al., in JAERI-M 82-114 (1982), p.53
4. H.Mitani and H.Kuroi, J.Nucl. Sci. Technol. 9 383 (1972)

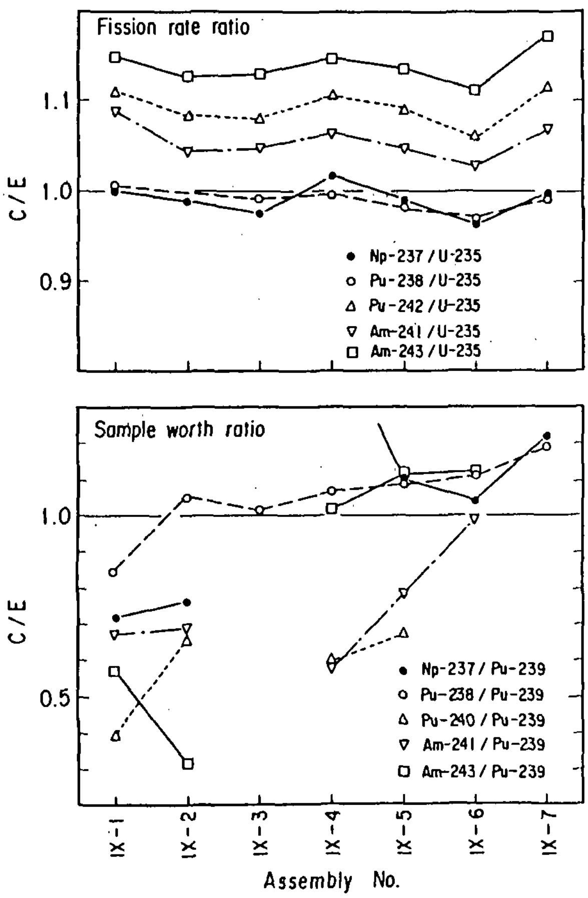

Fig. 1 Comparison of values between calculated (C) and measured (E) of actinide integral data (For the calculation, JENDL-2 was used)

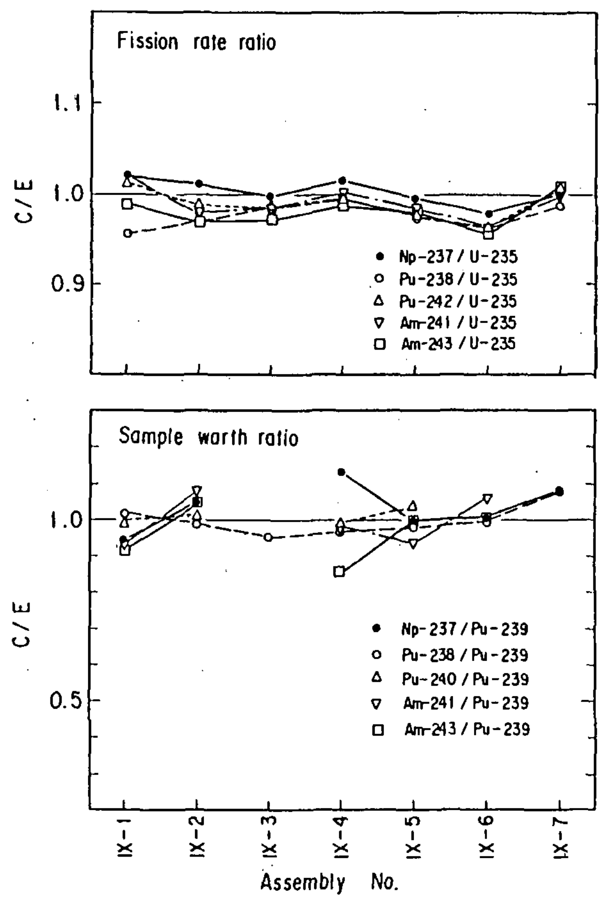

Fig. 2 Comparison of values between calculated (C) and measured (E) of actinide integral data (For the calculation, adjusted JENDL-2 was used)

III. Kyoto University

A. Research Reactor Institute

III-A-1

THE MEASUREMENT OF LEAKAGE NEUTRON SPECTRA FROM VARIOUS SPHERE PILES WITH 14MeV NEUTRONS

C. Ichihara, S. A. Hayashi, K. Kobayashi, I. Kimura*, J. Yamamoto**, M. Izumi** and A. Takahashi**

In order to check the existing nuclear data files such as ENDF/B-IV, JENDL-3 etc., neutron leakage spectra from various kinds of sphere piles have been measured using an intense pulsed neutron source at OKTAVIAN[1] and time-of-flight technique. Measured Samples include LiF, TEFLON($(CF_2)n$), Si, Cr, Mn, Co, Cu, Nb, Mo and W. The thickness of the piles were 0.5 to 4.7 mean free paths for 14MeV neutrons. The obtained data were compared with the theoretical calculations using several kinds of transport codes, ANISN[2], NITRAN[3] or MCNP[4] and the evaluated nuclear data files, ENDF/B-IV, JENDL-3T etc.. In Table 1, given are the sample dimensions, and the nuclear data and calculation codes used for the theoretical prediction.

The measured and calculated spectra for the piles are given in Fig. 1-(a) through 1-(j). In general, JENDL-3T data gave preferable calculated spectrum to the other data did, while they contain several fundamental problems resulting quite large differences of the spectra except for the Si pile. For Cu and Si piles, the calculated spectrum using JENDL-3T data gave almost satisfactory prediction. However, for Cr and Mn, the calculated spectra gave several mispredictions probably due to the error of (n,2n) and/or inelastic continuum scattering cross sections.

* Dept. Nucl. Eng., Kyoto University
** Dept. Nucl. Eng., Osaka University

REFERENCES

1. SUMITA, K., et al.: Proc.12-th Fusion Tech., 1, 687(1982)
2. ENGLE, W. W. Jr.: K-1693, (1967).
3. TAKAHASHI, A.,RUSCH D.: KfK-2822/1, (1979).
4. J. F.BRIESMEISTER ed.: MCNP-A General Monte Carlo Code for Neutron and Photon Transport, LA-7396-M, Rev.2, (1986)

Table-1 Characteristic parameters of the piles, calculation codes and nuclear data files used

Pile	Dia. (cm)	Sample (cm)	Thickness (MFPs)	Calc Code	Cross-section Libraries
LiF	61.0	27.5	3.5	MCNP	BMCCS1 ^{6}Li:LASL(101) ^{7}Li:ENDF/B-IV(1272) F:ENDF/B-IV(1277)
TEFLON	40.4	10.0	0.7	MCNP	BMCCS1 C:LASL(102) F:ENDF/B-IV(1277)
Si	61.0	20.0	0.4	ANISN	FSX125/J3T-1 and GICXFNS
Cr	40.4	10.0	0.7	ANISN	FSX125/J3T-1 and GICXFNS
Mn	61.0	27.5	3.4	ANISN	FSX125/J3T-1 and GICXFNS
Co	40.4	10.0	0.5	NITRAN	DDX Library from ENDF/B-IV
Cu	61.0	27.5	4.7	ANISN	FSX125/J3T-1 and GICXFNS
Nb	28.6	11.2	1.1	MCNP	BMCCS1 ENDF/B-IV(1191)
Mo	61.0	27.5	1.5	MCNP	BMCCS1 ENDL-73(533)
W	40.4	10.0	0.8	MCNP	BMCCS1 ENDL-73(540)

FSX125/J3T-1: 125-group library processed from JENDL-3T with PROF.GRAUCH/G-B
GICXFNS: 135-group library processed from ENDF/B-IV with NJOY

Fig. 1 Experimental and calculated spectra

(a) Lithium Fluoride
60 cm Sphere

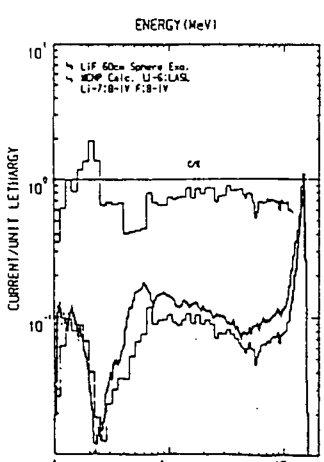

(b) TEFLON:$(CF_2)_n$
40 cm Sphere

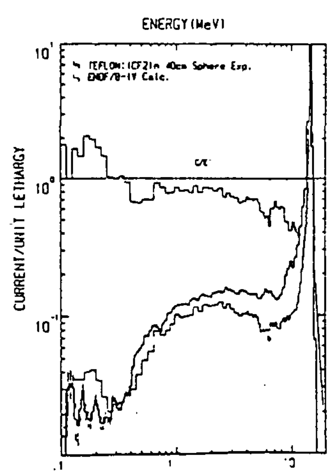

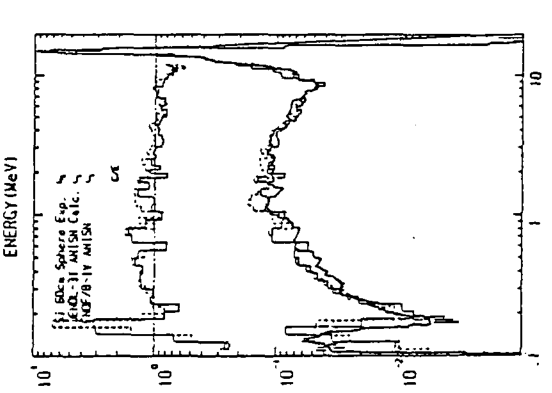

(c) Silicon 60 cm Sphere

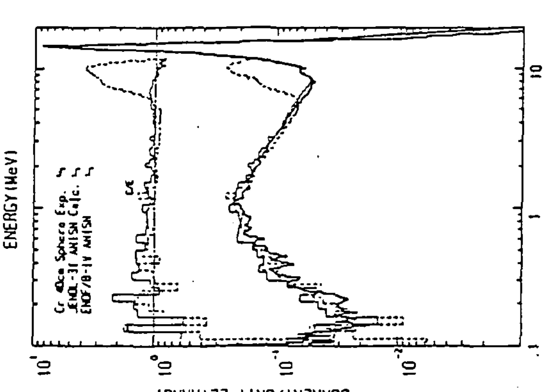

(d) Chromium 40 cm Sphere

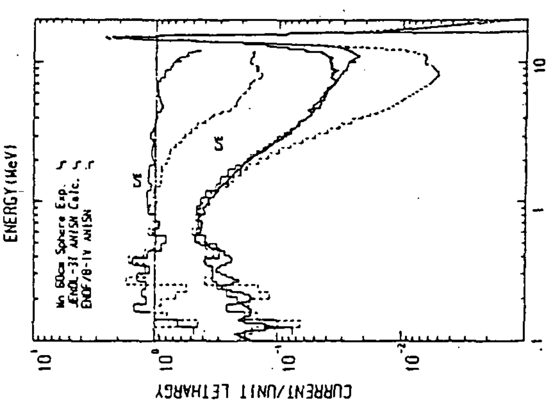

(e) Manganese 60 cm SPhere

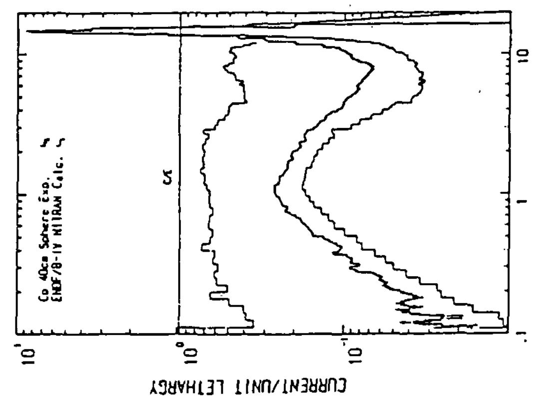

(f) Cobalt 40 cm Sphere

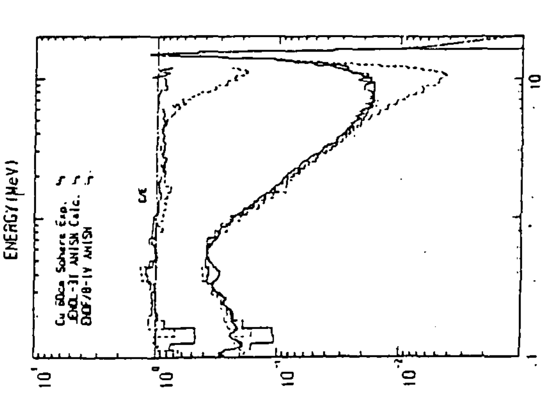

(g) Copper 60 cm Sphere

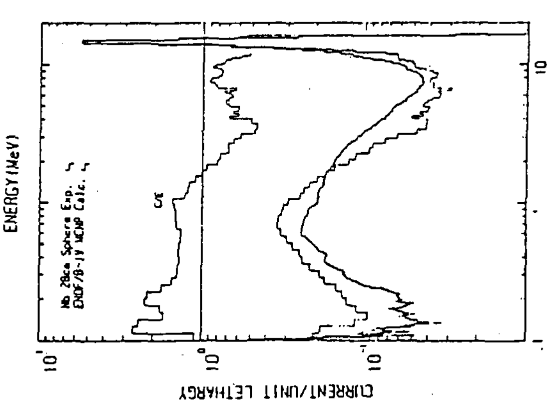

(h) Niobium 28 cm Sphere

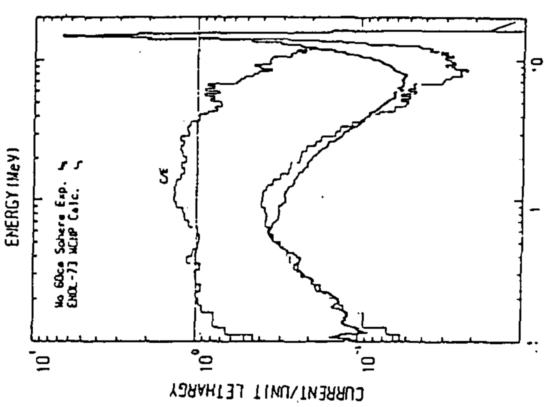

(i) Molybdenum 60 cm Sphere

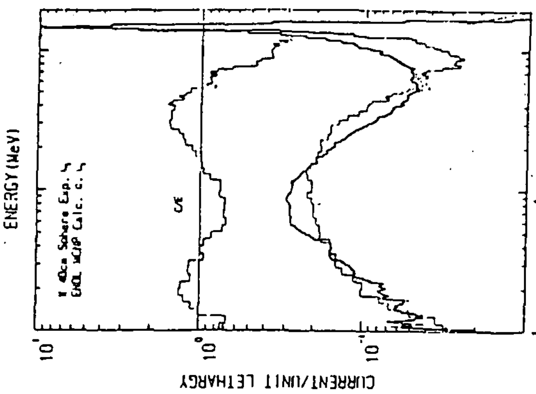

(J) Tungsten 40 cm Sphere

III-A-2 MEASUREMENT AND ANALYSIS OF NEUTRON SPECTRA IN STRUCTURAL MATERIALS USING AN ELECTRON-LINAC

S. A. Hayashi, I. Kimura#, K. Kobayashi, S. Yamamoto
T. Mori* and M. Nakagawa*

With a view to reassessing the currently available evaluated neutron cross sections for main structural materials of reactors and silicon, electron linac time-of-flight experiments were conducted to measure the energy spectra of neutrons in sample piles of the respective elements, in the energy region covering 10^0 - 10^3 keV. The measured neutron spectra were compared with the theoretical one obtained with one-dimensional transport calculation using the cross section data from either JENDL-2 or ENDF/B-IV. The spectra obtained for Fe, Ni, Cr, Mn and Si piles are shown in Figs. 1, 2, 3, 4 and 5, respectively[1]. The resulting findings are as follows:(1) Both files call for revising the resonance parameters of Fe and Ni in the energy region below 100 keV. (2) For Fe, ENDF/B-IV requires supplementation of additional data on inelastic scattering in the region below 840 keV. (3) For Cr, both files need reevaluation of the total cross section, notably in the energy region of 4 - 8 keV where it is characterized by a series of large resonances[2]. (4) For Mn, JENDL-2 requires supplementation the resonance parameters in the region above 100 keV[3]. (5) For Si, experimental neutron spectrum is higher than calculated one in the region of 200 - 500 keV[4].

* Japan Atomic Energy Research Institute
# Present affiliation :Dept. Nucl. Eng., Kyoto University

--References--

1) S.A. Hayashi et al., Inter. conf. on Nuclear Data for Sci. Technol., Mito, Japan (1988).

2) S. A. Hayashi et al., J. Nucl. Sci. Technol., **24**[9], 702 (1987).

3) S. Selvi, S. A. Hayashi et al., Atomkernenergie-kerntechnik, **45**[3], 183 (1983).

4) S. A. Hayashi et al., submitted to Ann. Rep. Res. Reactor Inst. Kyoto Univ., **21** (1988).

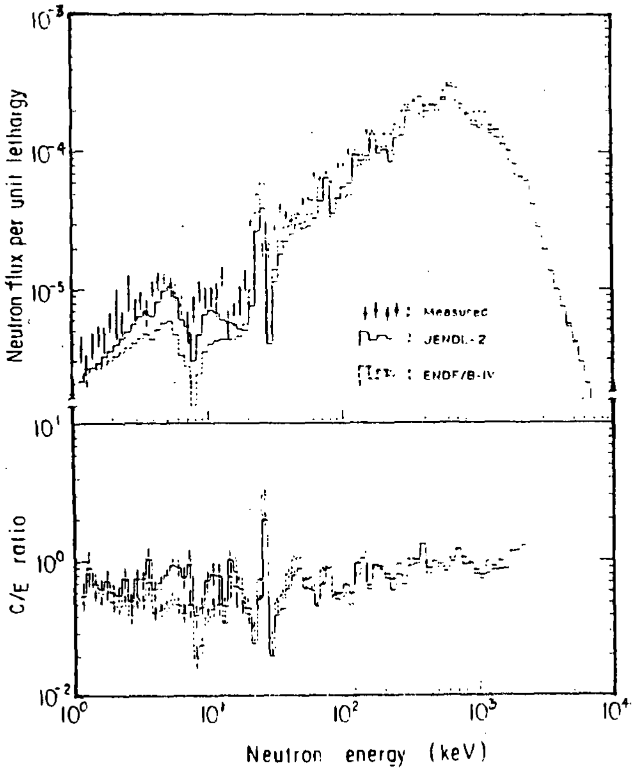

Fig.1 Angular neutron spectrum in direction of $\theta = 90°$ at 15 cm from target (upper diagram), and ratio of calculated to experimental values (lower diagram) —for case of Fe pile.

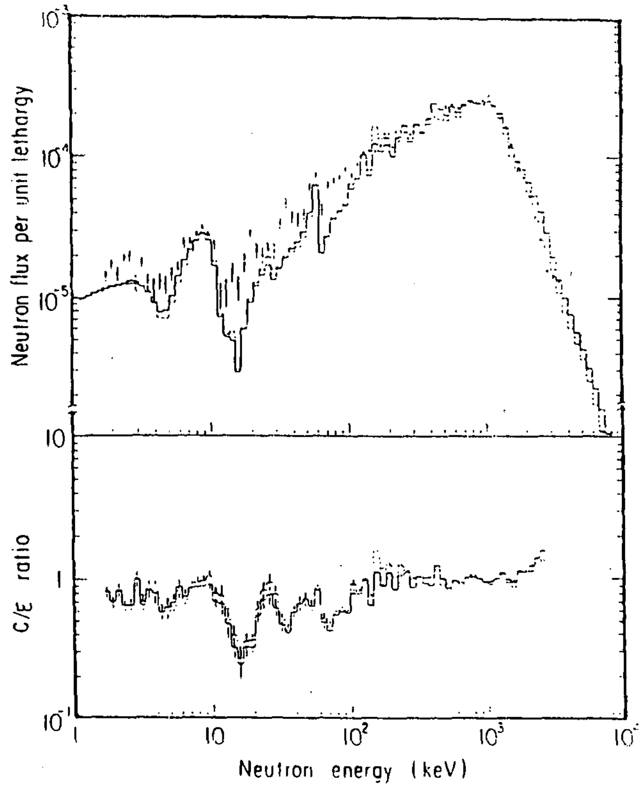

Fig.2 Angular neutron spectrum in direction of $\theta = 90°$ at 15 cm from target (upper diagram), and ratio of calculated to experimental values (lower diagram)—for case of Ni pile. All symbols same as in Fig. 1

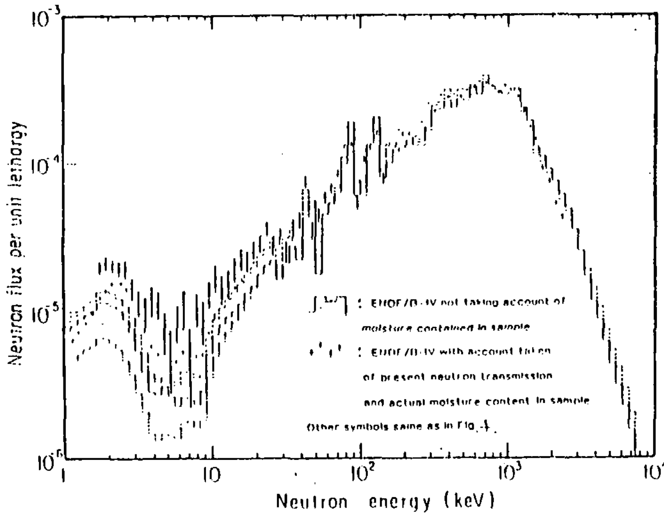

Fig. 3 Angular neutron spectrum in direction of $\theta = 90°$ at 15 cm from target--for case of Cr pile.

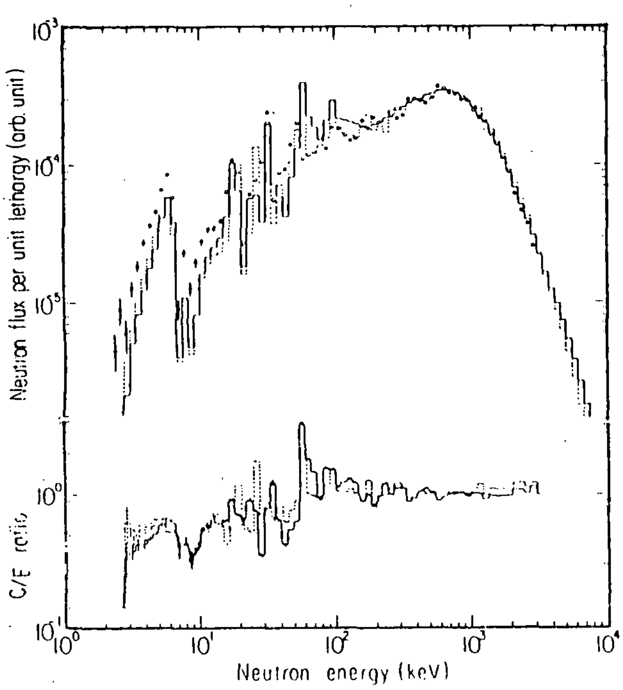

Fig. 4 Angular neutron spectrum in direction of $\theta = 90°$ at 15 cm from target (upper diagram), and ratio of calculated to experimental values (lower diagram)--for case of Mn pile. All symbols same as in Fig. 1.

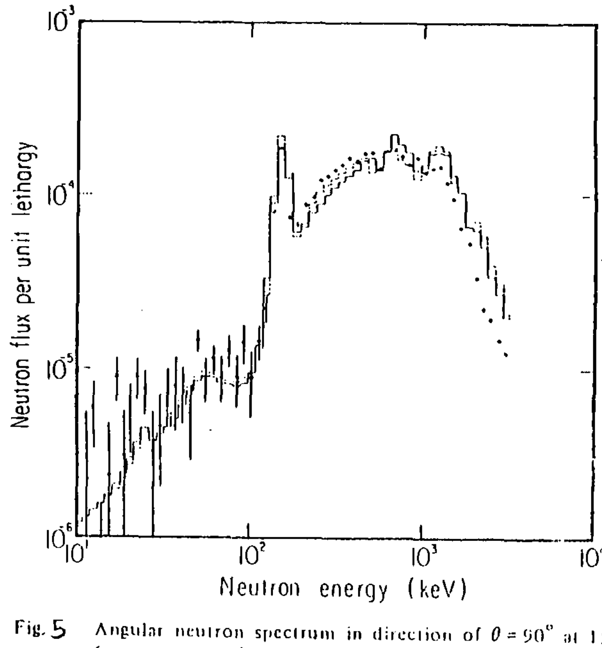

Fig. 5 Angular neutron spectrum in direction of $\theta = 90°$ at 15 cm from target --for case of Si pile. All symbols same as in Fig. 1

III-A-3

Application of a ^{6}LiD Thermal-14 MeV Neutron Converter to the Measurement of Activation Cross Sections

Katsuhei Kobayashi and Itsuro Kimura

A paper on this subject was submitted to the International Conference on Nuclear Data for Science and Technology, May 30 - June 3, 1988, held in Mito, Japan, with the following abstract:

By means of the following two reactions; ^{6}Li + n_{th} -- ^{4}He + T + 4.8 MeV and D + T -- ^{4}He + n, 14 MeV neutrons can be generated from thermal neutrons, whose flux conversion rate is estimated about 2 x 10^{-4}. A ^{6}Li converter, 10 x 10 cm square and 1 cm thick was prepared, and installed in a large thermal neutron irradiation facility of the Kyoto University Reactor, KUR, where the 14 MeV neutron flux of about 2.5 x 10^5 n/cm^2/sec was obtained.

The characteristics of the ^{6}LiD converters were measured: (1) energy of neutrons produced was determined to be 14.05 $\pm$ 0.07 MeV (Fig. 1) by the reaction rate ratio of ^{90}Zr(n,2n)/^{93}Nb(n,2n), and (2) the energy spectrum was obtained (Fig.2) by unfolding multi-foil activation data using the NEUPAC code.

Making use of the 14.1 MeV neutrons, twenty three kinds of activation cross sections were measured relative to that for the ^{27}Al(n, α)^{24}Na reaction as a standard value. The present results are summarized in Tables 1 and 2, and are compared with the evaluated data in ENDF/B-V and JENDL-2 and with the data in the IAEA Handbook and with the recent measurement by Ikeda et al.

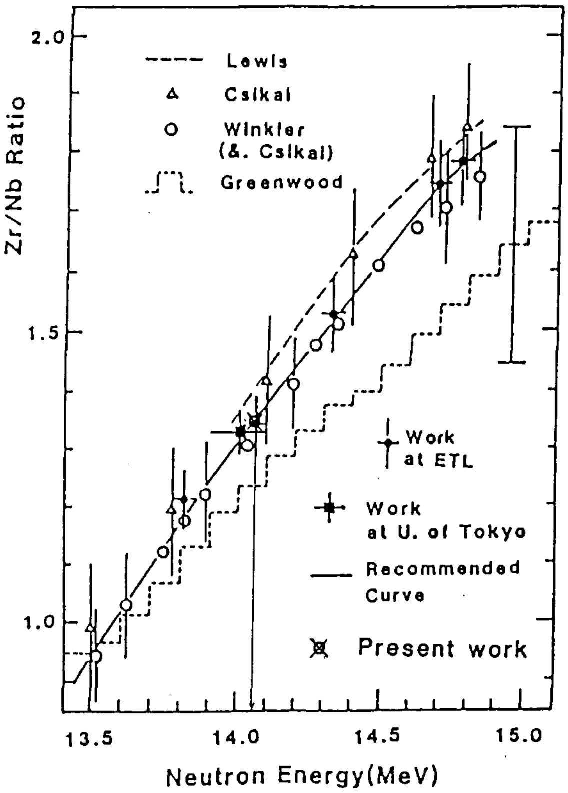

Fig. 1 Neutron energy dependencies of Zr/Nb activation rate ratio data.

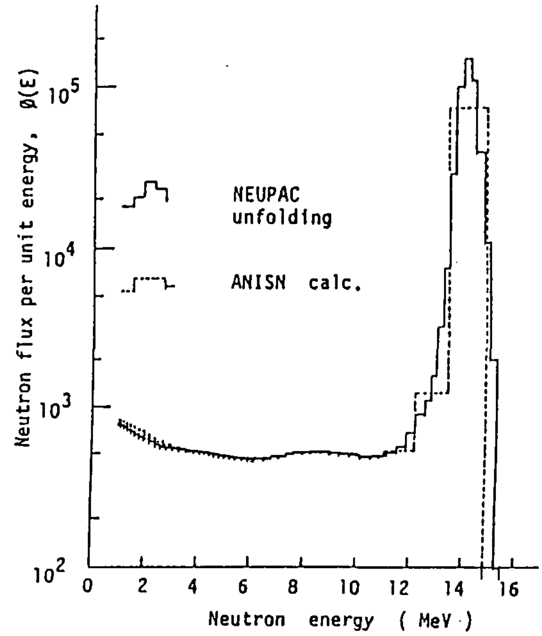

Fig. 2 Unfolded neutron spectrum from the ^{6}LiD converters.

Table 1 Comparison of the present measurements and the recent data (in mb).

Reaction	Present	ENDF/B-V[12)]	JENDL-2[11)]	IAEA Book[13)]	Ikeda[14)]*
$^{19}F(n,2n)^{18}F$	41.59 ± 1.70	- - -	42.94	55 ± 4	37.8 ± 2.0
$^{24}Mg(n,p)^{24}Na$	192.2 ± 6.6	- - -	- - -	181 ± 8	197.0 ± 9.8
$^{27}Al(n,\alpha)^{24}Na$	123.0 ± 3.8	123.0	120.9	119 - 121	123.6 ± 3.7
$^{27}Al(n,p)^{27}Mg$	77.07 ± 2.71	76.81	77.50	75 ± 4	70.6 ± 2.9
$^{46}Ti(n,p)^{46}Sc$	267.8 ± 9.3	257.7	- - -	242 ± 30	249 ± 13
$Ti(n,p)^{47}Sc$	289.6 ± 9.8	- - -	- - -	- - -	- - -
$^{48}Ti(n,p)^{48}Sc$	58.60 ± 1.88	63.50	- - -	66 ± 6	58.3 ± 2.8
$^{51}V(n,\alpha)^{48}Sc$	15.03 ± 0.65	- - -	15.00	16 ± 1.5	15.58 ± 0.81
$^{55}Mn(n,2n)^{54}Mn$	775.4 ± 28.6	722.3	770.9	809 - 890	752 ± 42
$^{54}Fe(n,p)^{54}Mn$	405.1 ± 15.3	359.6	359.9	332 - 365	343 ± 16
$^{56}Fe(n,p)^{56}Mn$	112.3 ± 3.9	108.8	113.9	98 ± 7	113.3 ± 5.8
$^{58}Ni(n,2n)^{57}Ni$	25.33 ± 0.83	25.35	21.50	30 ± 3	25.2 ± 1.3
$^{58}Ni(n,p)^{58}Co$	397.9 ± 13.3	415.3	400.0	375 - 378	356 ± 18
$^{59}Co(n,\alpha)^{56}Mn$	29.72 ± 1.04	28.95	30.00	29 ± 2	32.5 ± 1.6
$^{59}Co(n,2n)^{58}Co$	729.0 ± 29.0	749.0	639.9	720 - 788	705 ± 34
$^{64}Zn(n,p)^{64}Cu$	172.8 ± 12.7	- - -	- - -	160 - 164	- - -
$^{90}Zr(n,2n)^{89}Zr$	624.5 ± 20.5	- - -	- - -	764 - 768	613 ± 29
$^{90}Zr(n,2n)^{89m}Zr$	82.59 ± 5.01	- - -	- - -	86 ± 8	70.5 ± 4.1
$^{92}Mo(n,p)^{92m}Nb$	73.67 ± 4.14	- - -	61.40	60 - 64	72.6 ± 3.5
$^{93}Nb(n,2n)^{92m}Nb$	464.3 ± 15.1	- - -	1250	482 ± 35	469 ± 19
$^{115}In(n,n')^{115m}In$	65.03 ± 2.47	66.23	- - -	63 ± 6	- - -
$^{197}Au(n,2n)^{196}Au$	2125 ± 79	- - -	- - -	2160 ± 35	2004 ± 106
$^{204}Pb(n,2n)^{203}Pb$	1910 ± 63	- - -	2023	2103 ± 200	2155 ± 125
$^{204}Pb(n,n')^{204m}Pb$	63.81 ± 3.30	- - -	- - -	- - -	- - -

* Calculation by the interpolation between the measured data

Table 2 Summary of the present results.

ROW/CL		OUTPUT	%	ABS ERR
1	AL27NA	1.230D+02	3.07	3.774D+00
2	AL27NP	7.707D+01	3.52	2.711D+00
3	NI58NP	3.979D+02	3.33	1.313D+01
4	NI8N2N	2.533D+01	3.27	8.286D-01
5	ZRON2N	6.245D+02	3.28	2.048D+01
6	NB3N2N	4.643D+02	3.25	1.508D+01
7	CO59NA	2.972D+01	3.50	1.040D+00
8	TI46NP	2.678D+02	3.47	9.293D+00
9	TINX7N	2.896D+02	3.37	9.760D+00
10	TI48NP	5.860D+01	3.21	1.883D+00
11	MN5N2N	7.754D+02	3.69	2.860D+01
12	ZRMN2N	8.259D+01	6.07	5.011D+00
13	F19N2N	4.159D+01	4.08	1.697D+00
14	FE54NP	4.051D+02	3.78	1.529D+01
15	FE56NP	1.123D+02	3.49	3.915D+00
16	CO9N2N	7.290D+02	3.98	2.901D+01
17	IN15NN	6.503D+01	3.80	2.471D+00
18	MG24NP	1.922D+02	3.46	6.641D+00
19	PBO4NN	6.381D+01	5.17	3.299D+00
20	PB4N2N	1.910D+03	3.31	6.322D+01
21	V51NA	1.503D+01	4.31	6.470D-01
22	ZN64NP	1.728D+02	7.37	1.274D+01
23	MO92NP	7.367D+01	5.48	4.139D+00
24	AU7N2N	2.125D+03	3.70	7.863D+01

CORRELATION MATRIX (PRINTED VALUE HAS BEEN MULTIPLIED BY 100.)

ROW/COL	1	2	3	4	5	6	7	8	9	10	11	12	13	14	15	16	17	18	19	20	21	22	23	24
1	100																							
2	87	100																						
3	93	83	100																					
4	93	82	90	100																				
5	94	84	92	91	100																			
6	96	85	93	91	93	100																		
7	87	80	82	81	84	84	100																	
8	87	77	82	82	84	85	79	100																
9	90	80	85	84	86	88	82	85	100															
10	92	82	87	86	89	90	83	86	85	100														
11	84	75	79	78	80	81	76	77	79	81	100													
12	51	46	48	48	49	50	47	46	49	48	44	100												
13	75	70	70	70	72	72	70	66	69	70	65	39	100											
14	80	73	75	75	76	77	73	71	73	75	73	41	65	100										
15	86	79	81	80	82	83	80	76	79	81	77	45	72	78	100									
16	77	71	72	71	73	74	72	68	70	72	66	40	66	66	74	100								
17	81	75	76	75	77	78	76	72	74	76	70	42	73	71	78	71	100							
18	90	79	85	84	86	88	79	82	83	87	77	47	68	73	78	69	73	100						
19	60	53	56	56	58	59	53	55	56	58	51	32	45	48	52	46	49	57	100					
20	90	79	84	84	86	87	80	83	90	84	77	48	68	73	78	69	73	85	56	100				
21	71	63	68	67	69	72	63	63	65	67	60	37	54	58	62	55	60	65	43	65	100			
22	41	36	38	38	39	39	37	36	37	38	37	21	32	38	39	33	34	37	25	37	29	100		
23	56	50	53	53	54	56	50	50	51	53	48	29	43	46	49	44	47	51	34	51	48	23	100	
24	83	74	79	78	80	84	74	74	76	78	72	43	64	69	74	65	71	76	51	75	70	33	57	100

III-A-4

Integral Check on Nuclear Data of ^{232}Th with Neutron Spectra in a Thoria Pile and from a Thorium Slab

Katsuhei Kobayashi, Itsuro Kimura and Takamasa Mori*

A paper on this subject was published in Nucl. Sci. Eng., 99, 157 (1988), with the following abstract:

To make an integral check of the evaluated nuclear data for thorium in ENDF/B-IV, ENDF/B-V, and JENDL-2, the energy spectra of angular neutron fluxes calculated with these data bases were compared with those measured in a spherical thoria pile and from a metallic thorium slab by the Linac time-of-flight method in the 1 keV to 10 MeV energy range. The calculations were performed using the S_n code DTF-IV and the Monte Carlo code MCNP. General agreement can be seen between the measurement and the calculation with the above three data bases. In particular, the calculation with ENDF/B-V data shows best agreement with the measurement for the thoria pile at energies above about 4 MeV. However, the calculations using the ENDF/B-V and JENDL-2 data underpredicted the measurement by 30 to 40 % in the energy region from several hundred kilo-electron-volts to a few mega-electron-volts.

Sensitivity analysis for the neutron spectra in the above pile and from the slab was also carried out, and the results showed that both of the spectra were sensitive to the total and in elastic scattering cross sections. To determine the reason

* Japan Atomic Energy Research Instiute
Tokai-mura, Naka-gun, Ibaraki 319-11, Japan

for the discrepancy between the measured and calculated spectra, the partial cross section data in ENDF/B-V or JENDL-2 were substituted by those in ENDF/B-IV. The spectra calculated by replacing the inelastic scattering data for thorium in ENDF/B-V or JENDL-2 by those in ENDF/B-IV have shown good agreement with the ENDF/B-IV-based spectrum, which is rather close to the measurements found in all relevant energy regions.

III-A-5

Measurement of Cross Sections for Thermal Neutron Capture and the (n,2n) Reaction of ^{231}Pa

Tetsuo Hashimoto* and Katsuhei Kobayashi

A paper on this subject was published in J. Radioanal. Nucl. Chem., Articles, 120 185 (1988), with the following abstract:

The cross sections of both thermal neutron capture and the (n,2n) reactions for ^{231}Pa target have been determined by using gamma-ray and alpha-ray spectrometric methods following irradiation with neutrons possessing purely thermalized and fission-type reactor spectrum, respectively. Prior to the irradiation, a pre-chemical purification was applied to ensure the accurate determination of the target nuclide, ^{231}Pa. For the sake of alpha-spectrometric determination of the daughter ^{230}U, decayed out from parent ^{230}Pa, the chemical purification of uranium was also applied to the alpha-source preparation from the reactor-irradiated ^{231}Pa. The activity ratio of ^{230}U to ^{232}U was converted to an initial formation ratio of ^{230}Pa to ^{232}U and followed by an evaluation of cross section. The cross section value for the $^{231}Pa(n,\gamma)^{232}Pa$ reaction process was estimated to be 186 $\pm$ 13 barn for purely thermal neutrons. The $^{231}Pa(n,2n)^{230}Pa$ cross section value is 4.12 $\pm$ 0.32 mbarn for fission-type neutrons.

---

* Department of Chemistry, Faculty of Science, Niigata University, Ikarashi-Nino-cho, Niigata 950-21, Japan

III-A-6

Measurement of Resonance Parameters of ^{232}Th and their Integral Check through the Resonance Integral

Katsuhei Kobayashi, Yoshiaki Fujita and Itsuro Kimura

A paper on this subject will be published in Ann. Nucl. Energy, soon, with the following abstract:

By using the linac time-of-flight method, neutron transmission spectra through metallic Th samples were measured with a ^{6}Li glass scintillator placed at the 22 m station. Least-squares shape analysis using the SIOB code was employed to obtain the neutron and capture widths for the 21 s-wave resonances for ^{232}Th in the lower energy region. The results differed from old measurements and satisfactorily agreed with the recent measurements made by Olsen and Chrien.

In order to make an integral check of the resonance parameters, the resonance integral for the ^{232}Th(n,γ) reaction has been calculated by using the parameters measured above, and by using the evaluated parameters in JENDL-2, ENDF/B-IV and -V, and these calculated results have been compared with the measurement made in a standard 1/E spectrum field. The calculation has also been performed by exchanging the parameters in the evaluated data files for those presently measured. Resonance parameters in JENDL-2 have been found to be smaller than those measured, especially for the first two s-wave resonances.

III-A-7

Measurement of Self-Shielding Factors of Neutron Capture Cross Sections for ^{232}Th and ^{238}U in the Unresolved Resonance Region

Yoshiaki Fujita, Katsuhei Kobayashi, Shuji Yamamoto, Itsuro Kimura and Hiroyuki Oigawa*

A paper on this subject was presented in the Internatioal Confrene on Neutron Physics, Sept. 21 - 25, 1987, held in Kiev, USSR.

Self-shielding factors of neutron capture cross sections for Th-232 and U-238 have been measured in the resonance energy region from 1 to 35 keV, using the linac time-of-flight method at the Research Reactor Institute, Kyoto University. The self-shielding factor for an arbitrary dilution cross section has been obtained from a set of measured neutron transmission spectra and self-indication ratio measurements for several transmission samples of different thicknesses. The measured self-shielding factors have been compared with calculations performed using average resonance parameters from the evaluated nuclear data files JENDL-2 and ENDF/B-IV, as shown in Figs. 1 and 2. The calculated shielding factors for Th-232 are in good agreement with the measurements within an experimental error of about 5 %.

* Department of Nuclear Engineering, Kyoto University
Yoshida-honmachi, Sakyo-ku, Kyoto 606, Japan
Present address: Japan Atomic Energy Research Institute
Tokai-mura, Naka-gun, Ibaraki 319-11, Japan

For U-238, when the recent average parameters obtained by Olsen are employed, agreement between measurement and calculation is within 2 - 3 %. This value is better than those calculated using JENDL-2 and ENDF/B-IV data.

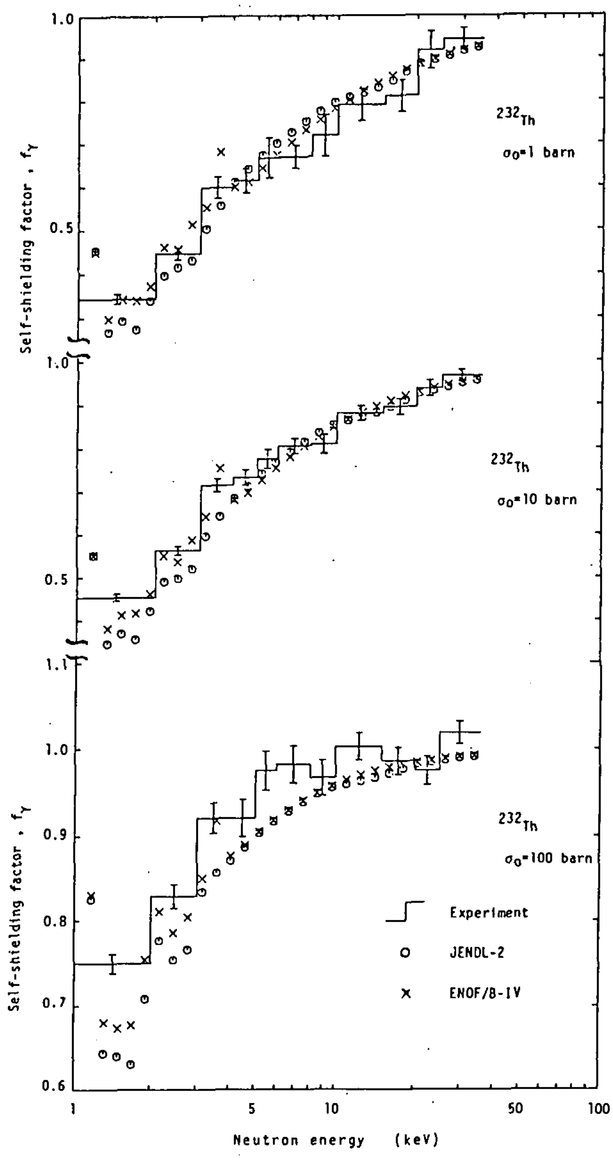

Fig. 1 Self-shielding factors of the neutron capture cross section of Th-232 for dilution cross sections, 1, 10, and 100 barn.

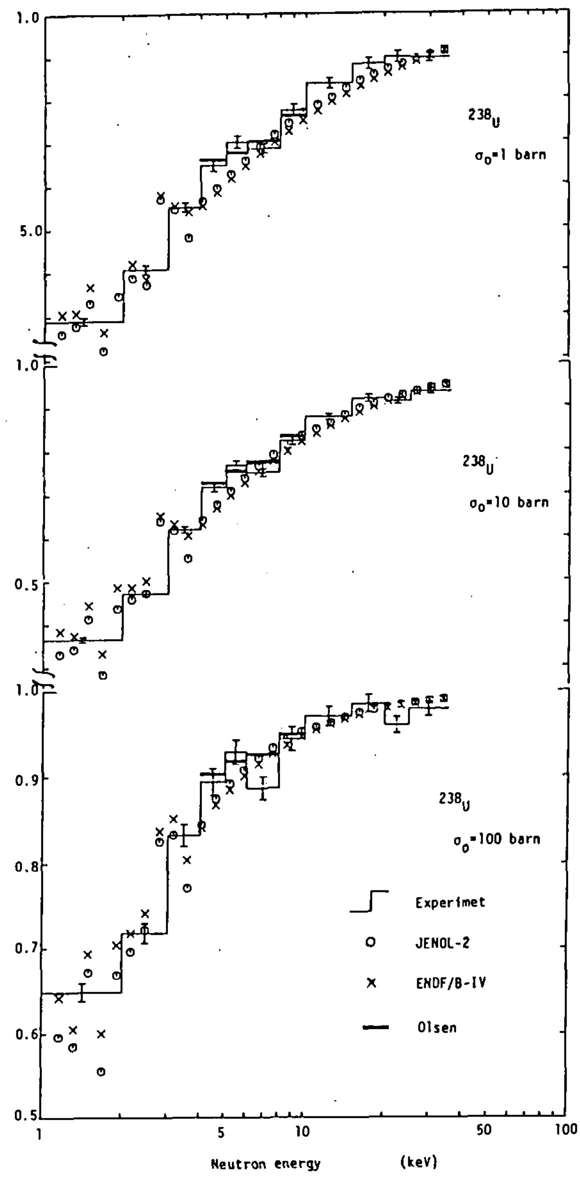

Fig. 2 Self-shielding factors of the neutron capture cross section of U-238 for dilution cross sections, 1, 10, and 100 barn.

III-A-8 Application of BGO for Neutron Capture Cross Section Measurements

Shuji Yamamoto, Katsuhei Kobayashi and Yoshiaki Fujita

A paper on this subject was submitted to the International Conference on Nuclear Data for Science and Technology, May 30 - June 3, 1988, held in Mito, Japan, with the following abstract:

A total absorption gamma-ray detector has been made using twelve BGO scintillator bricks of 5 x 5 x 7.5 cm^3, with an incentive to study the possibility of BGO for neutron capture cross section measurements of higher precision.

In this report, a study of the detection efficiency of the BGO for thermal neutron capture is presented. The efficiency has been measured at a neutron time-of-flight spectrometer at KURRI electron linear accelerator. Cd, In, Au and Fe were employed for capture samples as they have different types of capture gamma-rays. The efficiencies have been found between 80 to 100 %.

A study has been made on a technique to estimate the efficiency for a sample of unknown cross section and cascade gamma-ray spectrum using the information of the pulse height spectrum obtained with the BGO. At present, the estimation is only partly succeeded. For a sample of high multiplicity cascade gamma-rays, the BGO is satisfactorily used for capture cross section measurements. Further studies are needed before the BGO is used for samples of low gamma-ray multiplicity.

III-A-9

Application of a Resonance Capture Method to the Precise Measurement of Neutron Total Cross Sections

Katsuhei Kobayashi, Shuji Yamamoto and Yoshiaki Fujita

Filtered-beam neutrons are often applied to the precise measurement of neutron cross sections[1-4]. In the present experiment, we have paid attention to the signals from the resonance captures, which give many counts at the resonances. When we combine the capture measurement with a linac time-of-flight technique, the time spectrum shows similar resonant shape at the resonance as a filtered-beam neutron[1,2]. Moreover, for the background measurement, by putting the same material as the capture sample into the TOF beam, one can precisely determine the background level at the resonance capture peak. This experimental arrangement is that for the self-indication measurement[5].

The capture detection system consisted of eight pieces of BGD scintillators[6] was separated into two parts; front half of the detection system had four pieces of the BGO and the others were set behind, as seen in Fig. 1. Coincidence measurement was made for these two segments of the detectors to reduce the background counts and improve the signal-to-noise ratio. Figure 2 shows a typical example for the foreground and background measurements by the linac TOF method, when a metallic Ta plate of 2 mm thickness was used as a capture sample.

This resonance capture method has been applied to the precise measurement of neutron total cross sections of polyethylene and lead at neutron resonance energies of 4.28, 10.4, 14.0, 23.9, 35.9 and 39.1 eV for ^{181}Ta. The TOF method, the data aquisition and processing system are same as those in the previous measurement[7,8]. The present results are shown in Figs. 3 and 4, and Table 1. As seen in Fig. 3, the result of polyethylene is in very good agreement with that by the ENDF/B-IV data. However, for lead, there exists a large discrepancy between the present measurement and the evaluations in JENDL-2 and ENDF/B-IV. It is found that the total cross section of lead is almost constant in the relevant energy region.

References

1) R. C. Block, et al.: J. Nucl. Sci. Technol., 12, 1 (1975).
2) A. J. Mill and J. R. Harvey:RD/B/N4776 (1980).
3) Y. Fujita, et al.: J. Nucl. Sci. Technol., 20, 983 (1983).
4) O. Aizawa, et al.: J. Nucl. Sci. Technol., 20, 354 (1983).
5) R. C. Block, et al.: Nucl. Sci. Eng., 80, 263 (1982).
6) S. Yamamoto, et al.: Nucl. Instr. Meth., A249, 484 (1986).
7) K. Kobayashi, et al.: Ann. Nucl. Energy, 11, 315 (1984).
8) K. Kobayashi, et al.: Ann. Nucl. Energy, (1988) in print.

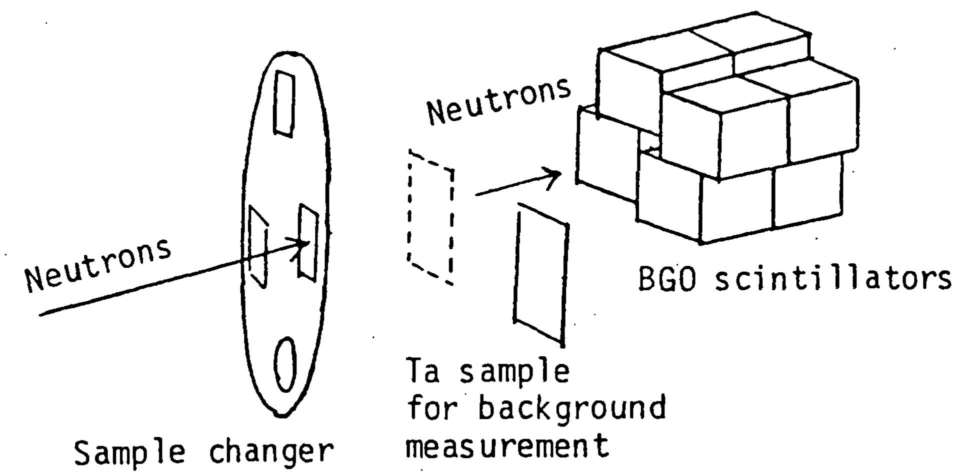

Fig. 1 The experimental arrangement.

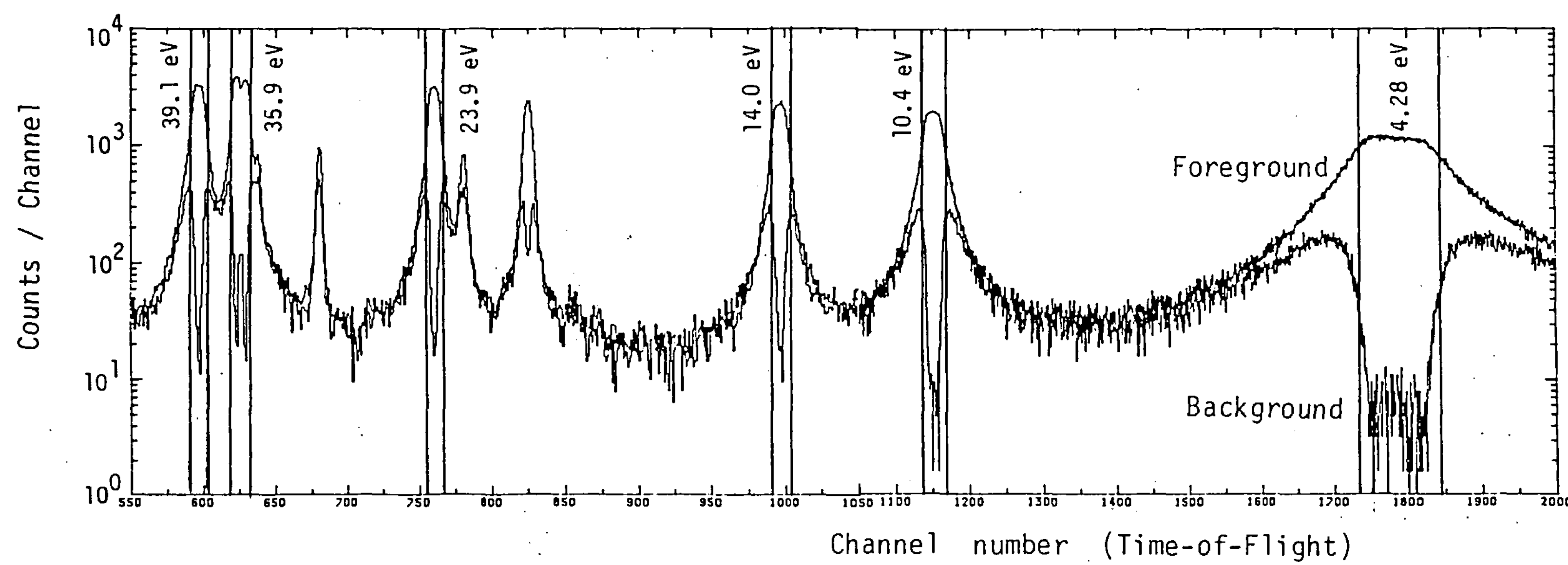

Fig. 2 A typical example for the foreground and background measurements using the resonance capture method.

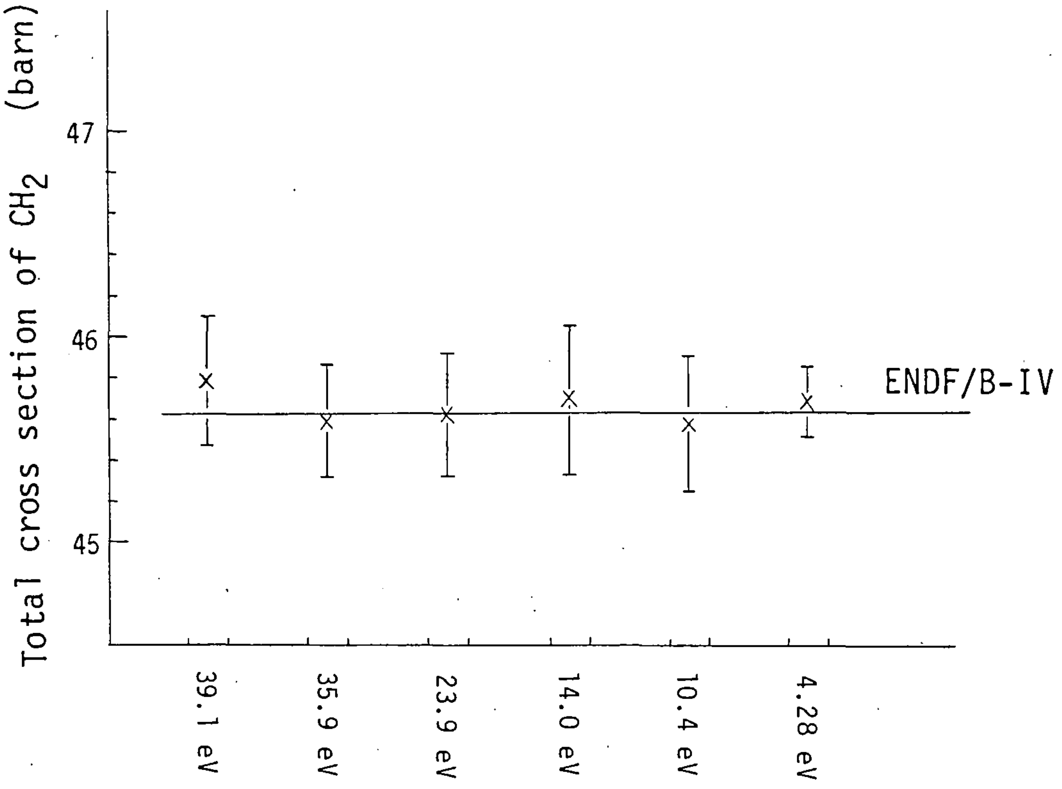

Fig. 3 Present results for the neutron total cross section of polyethylene.

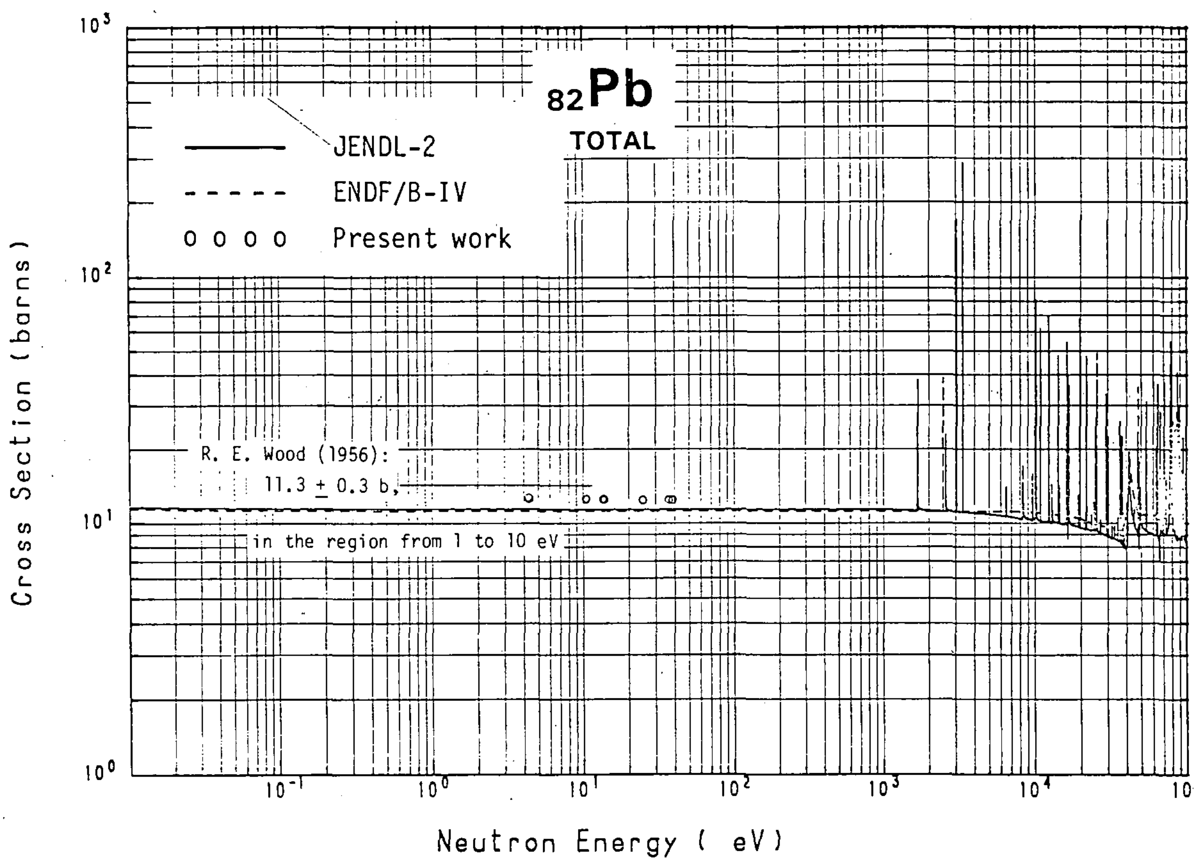

Fig. 4 Present results for the neutron total cross section of lead.

Table 1 Neutron total cross section of lead, measured with resonance captures from Ta-181.

Resonance energy (eV)	FWHM (eV)	Noise/Signal ratio [open beam]	Total cross section (barn)
4.28	0.30	0.0058	11.17 ± 0.025
10.4	0.34	0.0055	11.18 ± 0.036
14.0	0.26	0.0070	11.18 ± 0.051
23.9	0.54	0.0074	11.17 ± 0.040
35.9	1.17	0.0066	11.18 ± 0.037
39.1	1.11	0.0080	11.18 ± 0.045

III-A-10

Measurement of Resonance Integrals for Reactor Materials In the Standard 1/E Neutron Spectrum Field

Katsuhei Kobayashi, Itsuro Kimura, Shuji Yamamoto
Ryota Miki* and Tetsuo Itoh*

A paper on this subject was presented in the International Conference on Neutron Physics, Sept. 21 - 25, 1987, held in Kiev, USSR.

The neutron spectrum at the center of the internal graphite reflector between the two-divided cores of a low power research reactor, UTR-Kinki, was verified to be very close to a standard 1/E shape from about 1 eV to a few hundreds keV, by (1) calculation using a 2-D Sn transport code TWOTRAN, (2) unfolding multi-foil activation data by the NEUPAC code, and (3) measurement using the sandwich foil method. The results are shown in Figs. 1 and 2.

Making use of this standard 1/E neutron spectrum field, fifteen kinds of resonance integrals were measured for the (n,γ) reactions of reactor materials, using the $^{197}Au(n,\gamma)^{198}Au$ reaction as a standard value. A Monte Carlo calculation was employed to correct the neutron self-shielding in the activation foils. In the uncertainty analysis, variance-covariance data were taken into account and a correlation matrix was given to the measured data.

* Kinki University Atomic Energy Research Institute
3-4-1, Kowakae, Higashi-osaka-shi, Osaka 577, Japan

The present results are summarized in Table 1 and are compared with the values evaluated by Mughabghab and the JENDL-2 data. General agreement between the measurement and the evaluated data has been seen except for Ti-50, Ni-64, Nb-93, Ag-109, and Ta-181.

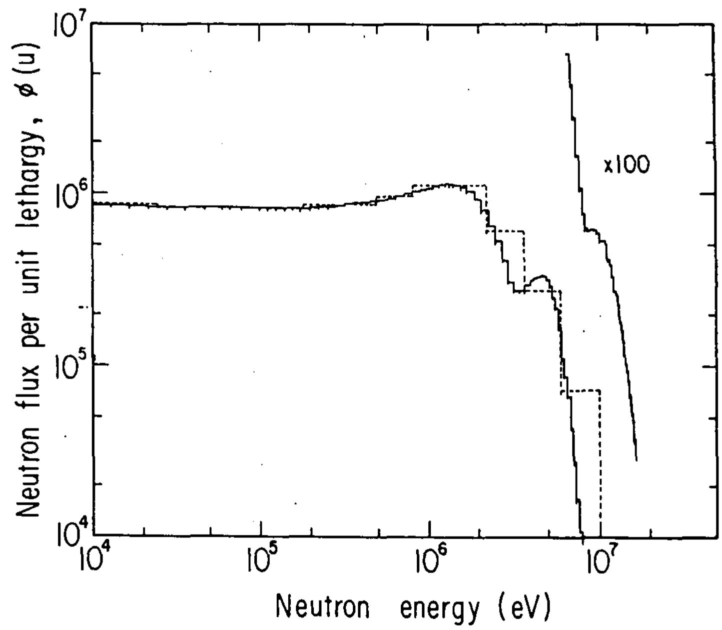

Fig. 1 Neutron energy spectrum in the central graphite region of UTR-KINKI.

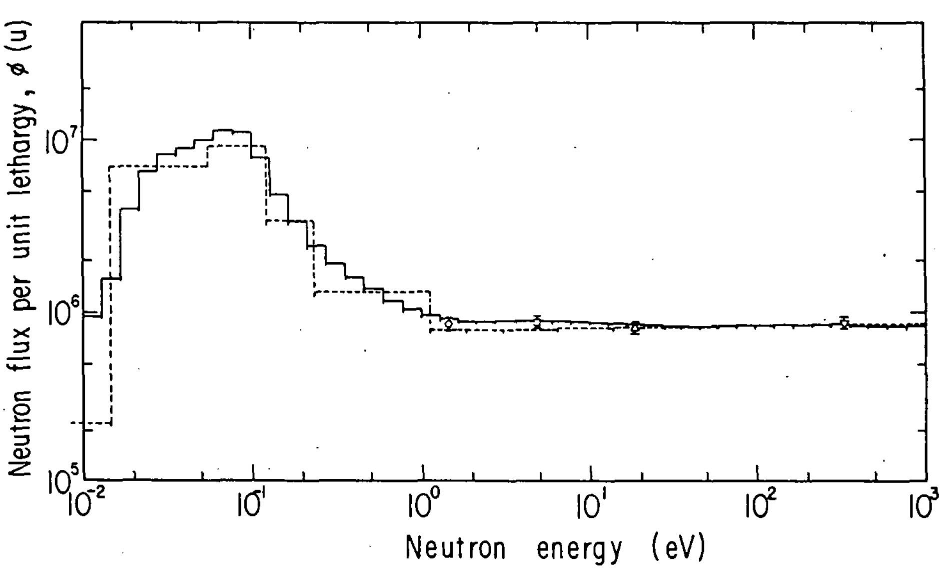

Fig. 2 Neutron energy spectrum in the central graphite region of UTR-KINKI.

——— NEUPAC unfolding
- - - - - SRAC code system calculation
○□△▽ sandwich foil method by In, Au, W and Mn, respectively.

Table 1 Summary of the present measurements of resonance integrals and comparison with the evaluated data.

Reaction	Present measurement																		Evaluated value (b)	
	Cross section (b)	(%)	Correlation matrix, (x 100)																JENDL-2	Mughabghab*
$^{197}Au(n,\gamma)^{198}Au$	1550	1.81	100																- - -	1550 ± 28
$^{23}Na(n,\gamma)^{24}Na$	0.3197	4.14	43	100															0.329	0.311±0.010
$^{50}Ti(n,\gamma)^{51}Ti$	0.1414	6.42	28	19	100														- - -	0.118±0.011
$^{51}V(n,\gamma)^{52}V$	2.799	5.99	30	27	25	100													2.534	2.7 ± 0.1
$^{55}Mn(n,\gamma)^{56}Mn$	13.90	2.94	60	35	20	22	100												14.63	14.0 ± 0.3
$^{59}Co(n,\gamma)^{60}Co$	73.34	4.91	37	32	30	37	27	100											75.65	74 ± 2
$^{64}Ni(n,\gamma)^{65}Ni$	0.9238	6.48	28	24	24	29	21	34	100										0.819	0.98 ± 0.15
$^{71}Ga(n,\gamma)^{72}Ga$	30.26	5.65	32	27	15	16	26	20	15	100									- - -	31.2 ± 1.9
$^{93}Nb(n,\gamma)^{94m}Nb$	6.246	6.10	29	22	22	25	22	30	23	16	100								9.59	8.5 ± 0.5
$^{107}Ag(n,\gamma)^{108}Ag$	106.4	6.73	27	22	25	20	20	29	23	14	21	100							- - -	100 ± 5
$^{109}Ag(n,\gamma)^{110m}Ag$	56.89	4.98	36	28	32	33	27	41	32	20	30	34	100						- - -	72.3 ± 4
$^{115}In(n,\gamma)^{116m}In$	2695	5.75	31	23	16	13	24	17	14	46	15	15	18	100					- - -	2650 ± 100
$^{181}Ta(n,\gamma)^{182}Ta$	655.4	4.24	43	29	33	40	31	46	37	22	36	32	46	20	100				743.4	660 ± 23
$^{186}W(n,\gamma)^{187}W$	510.7	4.76	38	25	32	32	28	40	29	20	31	30	39	20	44	100			- - -	485 ± 15
$^{232}Th(n,\gamma)^{233}Th$	85.71	3.43	53	29	17	19	71	22	17	21	18	16	23	20	26	23	100		79.93	85 ± 3
$^{238}U(n,\gamma)^{239}U$	274.8	4.09	44	25	15	16	66	19	15	18	16	14	19	17	22	20	64	100	279.0	277 ± 3

* cited from "Neutron Cross Sections", Academic Press, Inc. (1984).

III-A-11

$\nu(m^*)$ MEASUREMENT FOR THERMAL NEUTRON-INDUCED FISSION OF ^{233}U AND ^{235}U BY DOUBLE-VELOCITY DOUBLE-ENERGY METHOD

Y. Nakagome, I. Kanno[§], I. Kimura[¶]

Number of prompt neutrons as a function of individual fragment mass $\nu(m^*)$ was measured for the thermal neutron-induced fission of ^{233}U and ^{235}U. The experiments were carried out at the super mirror neutron guide tube facility of the Kyoto University Reactor. By measuring the velocities and energies of two fission fragments simultaneously, preneutron-emission fragment mass m* and postneutron-emission fragment mass m were obtained. $\nu(m^*)$ was deduced by subtracing m from m*. The fragment velocity was measured by a time-of-flight (TOF) method, and the start time was detected by a very thin plastic scintillator film detector. A silicon surface barrier detector was used to measure the fragment energy, which was also used as a stop detector of the TOF.

The result of $\nu(m^*)$ for $^{233}U(n,f)$, which is shown in Fig. 1, was in agreement with other data in the heavy fragment region, but was 20 to 50% larger than those in the light one. $\nu(m^*)$ for $^{235}U(n,f)$, which is shown in Fig. 2, showed a factor of 1.5 to 2 larger in the light fragment region and smaller in the heavy one than the other data. With the energy balance equation, the total kinetic energy was estimated using the $\nu(m^*)$-value and was in good agreement with the experimental result. Also

---

§ Present address, Japan Atomic Energy Research Institute, Tokai-mura

¶ Present address, Department of Nuclear Engineering, Kyoto University

using the energy balance equation, the $\nu(m^*)$-values were calculated by assuming the thermal equilibrium at the scission point. These values were quite different from the experimental results in both cases. We now calculate the $\nu(m^*)$-values by considering the effect of deformation of the fragment.

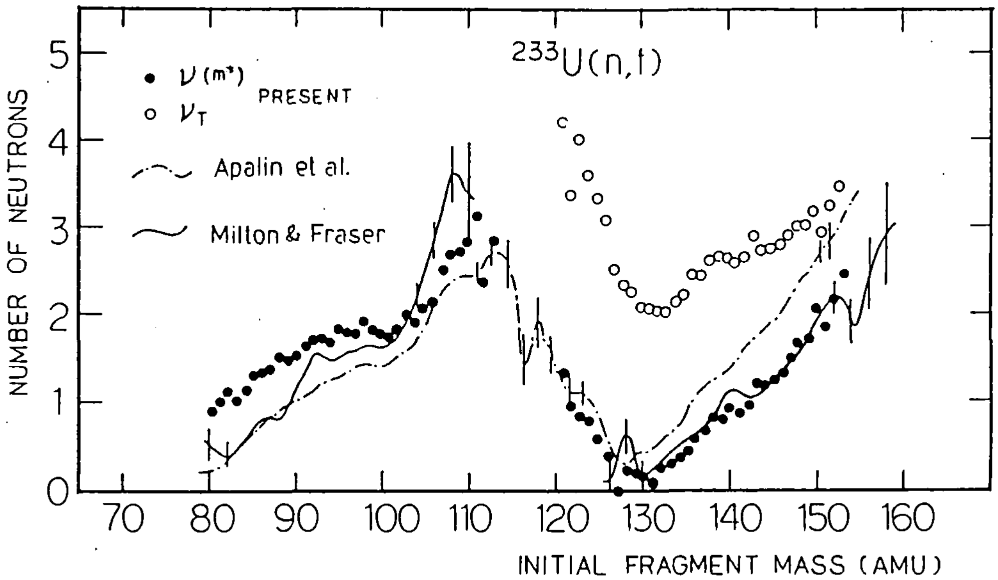

Fig. 1 Prompt neutron distribution $\nu(m^*)$ for thermal neutron-induced fission of ^{233}U

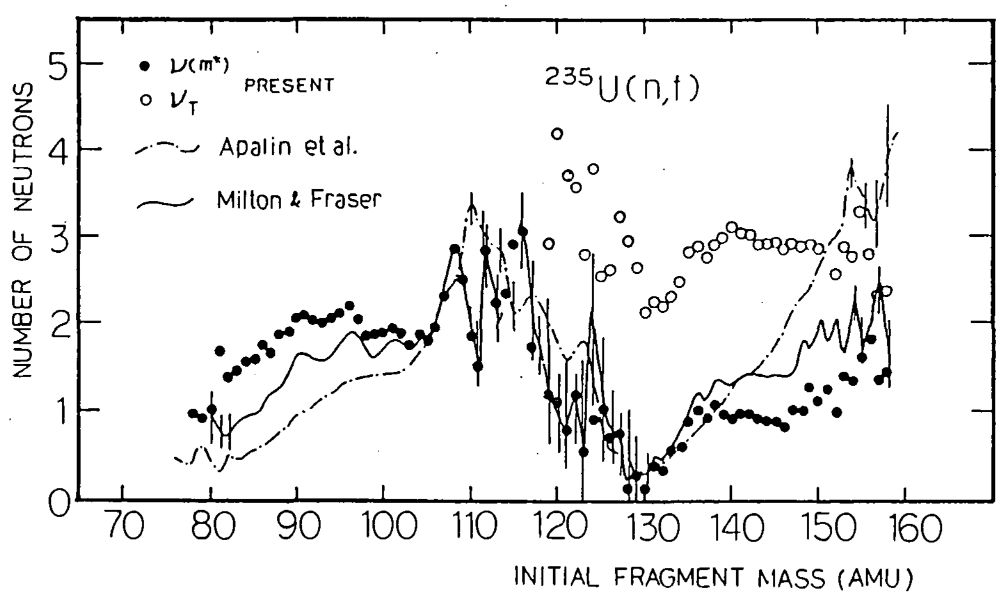

Fig. 2 Prompt neutron distribution for thermal neutron-induced fission of ^{235}U

III-A-12

Identification of a New Isotope ^{154}Pr

Y. Kawase and K. Okano

The heaviest isotope of praseodimium, ^{154}Pr, has been identified for the first time by the γ-ray measurements of mass-separated activities obtained by means of a helium-jet type on-line isotope separator for fission products. The oxidation technique[1] was employed to enhance the beam intensity of lanthanides. The A=154 isobars were ionized as lanthanide monoxides at high efficiencies, and mass-analysed with magnetic field setting at mass=170. The Nd-K X-ray and 10 γ-rays have been assigned to be generated by the β-decay of ^{154}Pr. The γ-ray spectrum taken with a high-resolution HPGe detector is shown in Fig. 1, and γ-ray energies and intensities in the decay of ^{154}Pr are listed in Table 1. The results of hale-life measurements are illustrated in Fig. 2, and are summarised in Table 2. The half-life has been determined to be 2.3 ± 0.1 s, which is slightly longer than the theoretical prediction of 1.5 s by H. V. Klapdor et al.[2] but a little shorter than the predicted value of 4.0 s by T. Tachibana et al.[3]. The spin and parity of the ground state of ^{154}Pr are considered to be 3^+ because the log ft values to 4^+

and 2^+ levels in ^{154}Nd are estimated to be about 5.4 and 4.8, respectively, and no β-feeding was found to the 6^+ level of ^{154}Nd in the present study.

References

[1] Y. Kawase and K. Okano, Proceedings of the 7th Int. Conf. on Ion Implantation Technolory, Kyoto, 1988.

[2] H. V. Klapdor et al., At. Data & Nucl. Data Tables, 31(1984)82.

[3] T. Tachibana et al., AIP Conf. Proc. No.164, Nuclei far from Stability, 1987, p.614.

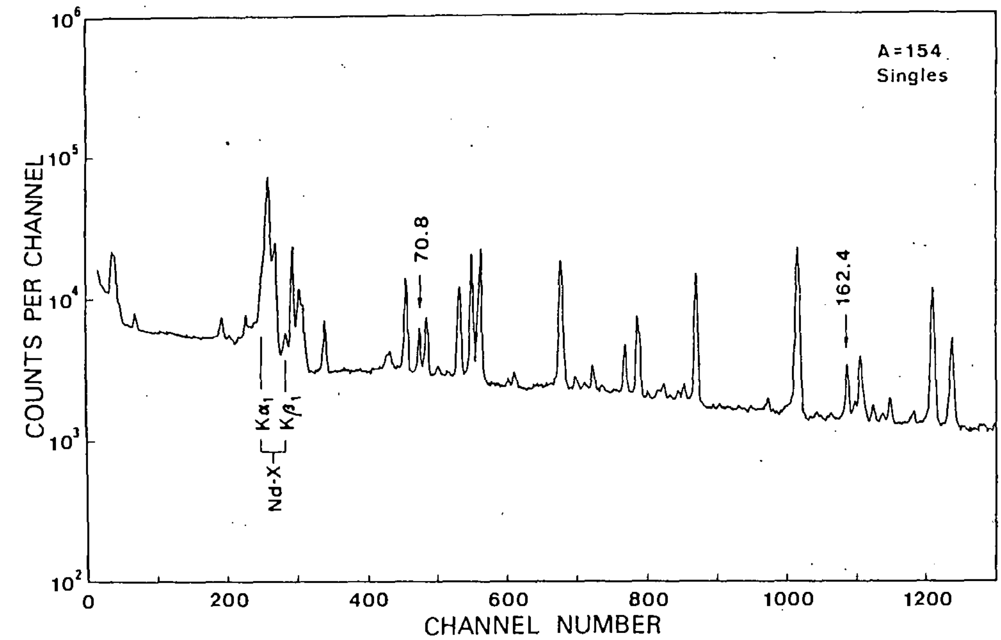

Fig. 1 Singles spectrum of A=154 isobars taken with a high-resolution LEPS spectrometer

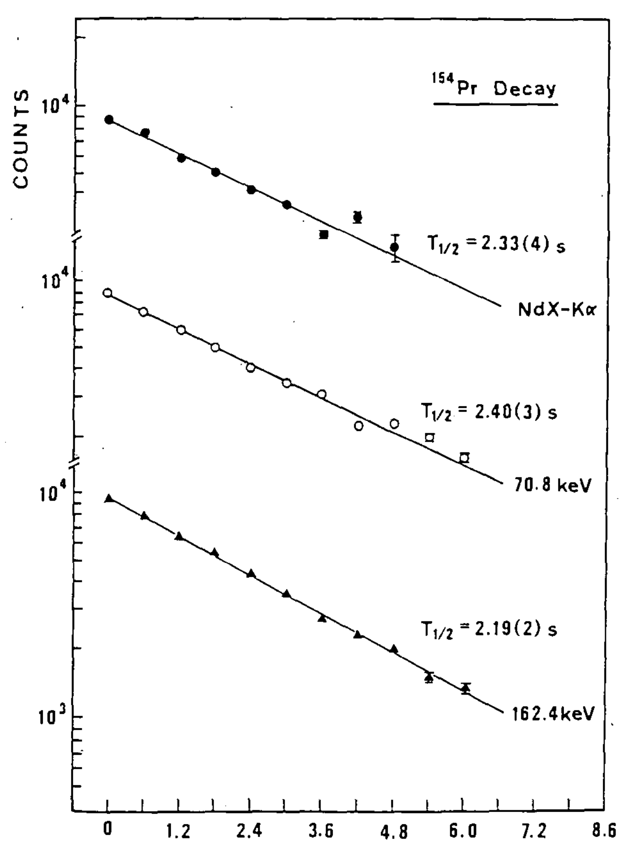

Fig. 2 Half-life measurements of ^{154}Pr

Table 1. Gamma-ray energies and intensities in the decay of 2.3 s ^{154}Pr

E_γ/keV	I_γ/ %	Transition
70.8(1)	73.8(15)	$2^+ - 0^+$
162.4(1)	100	$4^+ - 2^+$
520.5(5)	12.1(8)	
562.2(6)	33.6(11)	
581.4(6)	22.4(13)	
794.3(4)	16.2(8)	
895.1(5)	2.0(4)	
932.1(3)	76.9(18)	
956.9(3)	44.7(18)	
1184.4(4)	7.6(10)	

Table 2. Half-life measurements of the ^{154}Pr decay

E_γ/keV	$T_{1/2}$/s	I_γ/%	Transition
Nd-X K	2.33(4)		
70.8(1)	2.40(3)	73.8(15)	$2^+ - 0^+$
162.4(1)	2.19(2)	100	$4^+ - 2^+$

III-A-13 Gamma rays following the decay of ^{156}Pm

K. Okano and Y. Kawase

The identification of the nuclide ^{156}Pm has previously been reported.[1] Several new lines and the revised value of half-life have recently been measured by using KUR-ISOL with increased beam intensity of ^{156}Pm.[2] The results are summarized in Table 1 together with the other reported values. The revised half-life of ^{156}Pm, 27.4$\pm$0.5 sec, has been obtained as the average of half-lives of 75.7, 117.8, 174.0 and 934.0 keV gamma rays measured for successive 16$\times$10 sec using a 64K pulse-height analyzer. The lines listed in Table 1 have been assigned to ^{156}Pm from their half-lives. The energies of the 1st(2+), 2nd(4+) and 3rd(6+) excited states in ^{156}Sm have been revised as 75.7, 249.7 and 517.1 keV, respectively. The energy relations of gamma rays and the appearance of sum peaks at 1068.3 $\pm$ 0.3 and 1321.7 $\pm$ 0.4 keV indicate the existence of excited levels in ^{156}Sm at 1144.0 $\pm$ 0.18 keV decaying to the 249.7 keV level and at 1397.5 $\pm$ 0.12 keV decaying to the 249.7 and 517.1 keV levels. As these levels feed only to the 4+ and 6+ levels, the spins of these levels must be 4 $\sim$ 6, which allow allowed or first-forbidden β^--decay from the ground state of ^{156}Pm with assumed spin and parity of 4+ or 5-.[1] The intensities listed in Table 1 should be taken as tentative as no precise sum corrections are applied on account of the lack of the accurate decay scheme.

References

1) K. Okano, Y. Kawase and Y. Funakoshi, J. Phy. Soc. Jpn., 55 (1986) 715.

2) Y. Kawase and K. Okano, to be published in Nucl. Instr. Meth.

Table 1. Energies and relative intensities of gamma rays following the decay of ^{156}Pm

Ref.a E_γ (keV)	Ref.a I_γ	Ref.b E_γ (keV)	Ref.c E_γ (keV)	Present results E_γ (keV)	Present results I_γ
				29.7 (0.1)	1.4
75.8 (0.6)	37 (10)	75.7	75.9	75.7 (0.1)	24
		117.8	117.8	117.8 (0.1)	22
174.2 (0.1)	100	174.1	174.0	174.0 (0.1)	100
				213.8 (0.1)	8.9
				219.4 (0.2)	2.5
				223.5 (0.1)	2.0
267.4 (0.5)	19.7 (1.4)		267.8	267.4 (0.1)	22
				307.2 (0.2)	2.9
				376.8 (0.2)	1.6
				380.5 (0.2)	2.3
				460.9 (0.2)	2.1
				525.0 (0.2)	1.9
				624.1 (0.4)	1.8
				625.8 (0.2)	2.6
				684.6 (0.2)	3.0
				690.8 (0.1)	6.9
				756.6 (0.2)	3.4
				770.6 (0.2)	4.6
				799.8 (0.2)	5.6
				803.3 (0.3)	3.0
			880.9	880.4 (0.1)	17
			894.8	894.3 (0.1)	17
				904.3 (0.5)	2.0
				920.5 (0.4)	2.4
934.0 (0.6)	25.2 (1.7)		934.6	934.0 (0.1)	26
				1034.5 (0.4)	3.4
1148.0 (0.5)	35.2 (2.1)		1148.5	1147.9 (0.1)	36
				1187.6 (0.3)	4.0
1259.7 (0.7)	23.3 (1.3)		1260.1	1259.4 (0.2)	22
				1382.3 (0.2)	8.9
				1433.7 (0.2)	19
				1509.5 (0.3)	4.4
				1516.7 (0.2)	15

a) Ref. 1.
b) H. Mach, A. Piotrowski, R. L. Gill, R. F. Casten and D. D. Warner, Phys. Rev. Lett. 56 (1986) 1547.
c) R. C. Greenwood, R. A. Anderl and J. D. Cole, Phys. Rev. C, 35 (1987) 1965.

IV. Kyushu University

IV-A-1 A. Department of Nuclear Engineering

Faculty of Engineering

Empirical Formulas for 14-MeV (n,p) and (n,α) Cross Sections

I. Kumabe and K. Fukuda

A paper on this subject was published in Journal of Nuclear Science and Technology 24 (1987) 839-843 with the following abstract :

Empirical formulas for the 14 MeV (n,p) and (n,α) cross sections given by Levkovskii were modified separately in three ranges of mass number, in each of which, coefficients modifying Levkovskii's formulas were determined by least-squares fitting to experimental cross sections. The resulting modified formulas yielded cross sections representing markedly smaller chi-square deviations from experimental values, and moreover gathered closer to unity, compared with calculation using Levkovskii's original formulas.

IV-A-2

Preequilibrium Model Analysis of (p,n) Reactions on Isotopes of Zr and Mo

I. Kumabe and Y. Watanabe

A paper on this subject was published in Physical Review C 36 (1987) 543-550 with the following abstract :

The neutron energy spectra from the (p,n) reaction on $^{90,91,92,94}Zr$, $^{92,94,95,96,97,98,100}Mo$, and ^{110}Pd with 25 MeV protons and $^{90,91,92,94}Zr$ with 18 MeV protons are analyzed in terms of the preequilibrium exciton model introducing effective Q values, the pairing correlation, and the modified uniform spacing model in which the uniform spacing model is modified so as to have a wide spacing at the magic number. For all these targets, the calculated spectra using the above model for 25 MeV protons show good agreement with the experimental ones not only on the absolute cross sections in the neutron energy region of 12-18 MeV, but also on the observed spectra with pronounced structures in the neutron energy region higher than 18 MeV.

IV-A-3 Preequilibrium (p,p') Spectra for Nuclei around Neutron Number 50

Y. Watanabe, I. Kumabe, M. Hyakutake, N. Koori,

K. Ogawa, K. Orito, K. Akagi and N. Oda

A paper on this subject was published in Physical Review C 36 (1987) 1325-1334 with the following abstract :

Energy spectra of protons emitted from (p,p') scattering were measured for ^{90}Zr, ^{93}Nb, ^{92,94,96,98,100}Mo, ^{106}Pd, and Ag at an incident energy of 18 MeV. It was shown that there were no appreciable shell and odd-even effects on the preequilibrium proton spectra corresponding to excitations higher than 4 MeV of the residual nucleus. The experimental results were interpreted on the basis of the state densities generated from two sets of single particle levels using the recursion method by Williams et al.; one is based on the spherical Nilsson model, and the other on the modified uniform spacing model in which a shell gap is introduced into the uniform spacing model. The measured angle-integrated proton spectra were compared with those calculated on the basis of the exciton model and the Hauser-Feshbach model in which the isospin selection rule was taken into account. Good agreement between the experimental and calculated spectra was obtained for all targets in the continuum region in the outgoing proton energy region of 3-14 MeV.

IV-A-4

Preequilibrium (n,n') Cross Sections on Nuclei around Atomic Number 50 at E_n=14.1 MeV

Y. Watanabe, I. Kumabe, M. Hyakutake,

A. Takahashi*, H. Sugimoto*, E. Ichimura* and Y. Sasaki*

A paper on this subject was published in Physical Review C 37 (1988) 963-968 with the following abstract :

The energy spectra of neutrons emitted from 14.1-MeV-neutron-induced reactions on Ag, Cd, In, Sn, Sb, and Te were measured at 70° in order to investigate the shell and odd-even effects in the preequilibrium (n,n') process. The cross sections integrated over the outgoing energies of 7-10 MeV, where the preequilibrium process is dominant, increased monotonically with increasing atomic numbers of all scatterers except Te. The results of calculations based on the exciton model showed an underestimation in 7-10 MeV only for Te. This underestimation could be explained by taking into account the contribution from the collective excitations of the low energy octupole resonance by the direct process. As a result, it was found that there were no appreciable shell and odd-even effects in the preequilibrium (n,n') process that leaves the residual nucleus into the continuum region.

* Department of Nuclear Engineering, Osaka University, Osaka, 565 Japan

IV-A-5 Energy Spectra of Deuterons Emitted from (p,d) Reaction on Nuclei around Neutron Number 50

I. Kumabe, J. Yano, N. Koori, Y. Watanabe,
A. Iida, Y. Kubo and K. Yoshioka

It has been well known that the preequilibrium process plays an important role in reactions induced by 14 MeV neutrons.

Most of the important candidates for structural materials in a nuclear fusion reactor are metals or their alloys which contain atoms of the magic nuclei or nuclei around the magic number. Therefore studies of the shell effect in reactions are very important. Since available data for (n,d) reaction are very poor, detailed features of the reactions such as the shell effect on target nuclei are not well known for the preequilibrium particle emission.

In general, accurate experimental data are available for the reaction induced by charged particles than those for neutron induced reactions because of better counting statistics for reactions related to the charged particles.

In the present study we have undertaken to measure systematically and accurately the double differential cross sections of the (p,d) reaction, which is analogous to the (n,d) reaction, in order to clarify the shell effect on the (p,d) reaction. By analogy with analyses of the (p,d) reaction, we expect to clarify the shell effect on the 14 MeV (n,d) reaction.

Proton beams of 19 MeV from the tandem Van de Graaff accelerator at Kyushu University were analyzed by a beam analyzing magnet and brought into a scattering chamber. A detecting system mounted on a turntable inside the scattering chamber consisted of a ΔE-E counter telescope of two silicon surface barrier detectors. Emitted deuterons were identified and separated from other reaction products by means of a particle identifier.

Energy spectra of deuterons emitted from (p,d) reactions were meaured for $^{92,94,96,98,100}Mo$ at an incident energy of 19 MeV. The measured energy spectra at $\theta=50°$ are shown in Fig.1. The energy spectrum for the ^{92}Mo(p,d) reaction has three sharp peaks which correspond to the neutron pickup in orbits of $1g_{9/2}$, $2p_{1/2}$ and $2p_{3/2}$. For other Mo isotopes, the energy spectra below the energy indicated by the arrow correspond mainly to the one-neutron pickup from the N=50 core and show structure duller than that for ^{92}Mo, because of the neutron pickup from the deep states ($1g_{9/2}$, $2p_{1/2}$, $2p_{3/2}$) which produces the fragmentation of single particle levels.

Cross sections integrated over the deuteron energy below the energy indicated by the arrow, which correspond to the core excitation, are shown in Fig.2. The cross sections increase monotonically with increasing mass numbers. The Q values of the (p,d) reactions on Mo isotopes increase monotonically with increasing mass numbers. Therefore if the corrections of the cross sections by the penetrability of deuterons are carried out, each of the corrected cross sections is nearly equal between the measured isotopes. Thus it was found that there is no appreciable shell effect in the (p,d) cross section correspending to the excitation of the N=50 core.

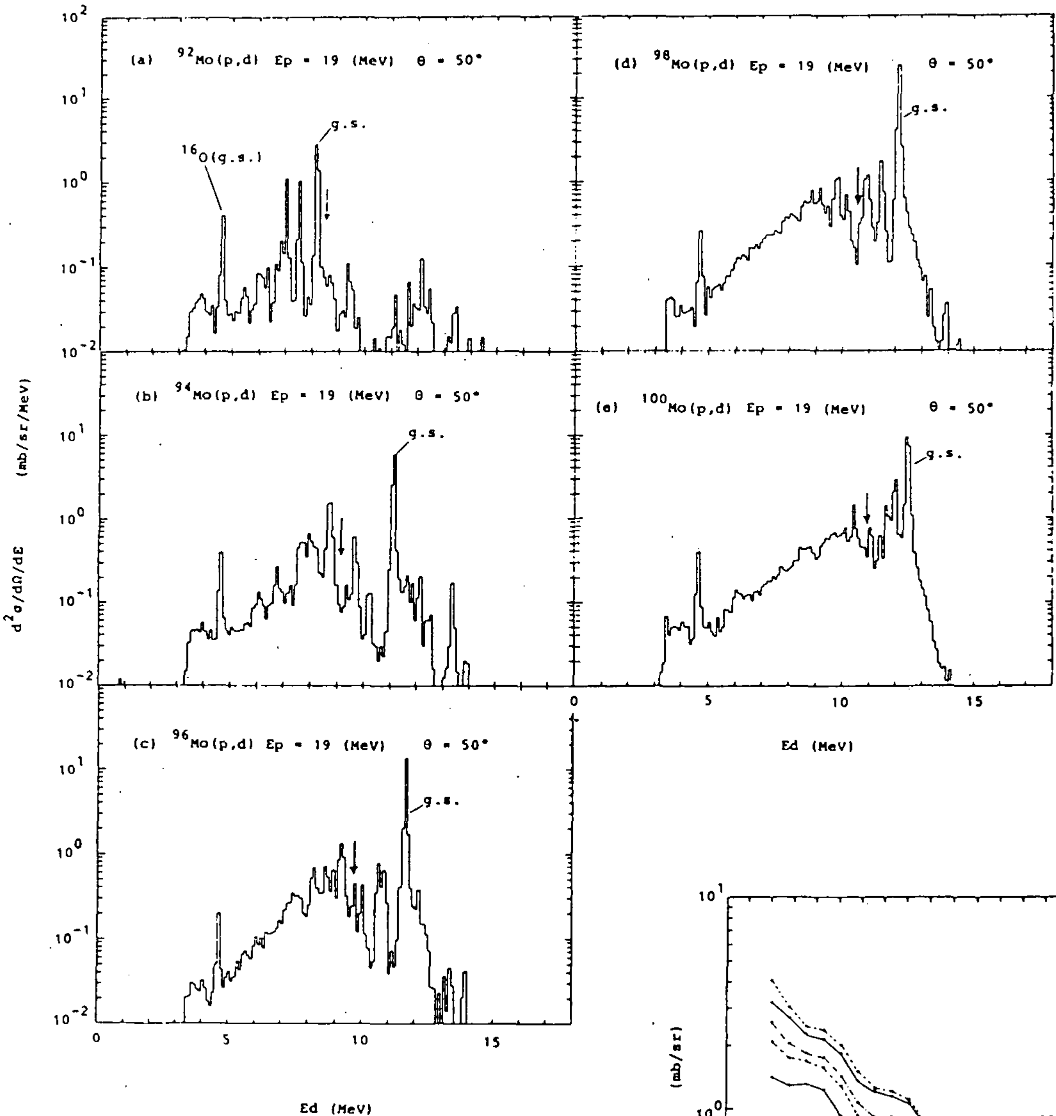

Fig. 1 Energy spectra of deuterons from the (p,d) reaction at θ_L=50°.

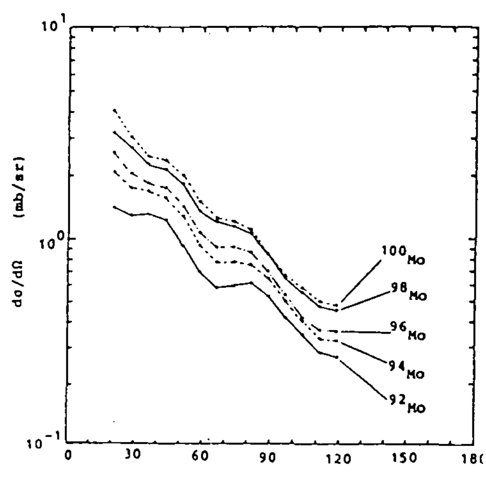

Fig. 2 Cross sections integrated over the deuteron energy below the energy indicated by the arrow in Fig. 1 , which correspond to the core excitation.

IV-A-6

Systematics and Parametrization of Continuum Angular Distributions

I. Kumabe, Y. Watanabe and Y. Nohtomi

Many theoretical approaches for calculating continuum angular distributions have been proposed. However they involve some serious approximations and / or computational complexities.

Kalbach and Mann[1](K & M), therefore, decided to approach the problem phenomenologically, studying the systematics of a wide variety of experimental angular distributions and then finding a convenient way to parametrize them. They have studied a large number of experimental angular distributions for particles emitted into the continuum in preequilibrium nuclear reactions in order to study their systematics. For pure multistep direct reactions it has been found that to first order the shapes of these angular distributions are determined by the energy of the outgoing particle. The formulation has been shown to have significant predictive ability for light ion reactions.

Although the angular distributions calculated by this systematics are in fairly good agreement with the experimental ones for the reaction induced by 14 MeV neutrons, this prediction shows slight underestimation at backward angles. K & M have performed the parametrization on the basis of the values of the parameters derived from the fits to mainly the 62 MeV (p,p') data. Therefore we have undertaken to carry out the reparametrization based on the values of the parameters derived from the fits to the data of the 18 and 25 MeV (p,n) reaction and the 18 MeV (p,p') reaction recently measured.

K & M assumed that the angular distributions are described in terms of Legendre polynomials for the reaction (a,b).

$$\frac{d^2\sigma}{d\Omega\,d\epsilon}(a,b)=a_0(\mathrm{tot})\sum_{l=0}^{l_{max}} b_l\,P_l(\cos\Theta)\,. \qquad (1)$$

The general idea of statistical multistep direct (MSD) and statistical multistep compound (MSC) processes seems useful.

In the case where the MSD/MSC distinction is a meaningful one, K & M assumed that the two components will show the same systematics in the reduced polynomial coefficients, except that only the even order polynomials will contribute to the MSC part. Thus the cross section of (1) becomes

$$\frac{d^2\sigma}{d\Omega\,d\epsilon}(a,b)=a_0(\mathrm{MSD})\sum_{l=0}^{l_{max}} b_l\,P_l(\cos\Theta)$$

$$+\,a_0(\mathrm{MSC})\sum_{\substack{l=0\\ \Delta l=2}}^{l_{max}} b_l\,P_l(\cos\Theta)\,. \qquad (2)$$

The various a_0 values are obviously related by $a_0(\mathrm{tot}) = a_0(\mathrm{MSD}) + a_0(\mathrm{MSC})$.

By analogy to the weighted transmission coefficients for a parabolic barrier, K & M have assumed that

$$b_l(\epsilon)=\frac{(2l+1)}{1+\exp[A_l(B_l-\epsilon)]}\,, \qquad (3)$$

where A and B are free variables.

The fit with experimental data gives the dependences:

$$A_l=0.036\ \mathrm{MeV}^{-1}+0.0039\ \mathrm{MeV}^{-1}\,l(l+1)\,, \qquad (4a)$$

$$B_l=92\ \mathrm{MeV}-90\ \mathrm{MeV}\,[l(l+1)]^{-1/2}\,. \qquad (4b)$$

Recently Scobel et al.[2] have measured the neutron energy and angular distributions for the (p,n) reaction on isotopes of Zr and Mo with 18 and 25 MeV protons. The numerical data[2] are available. More recently we have measured the energy spectra and the angular distributions of protons emitted from (p,p') scattering for ^{90}Zr, ^{93}Nb, $^{92,94,96,98,100}Mo$, ^{106}Pd and Ag at an incident energy of 18 MeV. We have chosen the reactions in the energy region in which the contribution of the compound process is negligibly small.

The procedure of parametrization is similar to that performed by K & M. A nonlinear least squares fitting routine was used to optimize the values of A_ℓ and B_ℓ in Eq.(3). The results of the least squares fittings give the following dependence,

$$A_\ell = 0.0561 + 0.0377 \cdot \ell \ (\mathrm{MeV}^{-1}) \tag{5a}$$

$$B_\ell = 47.9 - 27.1 \cdot \ell^{-1/2} \ (\mathrm{MeV}) \tag{5b}$$

To test the usefulness of the empirical parametrization derived here, comparisons of calculated angular distributions with 14 MeV (n,n')[3] and (n,p)[4] data were presnted. In Figs. 1-4, the solid and dashed curves are the calculated angular distributions using the present and K & M's parameters, respectively. The calculated angular distributions using the present parameters show excellent agreement with the experimental ones.

References

1) C. Kalbach and F.M. Mann : Phys. Rev. 23 (1981) 112.

2) W. Scobel et al.: Phys. Rev. C30 (1984) 1480, Lawrence Livermore National Laboratory Report No. UCID-20101, 1984 (unpublished)

3) Y. Irie et al.: Mem. Fac. Eng. Kyushu Univ. 37 (1977)

19.

4) G. Traxler et al.: Nucl. Sci. and Eng. <u>90</u> (1985) 174.

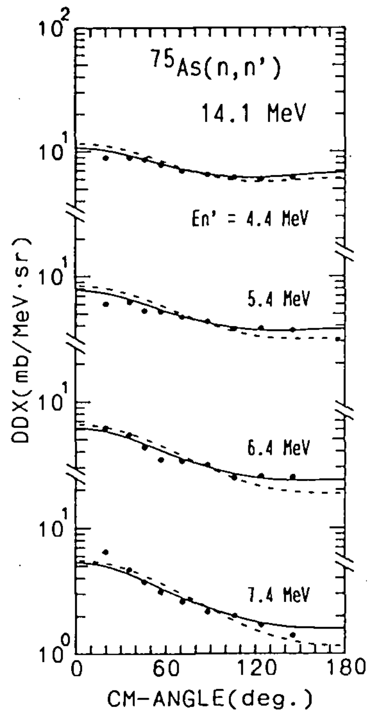

Fig.1

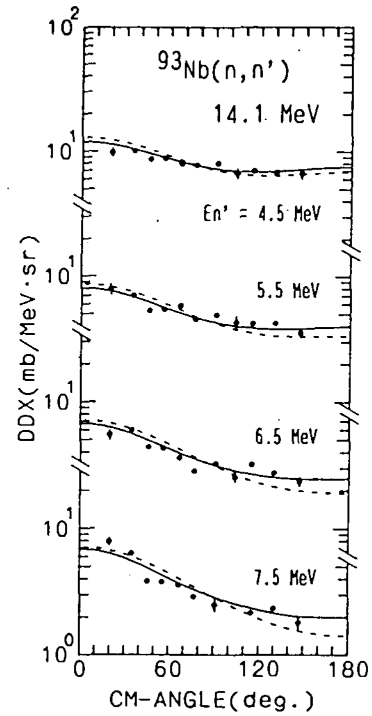

Fig.2

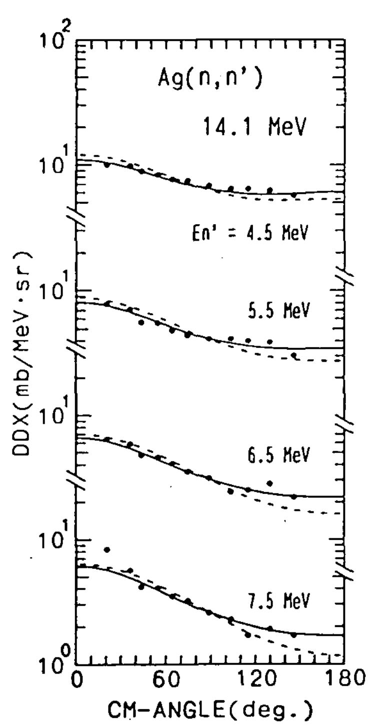

Fig.3

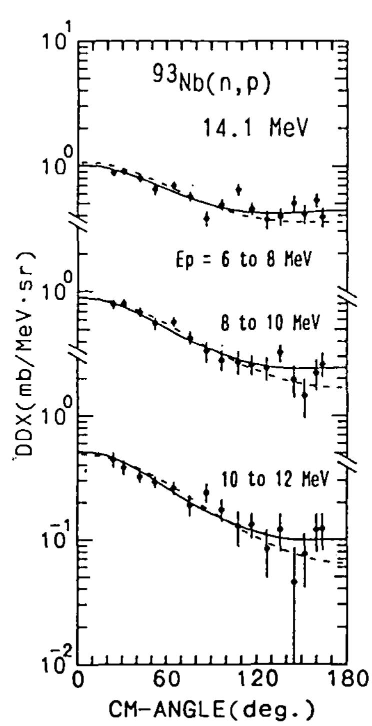

Fig.4

IV-A-7

Calculations of Preequilibrium angular distribution
(an improvement of the generalized exciton model)

Yukinobu Watanabe and Isao Kumabe

In nuclear reactions induced by the nucleon of several tens of MeV, preequilibrium process becomes important, in which process angular distributions of emitted particles are forward peaked. Several theories[1] have been proposed to calculate the angular distributions of the preequilibrium emissions. These are generally classified into semi-classical phenomenological approach (i.e. the generalized exciton model[2]: GEM) and quantum mechanical approach(i.e. the FKK theory[3]). So far the GEM has been applied to the calculations of double differential cross sections of 14-MeV (n,n') and 25.7-MeV (n,n') scatterings, and has been improved in some points[4,5,6]. However the problem still remains that calculated angular distributions show underestimation in backward angles with the increase of outgoing particle energies.

In the GEM calculations, single scattering kernel $G(\Omega,\Omega')$, which describes two-body collisions in nuclear matter, has a large effect on the shape of angular distribution. As followed by several workers[4,5,6], the kernel has been calculated using Kikuchi-Kawai expressions in which the momentum distribution of nucleons in a nucleus is assumed to be the uniform Fermi distribution at zero nuclear temperature. On the other hand, the recent analysis[7] of one-nucleon stripping reactions with high energy heavy ions has indicated that the momentum distribution near nuclear surface is given as follows;

$$\frac{dn(P_2)}{d\vec{P}_2} d\vec{P}_2 = N \left[e^{-P_2^2/P_0^2} + \varepsilon_0 e^{-P_2^2/q_0^2} \right] d\vec{P}_2 \qquad (1)$$

$$P_0 = 0.4\ P_F$$

$$q_0 = \sqrt{3}\ P_0$$

$$\varepsilon_0 = 0.03 \sim 0.1$$

where N is a normalization factor and ε_0 is a scaling parameter. This distribution will be referred to as two Gaussian distribution. From Eq.(1) it is found that there exists large momentum component more than the Fermi momentum P_F.

In Fig.1, we show the comparison between the calculated single scattering kernels using the uniform Fermi distribution and those using the two Gaussian distribution. In these calculations, ε_0 was taken as 0.07 and the Pauli principle was taken into account as follows;

$P_1 > P_F$ for prior collision

$P_{1'} > P_F$ and $P_{2'} > P_F$ for post collision

Both the calculated $G(\Omega,\Omega')$ are similar in the forward angles less than 100°, but are very different in the backward angles. As a result, we found that the probability of particle emission can be enhanced if the two Gaussian distribution is assumed in the GEM calculations.

Next, we have revised PREANG code[8] so as to implant the part of calculations of the above-mentioned $G(\Omega,\Omega')$ and calculated the double differential cross sections for several nucleon induced reactions. In the calculations, refraction effect were also taken into account by analogy with the scattering of a classical particle from a well-type potential according to the method mentioned in Ref.[5].

Figure 2 shows the comparison of experimental and calculated angular distributions for 18-MeV (p,xp) reaction on ^{96}Mo, 14.1-MeV (n,xn) reaction on In, and 25 MeV (p,n) reaction on ^{96}Mo[9]. Data for the 18-MeV (p,xp) and 14.1-MeV (n,xn) reactions were measured by the authors' groups; the details of experimental procedure have been described elsewhere[10,11]. The results using the two Gaussian distribution(solid curves) are in better agreement with the experimental values in backward angles(θ_{CM} > 120°) than those using the uniform Fermi distribution(dashed curves). As can been seen in Fig.2(c), refraction effect leads to a flattening of the angular distributions and further improvement of the underestimation at backward angles.

In conclusion, we found that the underestimation in backward angles is rather improved by using the two Gaussian distribution instead of the uniform Fermi distribution and considering refraction effect in the GEM calculations.

References

[1] P.E. Hodgson et al. in Proc. of the international Conf.on Nuclear Data for Basic and Applied Science, Santa Fe, 1985,(Gordon and Breath Science,NY,1986) Vol.2,p.1033.
[2] G. Mantzouranis et al. Phys. lett. 57B, 220 (1975).
[3] H. Feshbach et al. Ann. Phys. 125, 427 (1980).
[4] J.M. Akkermans et al. Phys. Rev. C 22, 73 (1980).
[5] C. Costa et al. Phys. Rev. C 25, 587 (1983).
[6] Y. Watanabe et al. Tech. Rep. of the Kyushu Univ. Vol.59, 469 (1986).
[7] Y. Haneishi and T. Fujita, Phys. Rev. C 33, 260 (1986).
[8] J.M. Akkermans and H. Gruppelaar, ECN-60 (1979).
[9] W. Scobel et al. LLNL Report No. UCID-20101, 1984 (unpublished)
[10] Y. Watanabe et al. Phys. Rev. C 37, 963 (1988).
[11] Y. Watanabe et al. Phys. Rev. C 36, 1325 (1987).

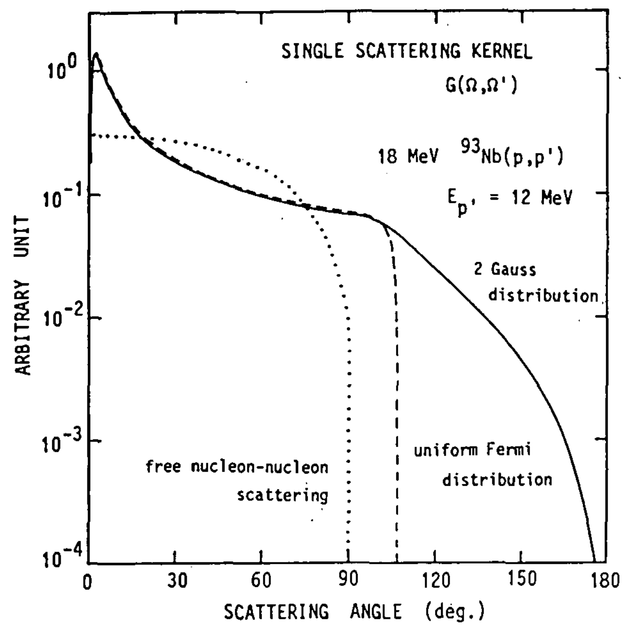

Fig.1 Comparison of the single scattering kernel $G(\Omega,\Omega')$

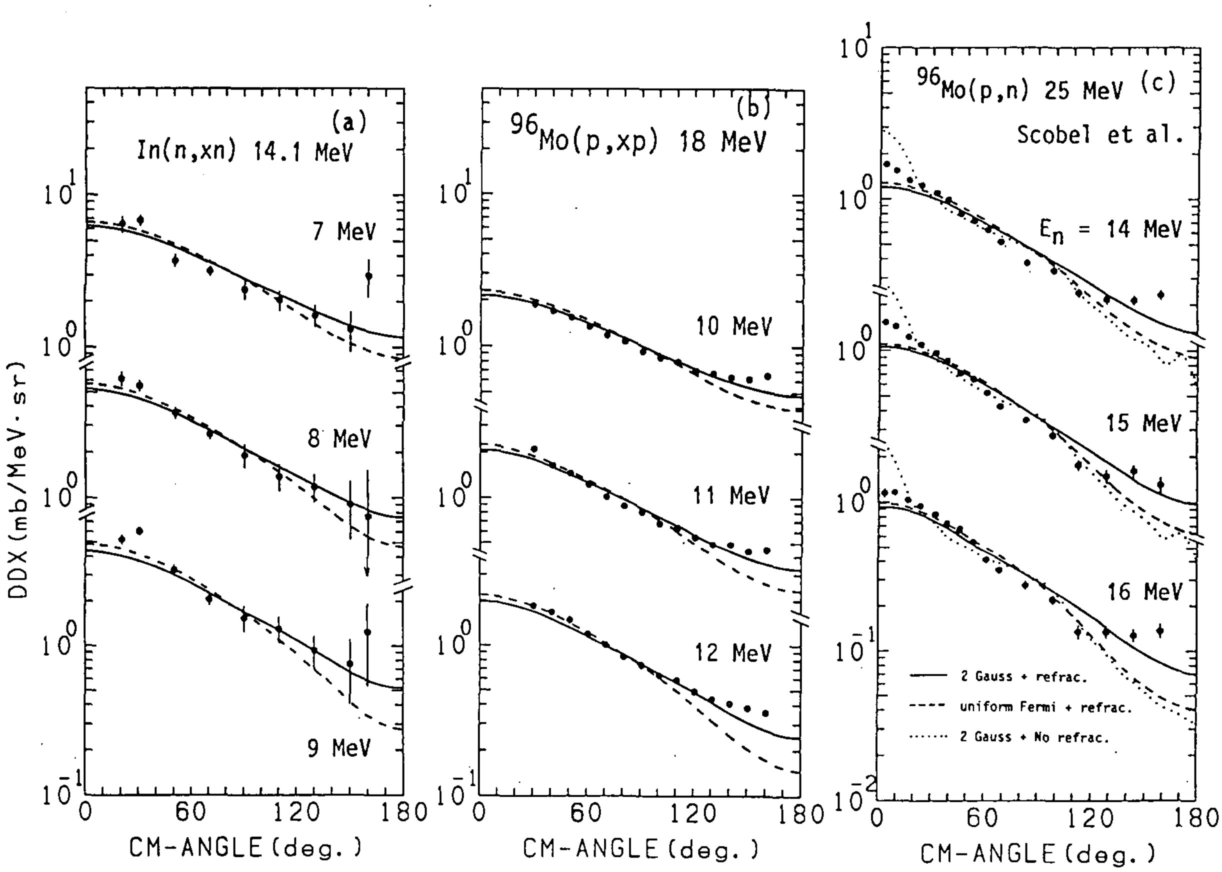

Fig.2 Calculated and experimental angular distributions.
(a) the In (n,xn) reaction with 14.1 MeV incident neutrons.
(b) the ^{96}Mo(p,xp) reaction with 18 MeV incident protons.
(c) the ^{96}Mo(p,n) reaction with 25 MeV incident protons.

IV-A-8

MEASUREMENTS OF ^{6}Li(p,p'), (p,d), AND (p,^{3}He) REACTIONS INDUCED BY POLARIZED PROTONS OF 14 MeV

N. Koori, I. Kumabe, M. Hyakutake,+ A. Iida, Y. Watanabe, K. Sagara,*
H. Nakamura,* K. Maeda,* T. Nakashima,* M. Kamimura,* and Y. Sakuragi**

As a series of polarized proton induced reactions on lithium isotopes, we have measured the ^{6}Li(p,p'), (p,d), and (p,^{3}He) reactions at 14 MeV. Comparison of the proton induced reactions with the neutron induced reactions would lead us to better understanding on mechanisms of breakup reactions on light nuclei. Sophisticated theories, such as the coupled discretized-continuum channel (CDCC) calculation, the Faddeev approach, etc. may be applied for analyses of reactions including three-body breakup reactions. We showed already applicability of these theories to the ^{7}Li(p,p') and (p,t) reactions around 14 MeV[1].

Elastic and Inelastic Scatterings:

The measurement was performed similarly to the previous measurement on lithium-7 using the tandem accelerator at Kyushu University. The differential cross sections and analyzing powers of ^{6}Li(p,p') scattering are shown in Fig.1. The spherical optical model (SOM) analysis gave a good fit to the measured data of the elastic scattering. The spin dependent terms were determined. The analyzing powers of the first excited state, however, could not be reproduced well in the frame of the DWBA calculation, in which the optical potential parameters were taken from the searched values. The fit could not be ameliorated, even if the form factors derived from the microscopic cluster model were used. Coupled channel calculations were performed with

+ Present address: Sasebo Technical College.
* Department of Physics, Faculty of Science, Kyushu University.
** Department of Physics, Faculty of Science, Osaka City University.

the ECIS79 code, in which three lowest states belonging to the K=1 band in the rotational model were assumed to be coupled each other. Although this coupled channel calculations could give a good fit to the elastic scattering data, they could not reproduce well the analyzing powers of inelastic scatterings similarly to the SOM and DWBA calculations.

DWBA Calculation for Discretized-Continuum States:

The proton continuum spectra, an example is shown in Fig.2, are mainly due to the $^{6}Li(p,p')d\alpha$ three-body breakup reaction. Instead of the complete CDCC calculations, we tried to calculate the spectra in the framework of the DWBA using the ^{6}Li form factors extended to the resonant and non-resonant discretized-continuum states by Kamimura et al.[2] As indicated in Fig.2, rather good agreement is obtained in a wide energy region, except in lower energies. More comprehensive CDCC calculation may improve the fit.

The $^{6}Li(p,d)p\alpha$ Three-Body Reaction:

An example of deuteron energy spectra from the $^{6}Li(p,d)p\alpha$ reaction is shown in Fig.3. The spectrum was calculated by means of the final state interaction (FSI) theory, where the p-α FSI, d-α FSI, and direct-breakup processes were taken into account as main contribution. The energy spectra were explained very well by means of the FSI theory. It is interesting that analyzing powers of the spectrum vary evidently at the FSI region, as indicated in Fig.3.

The $^{6}Li(p,^{3}He)\alpha$ Reaction:

The differential cross sections and analyzing powers of the reaction were measured and is presented in Fig.4. Comparing them with the $^{6}Li(n,t)\alpha$ reaction, their reaction mechanisms are very similar. Analysis of the reaction is in progress.

Brief report was presented at the Conference on Nuclear Data for Science and Technology, 1988.[3]

References

[1] N. Koori et al., Progress Report NEANDC(J)-125/U, Japan Atomic Energy Research Institute, (unpublished).

N. Koori et al., KUNE report 87-1, Dept. of Nuclear Engineering, Kyushu University, (unpublished).

[2] M. Kamimura et al. J. Phys. Soc. Jpn. Suppl. 55, (1986) 205.

[3] N. Koori et al., Contribution to the International Conference on Nuclear Data for Science and Technology, Mito,1988.

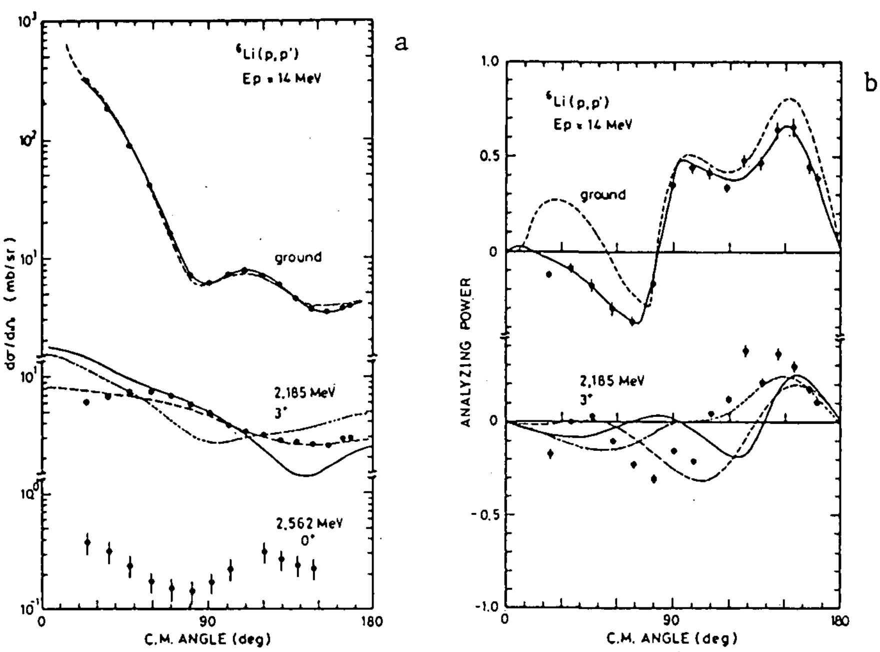

Fig. 1. Differential cross sections and analyzing powers of the $^{6}Li(p,p')$ scatterings. Solid lines and dashed lines indicate the results of the SOM and DWBA calculations. Dotted lines are for DWBA calculation with the form factors of microscopic cluster model.

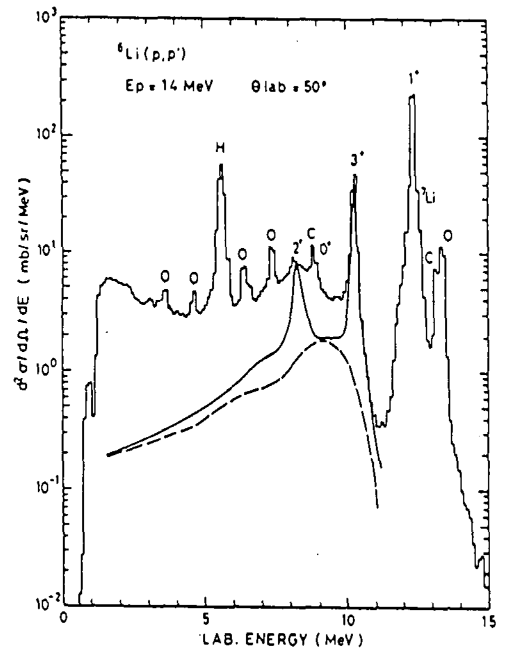

Fig. 2. An example of DDX of the $^6Li(p,p')d\alpha$ reaction. Solid line indicates the result of DWBA calculation with the form factors based on the microscopic cluster model.

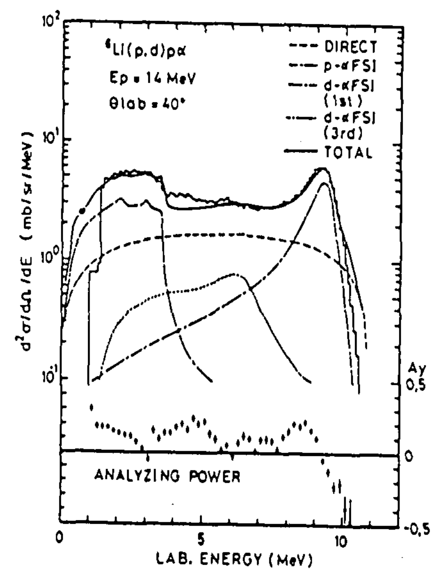

Fig. 3. An example of DDX of the $^6Li(p,d)p\alpha$ reaction. Lines indicate the contributions of final state interactions. Analyzing powers change clearly around the FSI region.

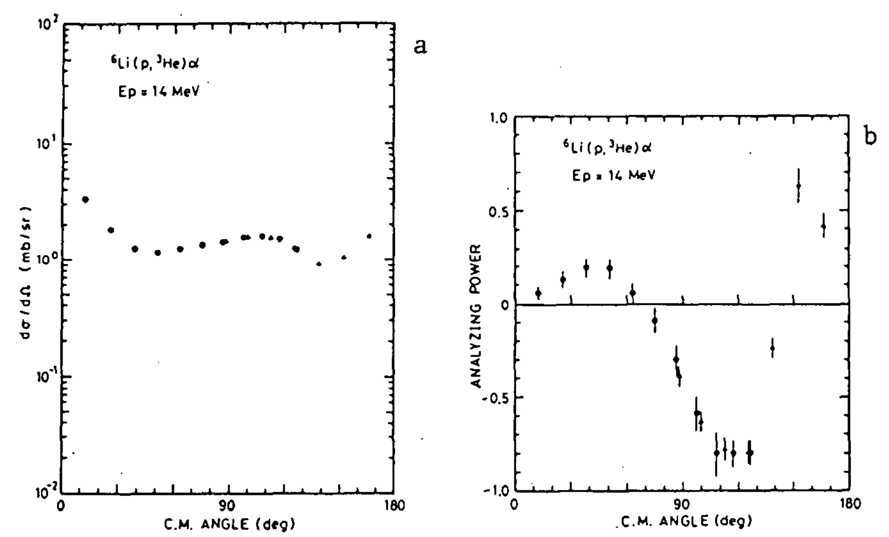

Fig. 4. Differential cross sections and analyzing powers for the $^6Li(p,^3He)\alpha$ reaction.

IV-A-9

IMPROVEMENT OF INTRANUCLEAR CASCADE MODEL CALCULATION FOR AN INCIDENT ENERGY RANGE 500-1000 MEV

Kenji Ishibashi and Akira Katase

The following two papers have been published or presented by our group in this period.

Kerntechnik 52(1988) No.6

"Improvements of high-energy transport calculations by using an intermediate process"

Abstract: The high-energy transport code calculates a nuclear reaction in two steps. There are considerable discrepancies in both mass yield and neutron energy spectrum of spallation reactions between calculated and experimental results. An intermediate process with three adjustable parameters is incorporated into the code as an additional calculation step to remedy the disagreement. The original rapid computation speed is maintained. The agreement between calculated and experimental results is considerably improved with a single set of parameters.

Presented at the International Conference on Nuclear Data for Science and Technology, May 30-June 3, 1988, Mito, Japan.

"Improvement on intranuclear cascade model calculation for an energy range 500-1000 MeV"

Abstract: High energy proton beams of about 1 GeV may be used for such engineering purposes as incineration of nuclear waste. Computer codes like High Energy Transport Code (HETC) are utilized for designing target systems. These codes treat high energy reactions on the basis of the intranuclear-cascade-evaporation model. They produce a discrepancy in experimental results in both neutron spectra and mass yields of residual nuclei. Improvement is made on the HETC to eliminate this disagreement. The intranuclear-cascade (INC) calculation is introduced between the processes of INC and evaporation. A better agreement is obtained betweeen the experimental and calculated results for both neutron spectra and residual mass yields.

B. Energy Conversion Engineering
Interdisciplinary Graduate School
of Engineering Sciences

IV-B-1

Expert System for Evaluation of Experimental Uncertainty from EXFOR File

Y. Uenohara, M. Tsukamoto, T. Mori, M. Kihara, and Y. Kanda

A paper on this subject was presented to International Conference on Nuclear Data for Science and Technology, Mito Japan, May 30 - June 3, 1988

Abstract

An expert system have been designed to estimate experimental uncertainties from comments and numerical data in EXFOR files. The expert system designed in the present work has knowledge bases and inference engines written in the computer programming language LISP. Scarce information in the report to be demanded in evaluation of errors is inferred and implemented from the other information given in the same report. The expert system is programmed to conduct reasonably these processes. Typical examples are presented.

IV-B-2

Covariance Matrices Evaluated by Different Methods for some Neutron-Dosimeter Reactions

Y. Kanda and Y. Uenohara

A paper on this subject was presented to International Conference on Nuclear Data for Science and Technology, Mito Japan, May 30 - June 3, 1988

Abstract

Covariance matrices between neutron-induced activation cross sections depends strongly on an evaluation method. The activation cross sections for neutron dosimeter can be evaluated from experimental data. In order to obtain covariances, differential and integral experiments are used in the evaluation. Correlation is localized in the limited energy regions where the measurements are abundant. In another way, the covariance matrices can be also evaluated by nuclear reaction model calculation in which are used the parameters estimated from experiments. Correlation is not localized but distributed over whole energy regions. These differences influence neutron spectra to be measured in unfolding from dosimeter activities.

IV-B-3

Estimation of Parameters in Nuclear Model Formula for Nuclides of Structural Materials

Y. Uenohara, H. Tsuji, and Y. Kanda

A paper on this subject was presented to International Conference on Nuclear Data for Science and Technology, Mito Japan, May 30 - June 3, 1988

Abstract

Optical model parameters and level density parameters for Hauser-Feshbach model calculations have been estimated systematically for Z = 22 to 28 nuclei by using Bayesian method. The experimental data for the estimation are total, (n,p), (n,α), and (n,2n) cross sections, and energy distribution of proton and α-particles emitted by neutron induced reactions. The prior optical model parameters of neutron, proton, and α-particles are taken from Beccetti-Greenlees', Menet et al.'s, and Huizenga-Igo's values, respectively. The prior level density parameters are taken from Gilbert-Cameron's values. The optical model and level density parameters estimated in the present work have been found to be reasonable comparing with the other works. The cross sections calculated with posterior parameters have been improved more than those done with prior ones.

IV-B-4

Evaluation of some Activation Cross Sections Measured by Monoenergetic and Fission Neutrons

Y. Kanda and Y. Uenohara

A paper on this subject was presented to International Conference on Nuclear Data for Science and Technology, Mito Japan, May 30 - June 3, 1988

Abstract

Neutron-induced activation cross sections applied in neutron dosimetry must be evaluated as accurate as possible and also their evaluated covariances are demanded in computer codes to unfold neutron spectra from dosimeter activities. The six activation cross sections, ^{27}Al(n,p), ^{27}Al(n,α), ^{54}Fe(n,p), ^{56}Fe(n,p), ^{59}Co(n,α), and ^{58}Ni(n,p) and their covariances have been simultaneously evaluated from differential experiments in which samples are activated with monoenergetic neutron sources and the integral experiments with ^{235}U(n,f) and ^{252}Cf(spontaneous) fission neutron spectra. The evaluated fission neutron spectra of JENDL-3T and Mannhart's work have been used for ^{235}U(n,f) and ^{252}Cf, respectively, in calculation of averaged cross sections. The evaluated cross sections are smaller than those only with the differential data.

IV-B-5

Some Activation Cross Sections Evaluated Simultaneously by Differential and Integral Data

Y. Kanda and Y. Uenohara

A paper on this subject was presented to International Conference on Neutron Physics, Kiev USSR, September 21-25, 1987

Abstract

The six activation cross sections, $^{27}Al(n,p)$, $^{27}Al(n,\alpha)$, $^{54}Fe(n,p)$, $^{56}Fe(n,p)$, $^{59}Co(n,\alpha)$, and $^{58}Ni(n,p)$ have been simultaneously evaluated from differential experiments by monoenergetic neutron and integral experiments with $^{235}U(n,f)$ and ^{252}Cf(spontaneous) fission neutron spectra. The results depend on nuclear temperatures in Maxwellian formula of the fission neutron spectra, which are used to calculate average cross sections.

IV-B-6

Measurement of Helium production cross section for 14MeV Neutrons

Y.Kanda, Y.Takao, Y.Uenohara, Y.Yamamoto, Y.Watanabe, S.Itadani, T.Takahashi, H.Eifuku and H.Nakashima

In a development of nuclear fusion reactors, first-wall damage is one of the most serious problems. The main cause of the damage is Helium atoms produced by (n,xα) reactions in structural materials. The Helium production cross sections of major elements in stainless steel, which is a candidate for structural materials of a nuclear fusion reactor, have been measured by Helium accumulation method using a Helium atom measurement system which was developed in our laboratory.

Samples were irradiated by about 10^{14} (n/cm^2) 14.8 MeV neutrons at OKTAVIAN(Osaka Univ.) and FNS(JAERI). Estimation of the cross sections is in progress. They are relatively measured with the Helium production cross section of Al for 14.8 MeV neutrons.

IV-B-7

Correlation of Nuclear Parameters in Hauser-Feshbach Model Formula Estimated from Experimental Cross Section Data

Y. Kanda, Y. Uenohara, and H. Tsuji

Abstract

Correlation of nuclear parameters, level density parameters, pairing energies and optical model parameters, in Hauser-Feshbach model formula have been estimated from experimental data of neutron-induced reactions for Co and Ni. Correlation matrices for the level density parameter resulted from three cases of different combination of the nuclear parameters are compared to discuss effect of parameters in the formula. The correlation of reaction cross sections calculated from the estimated parameters is compared with the one obtained in the new evaluation from both differential and integral experiments.

IV-B-8

Adjustment of Evaluated Fission Cross Sections by Integral Data

Y. Kanda*, Y. Uenohara*, D.L. Smith**, and J.W. Meadows**

A paper on this subject was presented to International Conference on Nuclear Data for Science and Technology, Mito Japan, May 30 - June 3, 1988

Abstract

Fission cross sections for ^{232}Th, ^{233}U, ^{234}U, ^{235}U, ^{236}U, ^{238}U, ^{237}Np and ^{239}Pu evaluated from differential experiments and compiled in JENDL-3T has been adjusted by using integral fission cross-section ratios measured for ^{232}Th/^{235}U, ^{237}Np/^{235}U, ^{238}U/^{235}U, ^{237}Np/^{238}U, ^{232}Th/^{237}Np, ^{236}U/^{235}U, ^{239}Pu/^{235}U, ^{233}U/^{235}U, ^{234}U/^{235}U, ^{234}U/^{238}U and ^{236}U/^{238}U in the continuum neutron spectrum produced by bombardment of a thick Be-metal target with 7 MeV deuterons. It has been demonstrated that the fission cross-section curves can be adjusted in the energy range between 1 and 10 MeV. The ratios of the calculated to experimental values for the integral fission cross-section ratios have been revised within ± 1.005 except for ^{232}Th whose result is 1.02. The original values are between 0.995 and 1.067 in JENDL-3T.

---

* Department of Energy Conversion Engineering, Kyushu University

** Applied Physics Division, Argonne National Laboratory

The adjustment method developed in the present work is valuable to evaluate accurate and consistent cross-sections in the MeV neutron energy region. Differential and integral data are complementary in a cross-section evaluation. The former is useful to determine shapes of the cross-section curves and the latter is valid to adjust their absolute values.

IV-B-9

Resonance Parameters of Tantalum-181 in Neutron Energy Range from 100 to 4,300eV

I. Tsubone[***], Y. Nakajima[*], and Y. Kanda[**]

A paper on this subject was published in the Jounal of Nuclear Science and Technology on December 1987[1)]

Abstract

Neutron transmission measurements were performed on natural tantalum (abundance ratio 99.988% for ^{181}Ta) in the energy range of 100~4,300eV using the Japan Atomic Energy Research Institute linac. The transmissions were measured using 55 and 190 m time-of-flight spectrometers for two and three samples of different thicknesses, respectively. These transmission data were simultaneously analyzed with a least

---

* Department of Physics, Japan Atomic Energy Research Institute.

** Department of Energy Conversion Engineering, Kyushu University.

*** On leave from Kyushu University as a research student in JAERI. Present Address: Design Division of Nuclear Instrumentation, Tokyo Factory, Fuji Electric Co., Ltd. Fuji-mati, Hino-shi 191.

squares fitting program based on multi-level Breit-Wigner formula, and resonance energies and neutron width were obtained for 696 resonances of ^{181}Ta.

The statistical analysis of these parameters gave the s-wave average level spacing of $\langle D \rangle = 4.10 \pm 0.14$eV and s-wave neutrron strength functions of $(1.67 \pm 0.13) \times 10^{-4}$, $(1.09 \pm 0.09) \times 10^{-4}$ and $(1.42 \pm 0.20) \times 10^{-4}$ for the energy intervals from 100～1,700eV, 1,700～3,400eV and 3,400～4,300eV, respectively. This significant difference among the neutron strength function for each energy interval is a prominent result of the present experiments and is of great interest.

Reference

1) I.Tsubone et al., J. Nucl. Sci. Technol. 24 975 (1987)

V. Musashi Institute of Technology

A. Atomic Energy Research Laboratory

V-A-1 **Measurement of Total Neutron Cross Sections for Sm, Gd and Dy in the Thermal Energy Region**

Kouichi Higurashi, Otohiko Aizawa, Tetsuo Matsumoto

and

Hiroyuki Kadotani+

A paper on this subject was submitted to the International Conference on Nuclear Data for Science and Technology, May 30 - June 3, 1988 Mito, Japan, with the following abstract:

The method to measure total neutron cross sections in the thermal energy region was established with the chopper and time-of-flight facility installed at the Musashi reactor (TRIGA-II, 100kW). To date, the facility was used primarily for measuring samples which were essentially scatterers. The method successfully developed in this research was newly applied to samples having very large absorption cross sections. Cross sections

+ Century Research Center Corporation

were measured for natural Sm, Gd and Dy by using the Al powder dilution method. Comparison of the measured cross sections with published data showed slightly lower values than the data published in BNL-325 3rd edition. The g-factors obtained by Westcott for these absorbers, however, were independently evaluated based on the result of this research, and found to be in good agreement with the published figures.

V-A-2 Measurement of Total Neutron Cross Sections for Some Organic Materials in Thermal Energy Region

H. Kadotani+, Y. Hariyama+, N. Fukumura++, N. Aihara++,

O. Aizawa and K. Hirano

A paper on this subject was submitted to the International Conference of Nuclear Data for Science and Technology, May 30 - June 3, 1988 Mito, Japan, with the following abstract:

The total cross sections of some organic moderators were measured for the thermal neutron energy region. The samples measured were normal dodecane, tri-butyl phosphate(TBP), and the mixture of 70 v/o of normal dodecane and 30 v/o of TBP which is typically used in a reprocessing plant. The cross sections were measured as the transmission of thermal neutrons through samples using the chopper and TOF facility installed at the Musashi reactor TRIGA-II, (100kW). It was found that, although the measured cross sections were almost the same for dodecane and TBP, they both show different behaviors compared with those of water. We propose to use the new spectral densities to calculate the cross sections for the above moderators within the framework of Nelkin's formalism for water.

\+ Century Research Center Corporation

++ Power Reactor and Nuclear Fuel Development Corporation

VI. Nagoya University

A. Department of Nuclear Engineering

Faculty of Engineering

VI-A-1

Measurement of Formation Cross-sections of Short-lived Nuclei Produced by 14 MeV Neutron

T. Katoh, H. Yoshida, A. Osa, Y. Gotoh, M. Miyachi, H. Ukon, M. Shibata, H. Yamamoto, K. Kawade, A. Takahashi* and T. Iida*

Measurement of formation cross-sections of short-lived nuclei produced by 14 MeV neutron were made by using the Intense Neutron Source(OKTAVIAN) at Osaka University. Measured reactions were ^{92}Mo(n,2n), ^{92}Mo(n,α), ^{63}Cu(n,2n), ^{65}Cu(n,α), ^{90}Zr(n,2n) and ^{55}Mn(n,α) reactions. Cross-sections were obtained by the activation method. Peumatic tubes were set at 6 directions for the incident deuteron beam direction for the purpose of transportation of samples. The neutron flux at the irradiation points were monitored by aluminum foils. Samples of natural molybdenum, zirconium, manganese and copper were irradiated together with the monitor foils. Gamma rays of induced short-lived nuclei were measured by a Ge detector, and then cross-sections were obtained from the amount of induced activities. The energy of neutron at each irradiation point was determined by the Zr-Nb method.

Measured cross-sections are shown in Figures together with previous results.

* Department of Nuclear Engineering, Osaka University

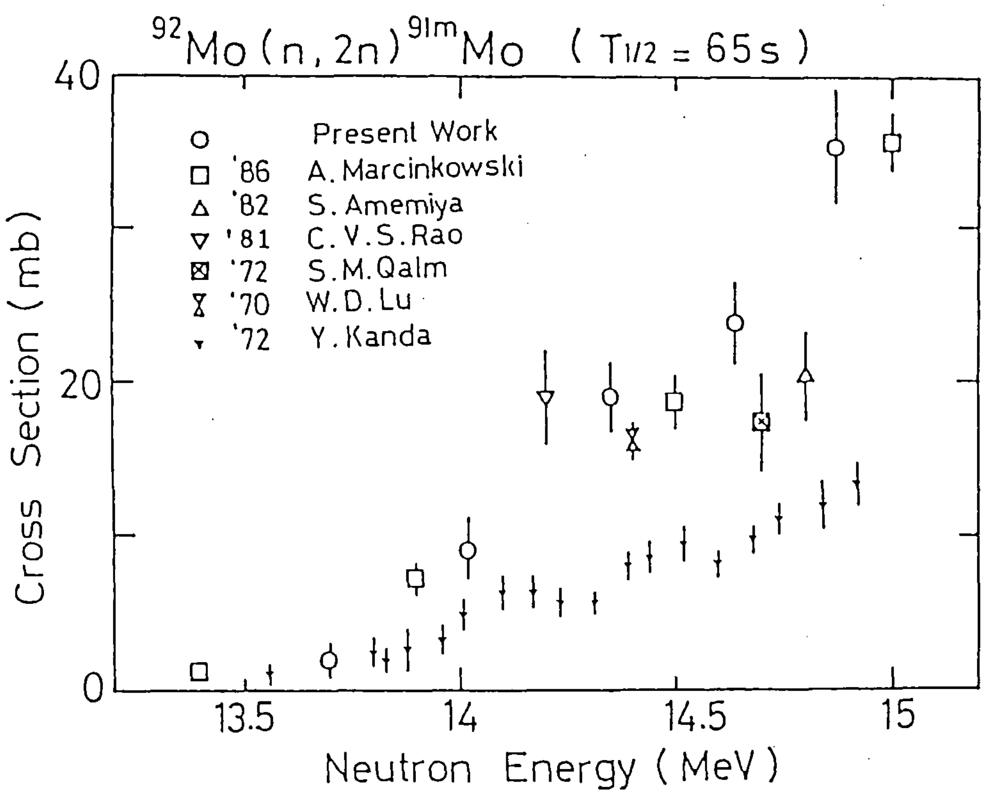

Fig. 1 Cross-sections of $^{92}Mo(n, 2n)^{91m}Mo$ reaction. The reference reaction for this measurement and the following 5 reactions was the $^{27}Al(n, p)^{27}Mg$ reaction.

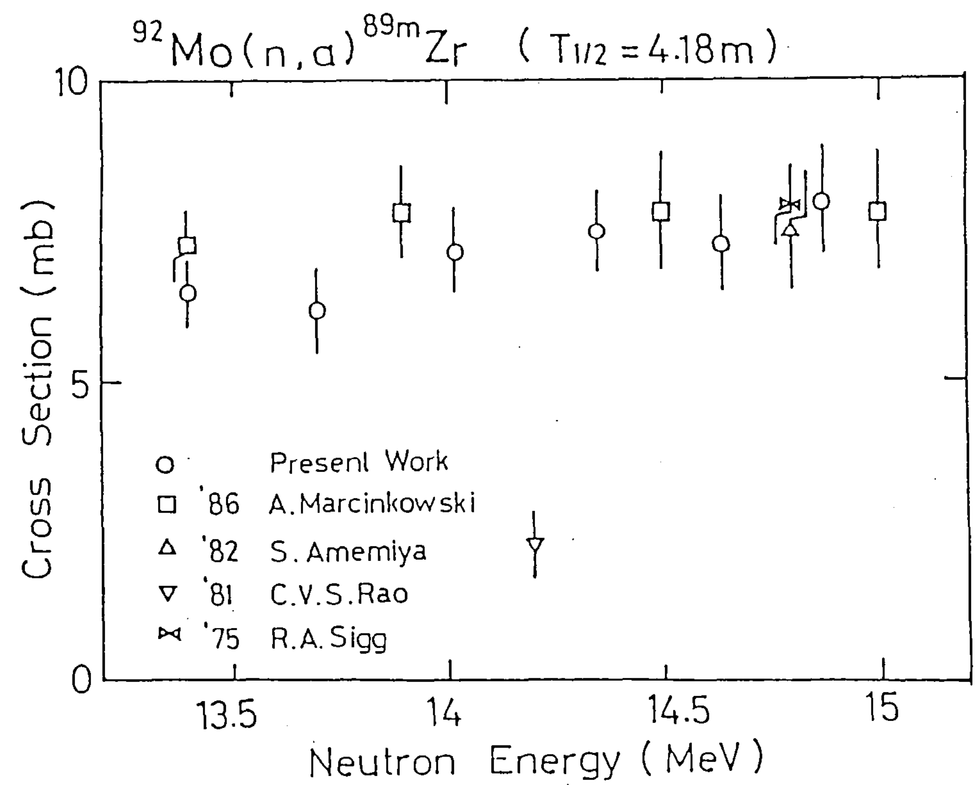

Fig. 2 Cross-sections of $^{92}Mo(n, \alpha)^{89m}Zr$ reaction.

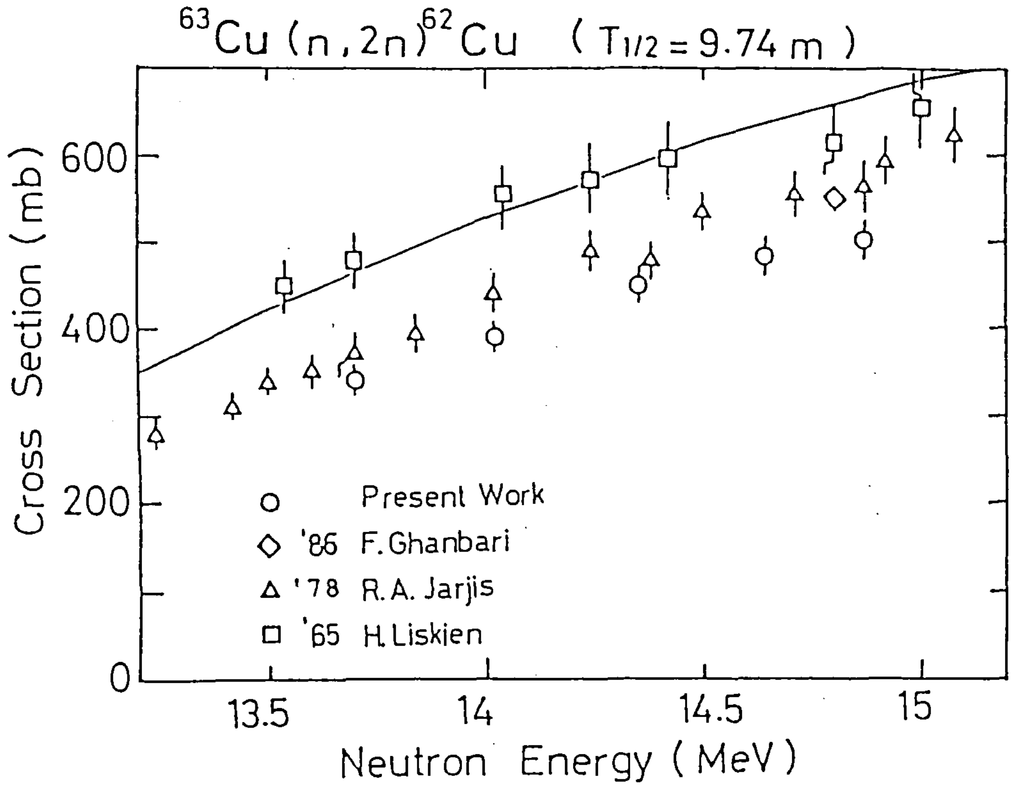

Fig. 3 Cross-sections of ^{63}Cu(n, 2n)^{62}Cu reaction.

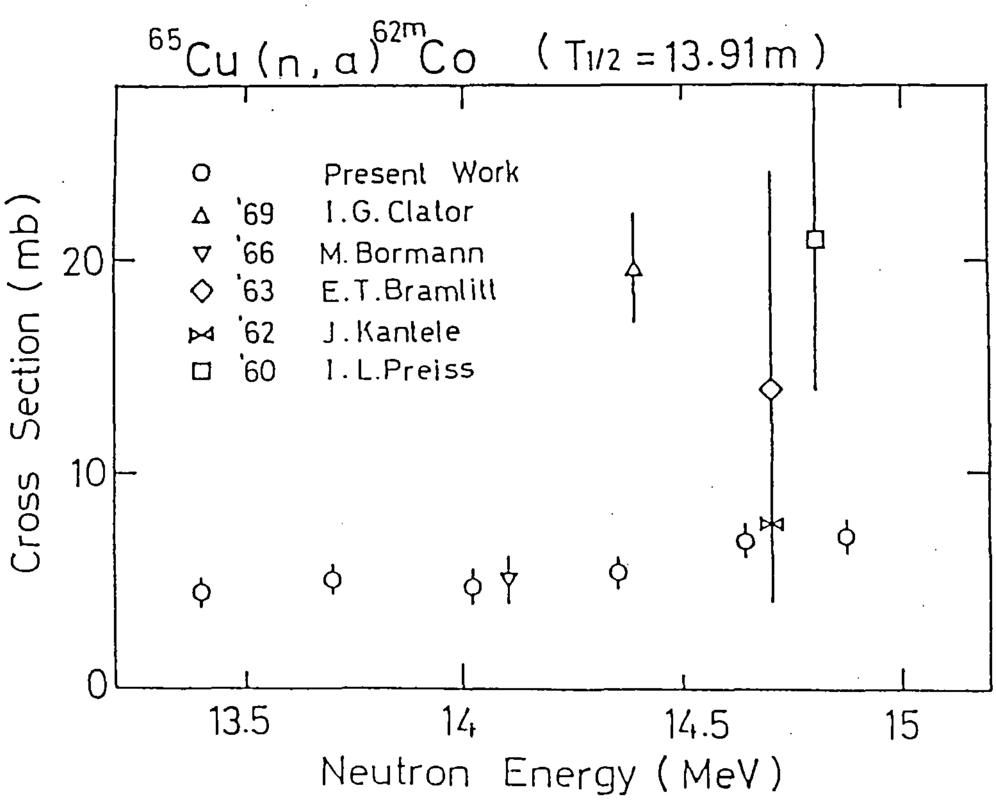

Fig. 4 Cross-sections of ^{65}Cu(n, α)^{62m}Co reaction.

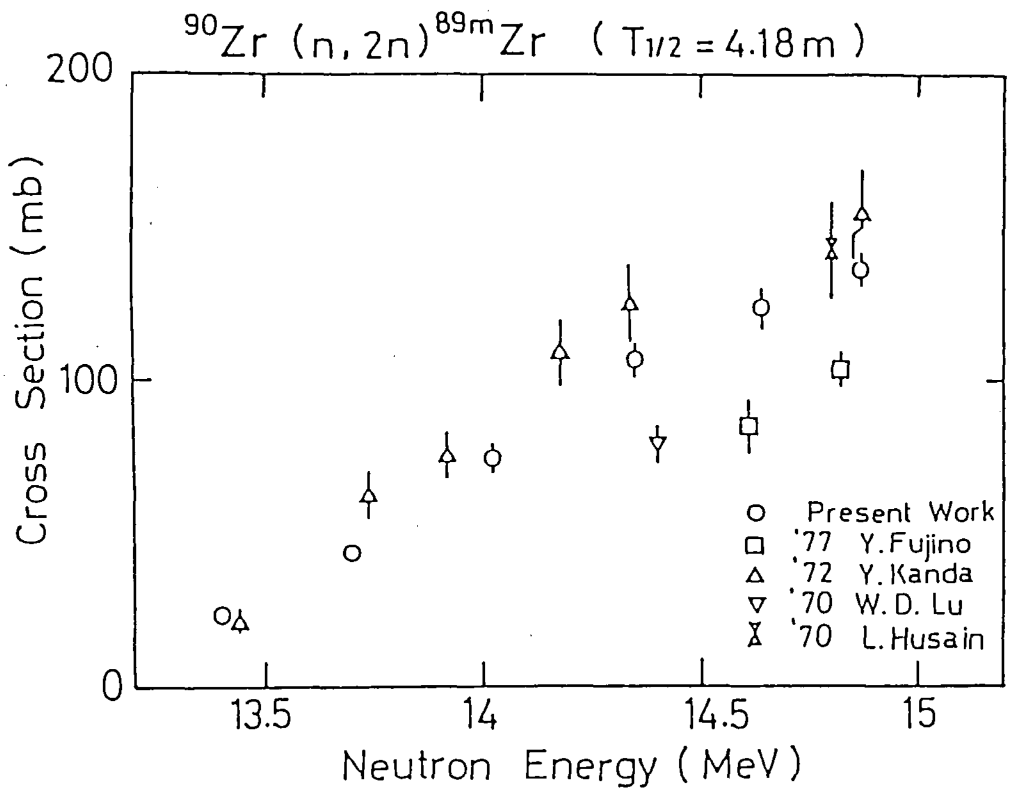

Fig. 5 Cross-sections of $^{90}Zr(n, 2n)^{89m}Zr$ reaction.

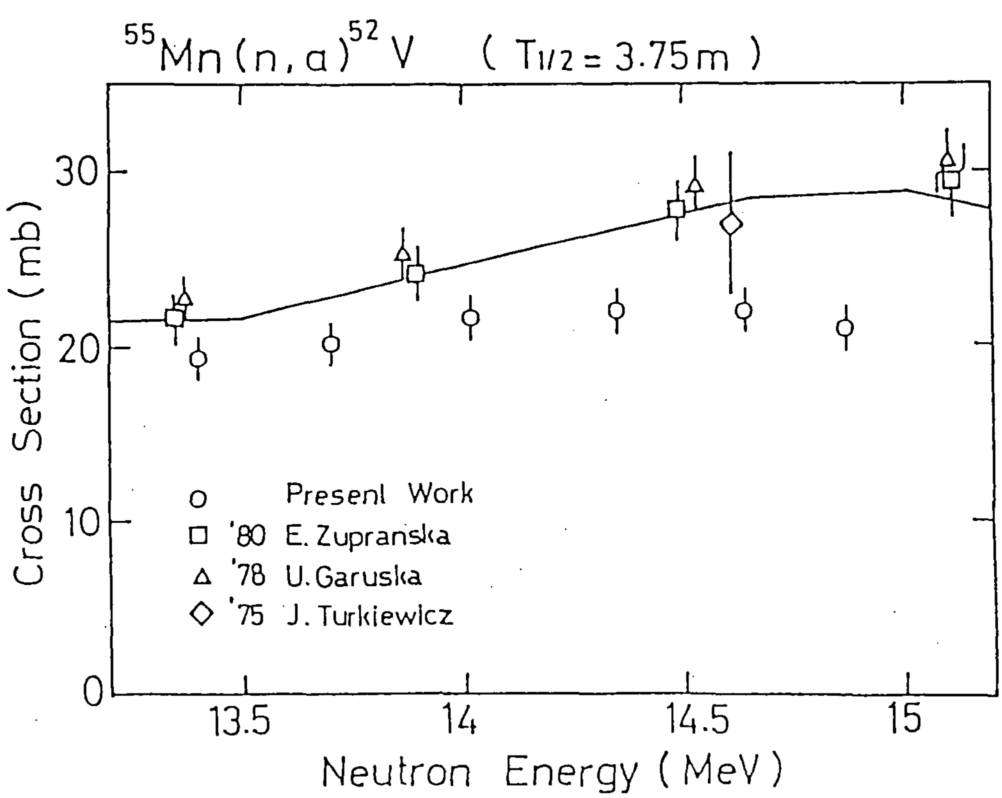

Fig. 6 Cross-sections of $^{55}Mn(n, \alpha)^{52}V$ reaction.

VII. Osaka University

A. Department of Chemistry

Faculty of Science

VII-A-1

Fission Fragment Formation Cross Sections in the Fission of ^{233}U, ^{235}U and ^{238}U with 90-MeV ^{12}C

H. Baba, M. J. Duh, N. Takahashi, A. Yokoyama,
S. Baba[+], K. Hata[+] and Y. Nagame[+]

In order to investigate the characteristics of charge distribution of heavy-ion fission in the heavy actinide region and deduce the neutron systematics, we carried out a radiochemical study of fission induced by ^{12}C using three uranium isotopes as targets. The targets were prepared by electrodeposition of uranium oxide on 26.2μm Al foils and bombarded with 90-MeV ^{12}C ions from the tandem accelerator at JAERI. The incident energy was adjusted so as to give the same excitation energy of 46 MeV for three compound systems by the use of Al degraders with appropriate thicknesses. Long and short irradiations of uranium targets were carried out; one for 2 hr and the other for 30 min. After the irradiation the targets were subjected to the non-destructive gamma-ray spectrometry. Chemical separation of antimony, tellurium, and iodine was undertaken in separate runs in order to detect as many isotopes as possible for the elements. Range measurements were also carried out to distinguish fission products from non-fission products due to the impurities. Cross sections were then determined for product masses A ranging from 72 to 151, which are summarized in the table.

+ Japan Atomic Energy Research Institute

Table. Fission fragment formation cross section in the ^{12}C-induced fision of ^{238}U, ^{235}U and ^{233}U. The symbols I and C given in the sixth column stand for the independent and cumulative yields, respectively.

Nuclide	Half-life	Cross section (mb) ^{238}U	^{235}U	^{233}U	Mode	Comments
^{72}Zn	46.5 h	0.99±0.15	0.97±0.19	0.75±0.13	C	
^{72}Ga	14.1 h			0.95±0.12	I	
^{73}Ga	4.86 h	2.9 ±0.7	2.6 ±0.2	3.73±0.06	C	
$^{82g+m}Br$	35.34 h		1.35±0.12	1.39±0.09	I	
^{85m}Kr	4.48 h	3.6 ±0.1	2.54±0.18	3.30±0.13	C	
^{88}Kr	2.84 h	12±3		13±1	C	
^{90m}Y	3.19 h			0.86±0.08	I	
^{91}Sr	9.52 h	6.3 ±0.3	7.6 ±0.5	9.2 ±0.3	C	
^{91m}Y	49.7 m	0.6 ±0.4	1.7 ±0.3	3.5 ±0.3	I	
^{92}Sr	2.71 h	6.0 ±0.4	5.5 ±0.2	7.2 ±0.6	C	
^{92}Y	3.54 h	1.39±0.12	1.38±0.11	0.66±0.06	I	
^{93}Y	10.1 h	11±4			C	
^{95}Zr	64.0 d	9.3 ±0.5	11.0 ±0.5	14.4 ±0.9	C	
^{96}Nb	23.4 h		1.37±0.09	3.14±0.12	I	
^{97}Zr	16.8 h	10.1 ±0.4	9.4 ±1.0	10.0 ±0.2	C	
^{98m}Nb	51.3 m	6.6 ±0.4	7.9 ±0.7	9.7 ±0.6	C	
^{99}Mo	65.94 h	14.0 ±0.4	13.6 ±1.0	16.9 ±1.4	C	
^{101}Mo	14.6 m	22±3		37±3	C	
^{101}Tc	14.2 m	28.4 ±0.9			I	
^{101m}Rh	4.4 d		0.22±0.03		C	
^{103}Ru	39.35 d	16.7 ±0.7	16.8 ±1.4	22.7 ±0.9	C	
^{104}Tc	18.4 m	15.7 ±0.6			C	
^{105}Ru	4.4 h	17.2 ±0.3	18.0 ±0.9	22.0 ±0.8	C	
$^{105g+m}Rh$	35.5 h	20.7 ±0.3	20.0 ±1.1	26.1 ±0.7	C	
^{107}Rh	21.7 m	18.2 ±0.7			C	
^{110g}In	69.1 m		4.9 ±0.3	7.8 ±0.3	I	
^{110}Sn	4 h	5.2 ±0.4	3.8 ±0.4	2.76±0.07	C	
^{111m}Pd	5.5 h	4.6 ±1.2	6.0 ±0.5	6.65±0.19	C	

Table (continued)

Nuclide	Half-life	Cross section (mb) ^{238}U	^{235}U	^{233}U	Mode	Comments
$^{111g+m}Ag$	7.45 d	18.5 ±0.6	30±5	24.8 ±1.1	C	
^{112}Pd	21.1 h	18.1 ±0.3	16.9 ±0.7	13.6 ±0.7	C	
$^{113g+m}Ag$	5.37 h	23±6	21±8	30±1	C	
^{115g}Cd	2.23 d	15.3 ±0.3	12.6 ±0.7	11.9 ±0.5	C	
^{115m}In	4.49 h	4.9 ±1.3	11.9 ±0.4	4.6 ±0.2	I	
^{117m}Cd	3.31 h	9.5 ±0.8	12.1 ±1.7	12.0 ±0.6	C	
^{117g}Cd	2.42 h	4.5 ±0.2	2.67±0.05		C	
^{117g}In	43.1 m	2.1 ±0.6			I	
^{120m}Sb	5.75 d		0.66±0.06		I	
$^{122g+m}Sb$	2.7 d	1.80±0.07	4.6 ±0.4	9.1 ±0.5	I	
$^{124g+m}Sb$	60.3 d	6.6 ±1.0	7.6 ±0.5	11.1 ±0.5	I	IT=80%
$^{126g(+m)}Sb$	12.4 d	7.6 ±0.2	6.0 ±0.5	4.37±0.14	I	IT=14%
^{126}I	19 d		2.0 ±0.5		I	
^{127}Sb	3.85 d	8.2 ±0.5		3.6 ±0.2	I	
〃	〃	8.5 ±0.4	5.0 ±0.3	3.33±0.07	C	
$^{128g(+m)}Sb$	9.01 h	3.8 ±0.3	1.78±0.11	1.15±0.10	I	IT=3.6%
〃	〃	3.5 ±0.2		1.14±0.14	C	
^{128}I	25 m	2.1 ±0.8		6.2 ±0.8	I	
^{129}Sb	4.4 h	1.5 ±0.2	1.24±0.12	1.02±0.10	C	
^{129g}Te	69.6 m	3.3 ±1.4		4.0 ±1.4	I	
^{129}Cs	32.1 h			1.3 ±0.2	C	
$^{130g+m}Sb$	40 m	0.98±0.05			C	
$^{130g+m}I$	12.36 h	7.9 ±0.7	8.5 ±0.2	7.7 ±0.4	I	IT=83%
^{131m}Te	30 h	3.6 ±0.2	2.40±0.14	1.61±0.08	C	
^{131g}Te	25 m		3.3 ±0.4	1.78±0.08	I	
^{131}I	8.02	13.6 ±0.6	9.5 ±0.5	7.3 ±0.5	C	
^{132}Te	3.26 d	4.6 ±0.8	2.61±0.20	1.68±0.05	C	
$^{132g+m}I$	2.30 h	8.3 ±0.6	5.5 ±0.8	4.9 ±0.5	I	IT=86%
^{132}Cs	6.48 d	2.5 ±0.8	4.3 ±1.8	6.7 ±0.6	I	
^{133m}Te	55.4 m	1.5 ±0.2	1.03±0.09	0.58±0.03	C	

Table (continued)

Nuclide	Half-life	Cross section (mb) ^{238}U	^{235}U	^{233}U	Mode	Comments
$^{133g+m}I$	20.8 h	7.2 ±0.4	4.0 ±0.2	3.4 ±0.2	I	
〃	〃	7.6 ±0.2	4.4 ±0.6	3.4 ±0.4	C	
^{133m}Xe	2.19 d	9.3 ±0.3	7.5 ±1.5	6.7 ±0.5	C	
^{133g}Xe	5.25 d	9.9 ±0.7	7.6 ±1.5	3.4 ±0.1	C	
$^{133g+m}Xe$	5.25 d	27±9	14±2	14±3	C	
^{134}Te	41.8 m	1.3 ±0.1	1.0 ±0.2	0.50±0.07	C	
^{134}I	52.6 m	3.2 ±0.2	2.8 ±0.2	2.4 ±0.2	I	
〃	〃	9.5 ±0.3	8.2 ±1.2	7.8 ±0.3	C	
^{134m}Cs	3.54 h	4.7 ±0.2			I	
^{135}I	6.61 h	2.7 ±0.3	1.8 ±0.7	1.3 ±0.2	C	
^{135m}Xe	15.6 m	3.5 ±0.5			I	
$^{135g+m}Xe$	9.10 h	5.4 ±0.1	4.6 ±0.2	2.96±0.16	I	
〃	〃	11.5 ±0.3	6.2 ±1.0	4.33±0.10	C	
^{135m}Ba	28.7 h	3.3 ±0.1	3.8 ±0.7	8.9 ±0.6	C	
$^{136g+m}Cs$	13.16	7.7 ±0.2	5.6 ±0.4	4.47±0.06	C	
^{137m}Ce	34.4 h	3.5 ±0.4			C	
^{138}Xe	14.1 m	20±3			C	
$^{138g+m}Cs$	32.2 m	5.3 ±1.2			C	
^{139}Ba	82.7 m	9.6 ±0.3	9.9 ±0.8	6.6 ±0.6	C	
^{140}Ba	12.75 d	6.4 ±0.2	3.9 ±0.3	3.41±0.06	C	
^{140}La	40.28 h	4.5 ±0.2	4.1 ±0.3	4.2 ±0.2	I	
^{141}Ce	32.5 d	13.4 ±0.3	12.3 ±0.5	7.4 ±0.7	C	
^{142}La	92.5 m	5.9 ±0.3	3.8 ±0.3	3.2 ±0.4	C	
^{143}Ce	33.0 h	9.5 ±0.3	6.6 ±0.5	5.8 ±0.2	C	
^{147}Nd	10.98 d	10.0 ±0.3	7.2 ±0.9	5.8 ±0.2	C	
^{148m}Pm	41.29 d		1.40±0.09	2.89±0.07	I	
^{149}Nd	1.73 h	13±5	4.6 ±0.3		C	
^{151}Pm	28.4 h	3.5 ±0.3	2.4 ±0.4	1.92±0.18	C	

VIII. Rikkyo (St. Paul's) University

A. Department of Physics

Faculty of Science

VIII-A-1

Cross Sections for the Neutron-Induced Reactions on ^{6}Li and ^{7}Li at 14.1 MeV

S. Shirato, S. Shibuya, Y. Ando and K. Shibata*

Remeasurement of the differential cross sections for the reactions $^{7}Li(n,t)^{5}He$ and $^{7}Li(n,d)^{6}He$ has been performed using 14.1 MeV neutrons provided by a new Cockcroft-Walton accelerator of the Rikkyo University. This measurement confirmed our previous data[1)] on the differential cross section for the $^{7}Li(n,t)^{5}He$ reaction, and a newly performed exact finite-range DWBA calculation reproduced the experimental data better than a previous calculation[2)].

A summary of our newly and previously measured cross sections for 14.1 MeV neutron-induced reactions on lithium isotopes has been reported at the International Conference on Nuclear Data for Science and Technology[3)]. Some problems existing in the data and DWBA calculations have been mentioned therein[3)].

References:

1) I. Furutate, T. Kokubu, Y. Ando, T. Motobayashi and S. Shirato, JAERI Report 1984, NEANDC(J)-116/U, INDC(JPN)-102/U, p. 81.
2) I. Furutate, Master thesis (Rikkyo University, 1986).
3) S. Shirato, S. Shibuya, Y. Ando and K. Shibata, Contributed paper submitted to the International Conference on Nuclear Data for Science and Technology, May 30 - June 3, 1988, Mito, Japan.

---

* Japan Atomic Energy Research Institute

IX. Tohoku University

A. Department of Nuclear Engineering

Faculty of Engineering

IX-A-1

MEASUREMENT OF ^{235}U FISSION CROSS SECTION AROUND 14 MeV

Tomohiko Iwasaki, Yoshiji Karino, Shigeo Matsuyama,
Fumitoshi Manabe, Mamoru Baba,
Kazutaka Kanda and Naohiro Hirakawa

A paper on this subject was presented at Int. Conf. "Nuclear data for Science and Technology" on May 30 - June 3, 1988 at Mito with the following abstract:

The neutron-induced fission cross section of U-235 was measured at five neutron energy points from 13.5 to 14.9 MeV by a newly developed detector which coupled a proton-recoil counter telescope with a fission chamber in back to back form. An experimental test of this detector was performed using the time correlated associated particle method. The experimental neutron sensitivity agreed with the analytical one within 1%. The fission cross section measurement was carried out for an U-235 sample with a purity of 99.91%. The overall uncertainties of the measurement were 2.5-2.8%. The present results agreed well in magnitude and in energy dependence , respectively, with the results by Cance and by Czirr.

IX-A-2

MEASUREMENT OF FAST NEUTRON INDUCED FISSION CROSS SECTION RATIOS OF ^{239}Pu AND ^{242}Pu RELATIVE TO ^{235}U

Naohiro Hirakawa, Tomohiko Iwasaki, Mamoru Baba,
Fumitoshi Manabe and Shigeo Matsuyama

A paper on this subject was presented at Int. Conf. "Nuclear Data for Science and Technology" on May 30 - June 3, 1988 at Mito with the following abstract:

Fission cross section ratios of Pu-239 and Pu-242 relative to U-235 were measured in the energy range from 0.6 to 7 MeV using the 4.5 MV Dynamitron accelerator of Tohoku University. A fast timing back to back fission chamber was used to detect fission events. The measurement was carried out with time of flight (TOF) method. The corrections to the measured data were carefully applied and uncertainty was analyzed taking the correlation between error sources into account. The overall uncertainty of the present results was about 2 %. The present results for Pu-239/U-235 are slightly higher than other experimental data and JENDL-2. For Pu-242/U-235, the present data agree with those of Meadows and Kuprijanov et al.

IX-A-3

DOUBLE-DIFFERENTIAL NEUTRON SCATTERING CROSS SECTIONS OF BERYLLIUM, CARBON, OXYGEN

Mamoru Baba, Masumi Ishikawa, Tsukasa Kikuchi,
Hidetaka Wakabayashi and Naohiro Hirakawa

A paper on this subject was presented at Int. Conf. "Nuclear Data for Science and Technology" on May 30 - June 3, 1988 at Mito with the following abstract:

The energy-angular double-differential neutron scattering cross sections have been measured for beryllium, carbon and oxygen at the incident neutron energies of 14.1 MeV and 18.0 MeV. The measured neutron emission spectra and partial scattering cross sections are presented in comparison with the evaluated values. The neutron spectra from beryllium were analyzed on the basis of a multi-particle decay model, and were reproduced reasonably by assuming contribution of simultaneous four-body breakup process.

IX-A-4

DOUBLE-DIFFERENTIAL NEUTRON EMISSION SPECTRA FOR Al, Ti, V, Cr, Mn, Fe, Ni, Cu, and Zr

M.Baba, M.Ishikawa, N.Yabuta, T.Kikuchi,
H.Wakabayashi and N.Hirakawa

A paper on this subject was presented at Int. Conf. "Nuclear Data for Science and Technology" on May 30 - June 3, 1988 at Mito with the following abstract :

The angle-dependent neutron emission spectra have been measured for nuclides cited above at the incident neutron energy of 14.1 MeV. For aluminum, iron, nickel, copper and zirconium, the measurements were performed as well at 18 MeV incident energy. The data were obtained at 7-12 laboratory angles for secondary neutrons down to 0.6 MeV. The emission neutrons show systematic angle dependence and their angular distribution were compared favorably with the calculation based on the Kalbach-Mann systematics.

X. Tokyo Institute of Technology

A. Research Laboratory for Nuclear Reactors

X-A-1 Mechanism of s-Wave and p-Wave Neutron Resonance Capture in Light and Medium-Weight Nuclei

H. Kitazawa and M. Igashira

Capture gamma-ray spectra of ^{16}O, ^{28}Si and ^{32}S have been measured to investigate the mechanism of neutron capture in s-wave and p-wave resonances with large reduced neutron width. Observed gamma-ray transitions from the 434-keV $p_{3/2}$-wave resonance of ^{16}O exhibit typical features of valence neutron capture in light nuclei. For the 565-keV and 806-keV $p_{3/2}$-wave resonances of ^{28}Si, a particle-vibrator coupling model indicates that in these resonance states core excitation is essential to explain the observed partial radiative widths. There is also some possibility of core excitation in the 203-keV $p_{1/2}$-wave resonance capture in ^{32}S. Moreover, a strong correlation between partial radiative widths and spectroscopic factors of the final states was found for gamma-ray transitions from the 188-keV s-wave resonance of ^{28}Si and the 103-keV s-wave resonance of ^{32}S. A discussion will follow on the particle-core coupling scheme in these resonance capture transitions.

Published in J. Phys. G: Nucl. Phys. 14 Suppl.

X-A-2 Evaluation of Neutron Cross Sections of the sd-Shell Nuclei ^{27}Al and $^{28,29,30}Si$

H. Kitazawa, Y. Harima, and T. Fukahori

On the basis of nuclear models we have evaluated neutron cross sections of ^{27}Al and $^{28,29,30}Si$ at the energies of 10^{-5} eV to 20 MeV. The model parameters, i.e. the nuclear level-density parameters in the Gilbert-Cameron formula and the optical potential parameters for neutron, proton and alpha particle, were determined independently of the previous work. Consequently it was found that the constant-temperature model function can be expressed in terms of a nuclear temperature common to the nuclei concerned in these neutron reactions. The potential parameters were so taken as to include the dependence of the real and imaginary potential depths on incident particle energies, being derived from a global optical potential. Moreover, we assumed the structure of rotational and vibrational levels in these nuclei in order to calculate neutron inelastic-scattering cross sections, taking account of some chatacteristic features of sd-shell nuclei which are predicted from the observed data on electron and proton scattering and on multipole transition strengths of gamma rays. The model calculations were mainly performed in the framework of the Hauser-Feshbach theory with width fluctuation. However, the expected strong excitation of collective states with neutrons was fully considered with a coupled-channel Born approximation. And also, the important contributions of direct and semidirect process were included into the calculations of neutron capture cross sections at En >

1.0 MeV. The calculated results were found to be in reasonable agreement with experimental values in the whole neutron-energy region.

Published in Proc. Int. Conf. on Nucl. Data for Sci. and Tech., Mito (1988).

X-A-3 Measurements of keV-Neutron Capture Gamma-Ray Spectra of Fe and Ni

M. Igashira, H. Matsumoto, T. Uchiyama, and H. Kitazawa

Photon-production nuclear data are indispensable for shielding design calculation, for radiation damage estimate, and for radiation heating calculation. However, the data are scanty, especially in the keV-neutron region. Therefore, we have measured keV-neutron capture gamma-ray spectra of Fe and Ni to provide these nuclear data.

Neutrons were generated by the $^7Li(p,n)^7Be$ reaction using the pulsed proton beam from the 3.2-MV Pelletron accelerator in Tokyo Institute of Technology. The average beam current was typically 10 μA for the pulse-repetition rate of 2 MHz and for the pulse width of about 1 ns. Capture samples were disks of 60 mm in diameter and 5 mm in thickness, and were located at a distance of 150 mm from the neutron source. Capture gamma rays were detected by an anti-Compton NaI(Tl) detector at an angle of 125° with respect to the proton beam direction. Measurements were performed using a time-of-flight technique at several neutron energies between 10 and 600 keV.

Background-subtracted gamma-ray pulse-height spectra were unfolded by the computer code FERDOR, using a response matrix of the gamma-ray detector. Correction for the gamma-ray attenuation in the sample was made by a Monte-Carlo calculation.

The observed spectra of Fe exhibit strong gamma-ray transitions from capture states to the ground state and first excited state of ^{57}Fe. The relative intensity of these transitions seems to decrease with the incident neutron energy. The spectra of Ni also exhibit strong transitions from capture states to low-lying states of residual nuclei.

Capture gamma-ray spectra of Fe were calculated by the computer code CASTHY based on the Hauser-Feshbach statistical model. In the calculations, the conventional Brink-Axel gamma-ray strength function was used for an E1 gamma-ray strength function, and the composite formula proposed by Gilbert and Cameron was used for a nuclear level-density distribution. Comparisons between the observed and calculated spectra disclose remarkable discrepancies between both spectra for gamma-ray transitions to low-lying states. An analysis of the Ni data is in progress.

Published in Proc. Int. Conf. on Nucl. Data for Sci. and Tech., Mito (1988).

X-A-4 Gamma Rays from Resonance Neutron Capture by ^{24}Mg

T. Uchiyama, M. Igashira and H. Kitazawa

In the mass region A=20-30, the p-wave neutron strength function shows strong peaking, and consequently neutron single-particle E1 transitions may be facilitated from p-wave resonance states to the low-lying states of residual nuclei which have large single-particle components. Moreover the M1 gamma-ray transitions which follow the core-particle spin-flip transitions, $(d_{5/2})^n \to (d_{5/2})^{n-1}\ d_{3/2}$, are expected in s-wave and d-wave resonance capture reactions. From this viewpoint we have planned to investigate a great variety of gamma-ray multipole transitions in resonance capture reactions on sd-shell nuclei.

In the present study, we have observed capture gamma-ray spectra from the 46.35-keV $d_{3/2}$-wave narrow resonance and the 83.5-keV $p_{3/2}$-wave strong resonance of ^{24}Mg. Measurements were performed using a time-of-flight technique. Pulsed neutrons were produced from the ^{7}Li(p,n)^{7}Be reaction by bombarding a Li-evapolated copper disk with the 1-ns bunched proton beam from the 3.2-MV pelletron accelerator in Tokyo Institute of Technology. The average beam current was typically 9 μA at the 2-MHz pulse repetition rate. The capture sample was a metal disk of natural magnesium (8.6×10^{-3} atm/b), which was placed 155 mm distant from the neutron source. Gamma rays were detected with an anti-Compton NaI(Tl) detector. The detector was located at a distance of 80 cm from the sample, and its axis made an angle of 125° with respect to the proton beam direction.

In the p-wave resonance capture, distinct gamma rays were observed for the transitions to the ground ($5/2^+$), 585keV ($1/2^+$), 1965keV ($5/2^+$) and 2564keV ($1/2^+$) states of ^{25}Mg. As a result, we found that the Lane-Mughabghab optical model formula of the valence capture model reproduces well the obseved partial radiative widths for these E1 transitions. In the d-wave resonance capture, only the ground-state transition was observed. The preliminary valence-model calculation which assumes the M1 transition and the free neutron g-factor shows a marked discrepancy with the observed partial radiative width for this transition.

Published in Proc. Int. Conf. on Nucl. Data for Sci. and Tech., Mito (1988).